mathematics

Article

A Refined Closed-Form Solution for Laterally Loaded Circular Membranes in Frictionless Contact with Rigid Flat Plates: Simultaneous Improvement of Out-of-Plane Equilibrium Equation and Geometric Equation

Fei-Yan Li [1], Xue Li [1], Qi Zhang [1], Xiao-Ting He [1,2] and Jun-Yi Sun [1,2,*]

1   School of Civil Engineering, Chongqing University, Chongqing 400045, China
2   Key Laboratory of New Technology for Construction of Cities in Mountain Area (Chongqing University), Ministry of Education, Chongqing 400045, China
*   Correspondence: sunjunyi@cqu.edu.cn; Tel.: +86-(0)23-6512-0720

Publisher's Note: MDPI stays neutral with regard to jurisdictional claims in published maps and institutional affiliations.

Abstract: Essential to the design and development of circular contact mode capacitive pressure sensors is the ability to accurately predict the contact radius, maximum stress, and shape of a laterally loaded circular membrane in frictionless contact with a concentric circular rigid flat plate. In this paper, this plate/membrane contact problem is solved analytically again by simultaneously improving both out-of-plane equilibrium equation and geometric equation, and a new and more refined closed-form solution is given to meet the need of accurate prediction. The new closed-form solution is numerically discussed in convergence and effectiveness and compared with the previous one, showing that it can greatly improve the prediction accuracy of the contact radius, maximum stress, and shape of the circular membrane in frictionless contact with the rigid flat plate.

1. Introduction

Rotationally symmetric membranes, as structures or structural components, are of much interest in a variety of applications such as bulge tests [1–3], blister tests [4–6] or constrained blister tests [7–10], and capacitive pressure sensors [11–14]. Attention in the literature has focused generally on circular membranes [15–19], relatively less on annular membranes [20–23]. The external loads applied to circular membranes cover lateral loading and normal loading, but only a few cases of normal loading are available in the literature [24,25]. Axisymmetric deformations with large deflections are allowed and formulated usually in terms of out-of-plane and in-plane equilibrium equations, geometric equations, and physical equations. During the establishment of these equations, some approximations or assumptions have to be considered, due to the strong nonlinearity of large deflection phenomena.

The first solution of circular membrane problems was presented originally by H. Hencky, who dealt analytically with the problem of axisymmetric deformation of a peripherally fixed circular membrane under uniformly distributed transverse loads and gave an analytical solution in the form of power series in 1915 [26]. Chien and Alekseev corrected a computational error in [26], a wrong value of a power series coefficient, in 1948 [27] and 1953 [28], respectively. This solution is often cited by related studies [5,15–19,29–31], and usually called the well-known Hencky's solution. During the derivation of the well-known Hencky's solution, in addition to the assumption of microdeformation of materials that is adopted in the establishment of physical equations, the assumption that the deflected

circular membrane only produces a relatively small rotation angle under uniformly distributed transverse loads is adopted in the establishment of out-of-plane and in-plane equilibrium equations and geometric equations. Therefore, later scholars have done a lot of improvement on well-known Hencky's solution [4,18,32]. The other two cases of transverse loading for peripherally fixed circular membranes are the concentrated loading at the central point of the circular membranes and the local uniform loading in the central portion of the circular membranes [15]. As for the normal loading of peripherally fixed circular membranes, the most typical example is gas pressure loading on membrane surfaces [24,25]. No matter how large the deflections are, the direction of action of gas pressure is always perpendicular to the deflected circular membranes under gas pressure, while the direction of transverse loading is always perpendicular to the undeflected circular membranes before loading.

　　　The first person to deal with annular membrane problems is S. A. Alekseev, an academician of the former Soviet Union Academy of Sciences, who algebraically solved the large deflection problem of an annular membrane whose outer edge is fixed and inner edge is connected centrally with a stiff, weightless, concentric, circular thin plate, where the external loads is applied at the central point of the stiff circular thin plate [20]. The algebraic solution, which was presented by Alekseev [20], is valid only when the Poisson's ratio of membranes is less than 1/3. Sun et al. [21] algebraically solved the problem considered originally by Alekseev [20] again and presented the algebraic solution suitable for Poisson's ratios less than, or equal to, or greater than 1/3. The Alekseev-type annular membrane structure, i.e., the one with an inner edge connected to a weightless, stiff, concentric, circular thin plate, was used for developing a membrane elastic deflection and parallel plate capacitor-based capacitive pressure sensor by Lian et al. [23], where the annular membrane and the circular thin plate are synchronously subjected to the uniformly distributed transverse loads, resulting in the parallel movement of the circular thin plate. Therefore, due to such a parallel movement the circular thin plate can be used to form a parallel plate capacitor and works as a movable electrode plate of the capacitor, thus achieving the capacitive pressure sensor mechanism of detecting pressure by measuring capacitance. The closed-form solution, which was given by Lian et al. [22], is not an algebraic solution, but in the form of power series. This closed-form solution is also the first power series solution for annular membrane problems. The annular membrane problems, if solved by using the power series method, are often more difficult to converge than circular membrane problems. This is because the stress or deflection variables can be expanded into a power series at the center of circular membranes (at the center of the domain of the independent variable), but in annular membrane problems, the stress or deflection variable has to be expanded into a power series at a point on the annular membranes (not at the center of the domain of the independent variable). Therefore, annular membrane problems often converge more slowly than circular membrane problems. This limitation means that for an annular membrane problem, the convergence of its power series solution can only be tested after the convergence of its undetermined constants has been confirmed. So, annular membrane problems, if solved by using power series method, are often much more complex than circular membrane problems.

　　　In this paper, we will deal with a plate/membrane contact problem, in which an initially flat, peripherally fixed circular membrane, which elastically deflects under uniformly distributed transverse loads, comes into contact with a concentric circular rigid flat plate that keeps a certain parallel gap from the initially flat circular membrane. Before touching the rigid plate, the circular membrane freely deflects, which is a standard circular membrane problem, the well-known Hencky problem. After coming into contact with the rigid plate, the circular membrane undergoes two classes of axisymmetric deformation: one is out-of-plane axisymmetric deflection in the plate/membrane non-contact area (an annular area); the other is in-plane axisymmetric stretching with or without plate/membrane friction in the plate/membrane contact area (a circular area). The case with plate/membrane friction is less studied because of its complexity, while the frictionless case is relatively

more studied, such as the membrane/substrate delamination [5,6], adhesion [7,9,10], and capacitive pressure sensors [11–14], etc. It should be pointed out that there must be friction in the movement of a deflected circular membrane in contact with a rigid flat plate and the larger the contact area, the greater the friction. Therefore, the frictionless case is just an ideal case, and in practice is an approximation to relatively small friction. The plate/membrane friction can often be reduced, for example, by coating the rigid flat plate with a smooth substance, and this is where the studies on frictionless contact problems are of value. Earlier studies on frictionless contact problems often tended to use some strict approximations or assumptions, such as assumptions of equi-biaxial constant stress state and small rotation angle of membrane [33]. Wang et al. gave up the assumption of equi-biaxial constant stress state and presented a closed-form solution of this plate/membrane frictionless contact problem for the first time [34]. Lian et al. gave up the assumption of equi-biaxial constant stress state and analytically solved this plate/membrane frictionless contact problem again, where the assumption of small rotation angle of membrane was also given up during the establishment of the out-of-plane equilibrium equation [35]. In this paper, this plate/membrane frictionless contact problem is further solved analytically and a new and more refined closed-form solution is presented. The further and specific applications of this new and more refined closed-form solution are mainly the development of conductive membrane-based capacitive pressure sensors [36–39].

The assumptions used in the existing studies have been further given up in this study. Firstly, the assumption that the stress state is equi-biaxial and constant is completely given up during the derivation of the closed-form solution. Secondly, the assumption that the rotation angle of membrane is small enough is given up in the establishment of both the out-of-plane equilibrium equation and the geometric equations. In the following section, the problem under consideration is reformulated and is analytically solved in terms of the plate/membrane non-contact region and the plate/membrane contact region. In Section 3, some important issues are addressed, such as whether the power series solutions for stress and deflection converge, whether the new and more refined closed-form solution presented can return to a classical circular membrane solution when the plate/membrane contact area approaches zero, and how accurate the present closed-form solution is in comparison with the previous closed-form solution. Concluding remarks are given in Section 4.

2. Membrane Equations and Its Solution

As shown in Figure 1, an initially flat, peripherally fixed circular membrane with Young's modulus E, Poisson's ratio ν, thickness h, and radius a, which elastically deflects under uniformly distributed transverse loads q, comes into contact with a concentric circular frictionless rigid flat plate that keeps a certain parallel gap g from the initially flat circular membrane, resulting in a circular contact area with radius b. In Figure 1, the dash-dotted line represents the geometric middle plane of the initially flat circular membrane, o is the origin of the introduced cylindrical coordinate system (r, φ, w) and is located in the centroid of the geometric middle plane, r is the radial coordinate, φ is the angle coordinate (but is not given in Figure 1 due to the characteristic of axisymmetric deformation), w denotes the axial coordinate and also denotes the deflection (transversal displacement) of the circular membrane under loads q, the polar coordinate plane (r, φ) passes through the geometric middle plane.

The size of the uniformly-distributed transverse loads q that makes the circular membrane go from free deflection to confined deflection depends on the size of the gap g, and for a given gap g, can be determined by using a circular membrane solution, that is, before the circular membrane comes into contact with the rigid plate, its maximum deflection (i.e., the deflection at $r = 0$) under the loads q should be exactly equal to the given gap g. The value of the loads q, thus determined, corresponds to the lower limit of the pressure measurement range of touch mode capacitive pressure sensors [13,14]. After coming into contact with the rigid plate, the deflected circular membrane may be divided into two portions: one is an annular area without plate/membrane contact and the other is a circular area with

plate/membrane contact. In the plate/membrane non-contact area, the circular membrane undergoes the out-of-plane axisymmetric deflection, while in the plate/membrane frictionless contact area, it undergoes the in-plane axisymmetric stretching, a plane problem in the plane in which the rigid plate is located. On the connecting ring between the annular region and the circular region, the stresses, strains, and displacements should be continuous. Such a continuity may be used as definite solution conditions. For convenience, let us deal first with the annular portion of the deflected circular membrane, then with its circular portion. Throughout the derivation, it is assumed that the circular membrane always has a constant thickness h during its deflection, i.e., the change of membrane thickness is ignored.
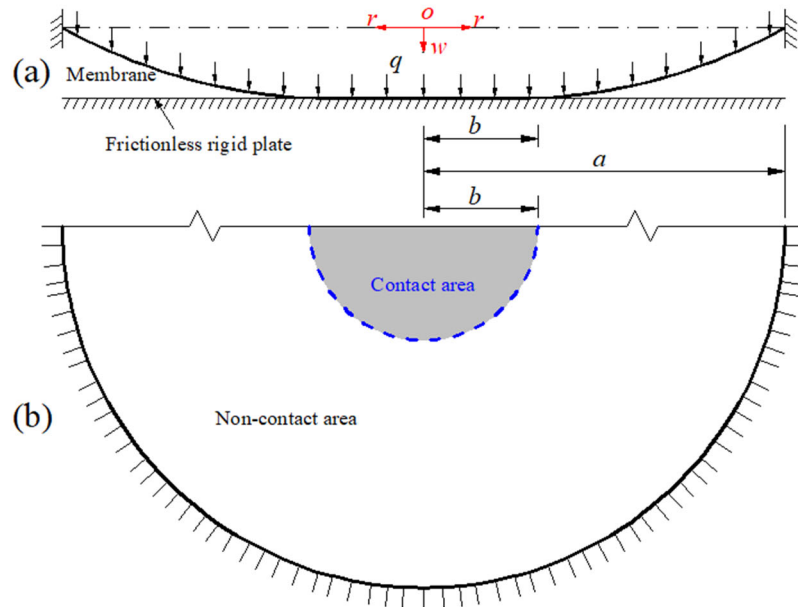
Figure 1. Sketch of a deflected circular membrane in contact with a frictionless rigid plate: (**a**) cross-section view along a diameter, and (**b**) half of plan view.

In the plate/membrane non-contact annular area, a free body of radius $b \leq r \leq a$ is taken from the annular portion of the deflected circular membrane to study its static problem of equilibrium, as shown in Figure 2, where σ_r is the radial stress (the mean stress over the cross section of the deflected membrane) and θ is the rotation angle of the deflected membrane, the meridional rotation angle.
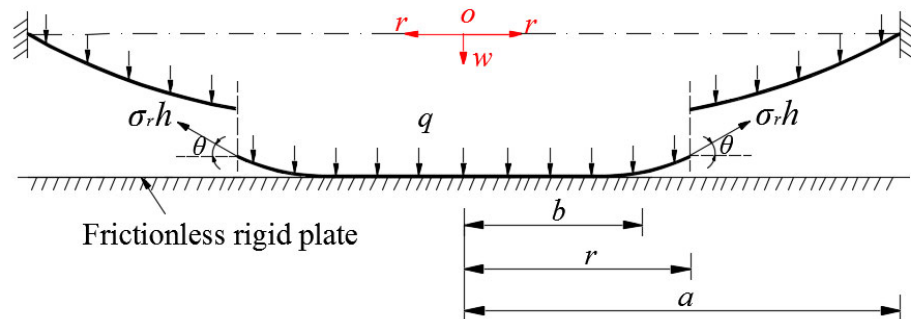
Figure 2. Equilibrium diagram of a free body with radius $b \leq r \leq a$.

In the vertical direction perpendicular to the initially flat circular membrane and the rigid plate (see Figure 2), there are three vertical forces: the total force $\pi r^2 q$ of the uniformly distributed transverse loads q within radius r, the total reaction force $\pi b^2 q$ from the rigid

plate, and the total vertical force $2\pi r \sigma_r h \sin\theta$ produced by the membrane force $\sigma_r h$, where $b \leq r \leq a$. Thus, the out-of-plane equilibrium condition is

$$\pi r^2 q - \pi b^2 q - 2\pi r \sigma_r h \sin\theta = 0. \tag{1}$$

If the deflection (transversal displacement) of the deflected circular membrane under the uniformly distributed transverse loads q is denoted by w, then

$$\sin\theta = 1/\sqrt{1 + 1/\tan^2\theta} = 1/\sqrt{1 + 1/(-dw/dr)^2}. \tag{2}$$

Substituting Equation (2) into Equation (1) one has

$$(r^2 - b^2)q\sqrt{1 + 1/(dw/dr)^2} = 2r\sigma_r h. \tag{3}$$

The in-plane equilibrium condition is the same as before

$$\frac{d}{dr}(r\sigma_r h) - \sigma_t h = 0, \tag{4}$$

where σ_t denotes circumferential stress. As for the relationships of the strain and displacement (the geometric equations), we here replace the previous geometric equation in [35] with a more accurate one in [18]

$$e_r = \left[\left(1 + \frac{du}{dr}\right)^2 + \left(\frac{dw}{dr}\right)^2\right]^{1/2} - 1 \tag{5}$$

and

$$e_t = \frac{u}{r}, \tag{6}$$

where e_r, e_t, and u denote the radial and circumferential strain, and radial displacement, respectively. During the derivation of Equation (5), the assumption of small rotation angle of membrane was given up, see reference [18] for details. Moreover, the circular membrane is still assumed to be linearly elastic, so the relationships between stress and strain satisfy the generalized Hooke's law

$$\sigma_r = \frac{E}{1 - v^2}(e_r + ve_t) \tag{7}$$

and

$$\sigma_t = \frac{E}{1 - v^2}(e_t + ve_r). \tag{8}$$

Substituting Equations (5) and (6) into Equations (7) and (8) yields

$$\sigma_r = \frac{E}{1 - v^2}\left\{\left[\left(1 + \frac{du}{dr}\right)^2 + \left(\frac{dw}{dr}\right)^2\right]^{1/2} - 1 + v\frac{u}{r}\right\} \tag{9}$$

and

$$\sigma_t = \frac{E}{1 - v^2}\left\{\frac{u}{r} + v\left[\left(1 + \frac{du}{dr}\right)^2 + \left(\frac{dw}{dr}\right)^2\right]^{1/2} - v\right\}. \tag{10}$$

By means of Equations (4), (9) and (10), one has

$$\frac{u}{r} = \frac{1}{E}(\sigma_t - v\sigma_r) = \frac{1}{E}\left[\frac{d}{dr}(r\sigma_r) - v\sigma_r\right]. \tag{11}$$

After substituting the u in Equation (11) into Equation (9), then the consistency equation may be written as

$$\left[\frac{1}{E}\sigma_r - \frac{v}{E}\frac{d}{dr}(r\sigma_r) + 1\right]^2 - \left\{\frac{1}{E}\frac{d}{dr}[r\frac{d}{dr}(r\sigma_r)] - \frac{v}{E}\frac{d}{dr}(r\sigma_r) + 1\right\}^2 - (\frac{dw}{dr})^2 = 0. \quad (12)$$

Therefore, the radial stress σ_r and deflection $w(r)$ within $b \leq r \leq a$ can be determined by simultaneously solving Equations (3) and (12). Their definite solution conditions are the boundary conditions at $r = a$ and the continuity conditions at $r = b$. However, the continuity conditions at $r = b$ can only be determined after the plane problem in the plate/membrane circular area is solved.

In the plate/membrane contact area with radius $0 \leq r \leq b$, the circular portion of the deflected circular membrane always undergoes the in-plane axisymmetric stretching in the plane in which the rigid plate is located. Obviously, for a plane problem the first derivative of the deflection $w(r)$ is always zero, i.e., $dw/dr = 0$. Therefore, Equations (5) and (6) give

$$e_r = \frac{du}{dr} \quad (13)$$

and

$$e_t = \frac{u}{r}. \quad (14)$$

Substituting Equations (13) and (14) into Equations (7) and (8) yields

$$\sigma_r = \frac{E}{1-v^2}(\frac{du}{dr} + v\frac{u}{r}) \quad (15)$$

and

$$\sigma_t = \frac{E}{1-v^2}(\frac{u}{r} + v\frac{du}{dr}). \quad (16)$$

Substituting Equations (15) and (16) into Equation (4), one has

$$r\frac{d^2u}{dr^2} + \frac{du}{dr} - \frac{u}{r} = 0. \quad (17)$$

Equation (17) satisfies the form of the Euler equation, therefore its general solution of Equation (17) may be written as

$$u(r) = C_1 r + \frac{C_2}{r}, \quad (18)$$

where C_1 and C_2 are two unknown constants. It is not difficult to understand that in order for the radial displacement u to be finite at $r = 0$, C_2 has to be equal to zero. If $u = u(b)$ at $r = b$, then $C_1 = u(b)/b$, thus

$$u(r) = \frac{u(b)}{b}r. \quad (19)$$

Therefore, substituting Equation (19) into Equations (13)–(16) yields

$$e_r = e_t = \frac{u(b)}{b} \quad (20)$$

and

$$\sigma_r = \sigma_t = \frac{E}{1-v}\frac{u(b)}{b} \quad (21)$$

Equations (20) and (21) show that the strain and stress are always uniformly distributed in the plate/membrane contact area within $0 \leq r \leq b$.

Now, let us proceed to the determination of the definite solution conditions in the plate/membrane non-contact annular area within $b \leq r \leq a$. The boundary conditions at $r = a$ are

$$w = 0 \text{ at } r = a, \tag{22}$$

and

$$u = 0 \text{ at } r = a. \tag{23}$$

The continuity conditions at $r = b$ are

$$w = g \text{ at } r = b, \tag{24}$$

$$\left(\frac{u}{r}\right)_A = \left(\frac{u}{r}\right)_B = \frac{u(b)}{b} \text{ at } r = b, \tag{25}$$

and

$$(\sigma_r)_A = (\sigma_r)_B = \frac{E}{1-\nu} \frac{u(b)}{b} \text{ at } r = b, \tag{26}$$

where $(\ )_A$ and $(\ )_B$ represent the values of various variables on two sides of the interconnecting circle with radius b, and the subscript A refers to the side of plate/membrane non-contact while the subscript B refers to the side of plate/membrane contact.

Let us introduce the following dimensionless variables

$$Q = \frac{qa}{Eh}, \ W = \frac{w}{a}, \ S_r = \frac{\sigma_r}{E}, \ S_t = \frac{\sigma_t}{E}, \ x = \frac{r}{a}, \ \alpha = \frac{b}{a}, \tag{27}$$

and transform Equations (3), (4), (12) and (22)–(26) into

$$[4x^2 S_r{}^2 - Q^2(x^2 - \alpha^2)^2]\left(\frac{\mathrm{d}W}{\mathrm{d}x}\right)^2 - Q^2(x^2 - \alpha^2)^2 = 0, \tag{28}$$

$$S_t = S_r + x\frac{\mathrm{d}S_r}{\mathrm{d}x}, \tag{29}$$

$$\left[S_r - \nu\frac{\mathrm{d}}{\mathrm{d}x}(xS_r) + 1\right]^2 - \left\{\frac{\mathrm{d}}{\mathrm{d}x}\left[x\frac{\mathrm{d}}{\mathrm{d}x}(xS_r)\right] - \nu\frac{\mathrm{d}}{\mathrm{d}x}(xS_r) + 1\right\}^2 - \left(\frac{\mathrm{d}W}{\mathrm{d}x}\right)^2 = 0, \tag{30}$$

$$W = 0 \text{ at } x = 1, \tag{31}$$

$$S_t - \nu S_r = 0 \text{ at } x = 1, \tag{32}$$

$$W = \frac{g}{a} \text{ at } x = \alpha, \tag{33}$$

$$(S_t - \nu S_r)_A = (S_t - \nu S_r)_B = \frac{u(b)}{b} \text{ at } x = \alpha \tag{34}$$

and

$$(S_r)_A = (S_r)_B = \frac{1}{1-\nu}\frac{u(b)}{b} \text{ at } x = \alpha. \tag{35}$$

It can be obtained by eliminating $(\mathrm{d}w/\mathrm{d}r)^2$ from Equations (28) and (30) that

$$[4x^2 S_r{}^2 - Q^2(x^2 - \alpha^2)^2]\left\{\left[S_r - \nu\frac{\mathrm{d}}{\mathrm{d}x}(xS_r) + 1\right]^2 - \left\{\frac{\mathrm{d}}{\mathrm{d}x}\left[x\frac{\mathrm{d}}{\mathrm{d}x}(xS_r)\right] - \nu\frac{\mathrm{d}}{\mathrm{d}x}(xS_r) + 1\right\}^2\right\} \\ - Q^2(x^2 - \alpha^2)^2 = 0 \tag{36}$$

Since both stress and deflection are finite in the region of $x \leq 1$ (i.e., $r \leq a$), S_r and W can be expanded as a power series of $x - (1 + \alpha)/2$. If letting $\beta = (1 + \alpha)/2$, then

$$S_r = \sum_{i=0}^{\infty} c_i(x - \beta)^i \tag{37}$$

and

$$W = \sum_{i=0}^{\infty} d_i(x - \beta)^i. \tag{38}$$

By substituting Equation (37) into Equation (36), the coefficients c_i ($i = 2, 3, 4, \ldots$) can be expressed as the polynomials of c_0, c_1, and α, which are listed in Appendix A. Then, substituting Equations (37) and (38) into Equation (28) or Equation (30), the coefficients d_i ($i = 1, 2, 3, \ldots$) can also be expressed as the polynomials of c_0, c_1, and α, which are listed in Appendix B.

The remaining three coefficients c_0, c_1, and d_0 are usually known as undetermined constants, while the dimensionless variable α ($\alpha = b/a$) also plays the role of an undetermined coefficient here. The c_0, c_1, α, and d_0 can be determined by using the boundary conditions and continuity conditions as follows. From Equation (38), Equations (31) and (33) give

$$\sum_{i=0}^{\infty} d_i(1 - \beta)^i = 0 \tag{39}$$

and

$$\sum_{i=0}^{\infty} d_i(\alpha - \beta)^i = \frac{g}{a}. \tag{40}$$

Equation (40) minus Equation (39) is

$$\sum_{i=1}^{\infty} d_i[(\alpha - \beta)^i - (1 - \beta)^i] = \frac{g}{a}. \tag{41}$$

From Equations (29) and (37), Equations (32), (34) and (35) yield

$$(1 - \nu)\sum_{i=0}^{\infty} c_i(1 - \beta)^i + \sum_{i=1}^{\infty} ic_i(1 - \beta)^{i-1} = 0, \tag{42}$$

$$(1 - \nu)\sum_{i=0}^{\infty} c_i(\alpha - \beta)^i + \alpha\sum_{i=1}^{\infty} ic_i(\alpha - \beta)^{i-1} = \frac{u(b)}{b} \tag{43}$$

and

$$\sum_{i=0}^{\infty} c_i(\alpha - \beta)^i = \frac{1}{1 - \nu}\frac{u(b)}{b}. \tag{44}$$

Eliminating the $u(b)/b$ from Equations (43) and (44), one has

$$\alpha\sum_{i=1}^{\infty} ic_i(\alpha - \beta)^{i-1} = 0. \tag{45}$$

For the given problem where a, h, E, ν, g, and q are known in advance, the undetermined constants c_0, c_1, and α can be determined by the simultaneous solutions of Equations (41), (42) and (45). Furthermore, with the known c_0, c_1, and α, the undetermined constant d_0 can be determined by Equation (39) or Equation (40). The problem dealt with here is thus solved. In addition, from Equations (27), (37) and (38), the expressions for dimensional stress and deflection may finally be written as

$$\sigma_r = E\sum_{i=0}^{\infty} c_i\left(\frac{r}{a} - \frac{b}{2a} - \frac{1}{2}\right)^i \tag{46}$$

and

$$w = a\sum_{i=0}^{\infty} d_i\left(\frac{r}{a} - \frac{b}{2a} - \frac{1}{2}\right)^i. \tag{47}$$

3. Results and Discussion

3.1. Convergence of the Closed-Form Solution Obtained in Section 2

As can be seen from Appendices A and B, the expressions for the power series coefficients c_i and d_i are too complex to discuss convergence in terms of general solutions, so the convergence can only be discussed in terms of the particular solutions for stress and deflection. To this end, a numerical example is conducted; an initially flat, peripherally fixed circular membrane with radius a = 100 mm, thickness h = 1 mm, Young's modulus E = 7.84 MPa, Poisson's ratio v = 0.47, which keeps a parallel gap of g = 10 mm from a concentric circular rigid flat plate, is subjected to a uniformly distributed transverse loads of q = 0.0018 MPa. The uniformly distributed transverse loads q that makes the circular membrane just touch the concentric circular rigid flat plate is about q = 0.00035215 MPa, that is, the uniformly distributed transverse loads q that makes the circular membrane just produces the maximum deflection (i.e., the deflection at r = 0) of g = 10 mm is q = 0.00035215 MPa, which is calculated by using the circular membrane solution given in reference [18]. Therefore, the circular membrane under q = 0.0018 MPa must have formed a frictionless contact area of radius b with the concentric circular rigid flat plate.

Therefore, the solution of the unknown contact radius b (or the undetermined constant $\alpha = b/a$) and the undetermined constants c_0, c_1, and d_0 are the main tasks of the following numerical calculations. To this end, let us truncate the infinite power series in Equations (39), (41), (42) and (45) to the nth terms, that is,

$$\sum_{i=0}^{n} d_i(1-\beta)^i = 0, \tag{48}$$

$$\sum_{i=1}^{n} d_i[(\alpha-\beta)^i - (1-\beta)^i] = \frac{g}{a}, \tag{49}$$

$$(1-v)\sum_{i=0}^{n} c_i(1-\beta)^i + \sum_{i=1}^{n} ic_i(1-\beta)^{i-1} = 0 \tag{50}$$

and

$$\alpha\sum_{i=1}^{n} ic_i(\alpha-\beta)^{i-1} = 0. \tag{51}$$

The parameter n in Equations (48)–(51) can first take 2 to start the numerical calculations of the undetermined constants c_0, c_1, α, and d_0, then take 3, 4, ... , until 14. The results of numerical calculation of c_0, c_1, α, and d_0 are listed in Table 1. The variations of c_0, c_1, α, and d_0 with n are shown in Figure 3, where the dash-dotted lines show the convergence trends of the data points of even terms (n = 2, 4, 6 ...) and the dashed lines show that of odd terms (n = 3, 5, 7 ...). From Figure 3, it can be seen that the data sequences for c_0, c_1, α, and d_0 have a very good convergence trend and show a very good saturation when the parameter n takes 10 or 11, which indicates that the undetermined constants c_0, c_1, α and d_0 when q = 0.0018 MPa can take the numerical values calculated by n = 10 or 11.

Table 1. The numerical calculation results of the undetermined constants c_0, c_1, α, and d_0, where $q = 1.8 \times 10^{-3}$ MPa.

n	α	c_0	c_1	d_0
2	0.550304	0.020333	−0.004946	0.074512
3	0.506556	0.023992	−0.002929	0.073227
4	0.511924	0.023563	−0.002825	0.074291
5	0.508790	0.023837	−0.002708	0.074196
6	0.506674	0.024005	−0.002746	0.074260

Table 1. *Cont.*

n	α	c_0	c_1	d_0
7	0.507546	0.023943	-0.002764	0.074264
8	0.506410	0.024033	-0.002784	0.074266
9	0.506772	0.024006	-0.002793	0.074270
10	0.506318	0.024039	-0.002830	0.074262
11	0.506448	0.024046	-0.002850	0.074265
12	0.506230	0.024045	-0.002855	0.074264
13	0.506210	0.024047	-0.002860	0.074263
14	0.506210	0.024047	-0.002860	0.074263

(**a**)

(**b**)

(**c**)

Figure 3. *Cont.*

(**d**)
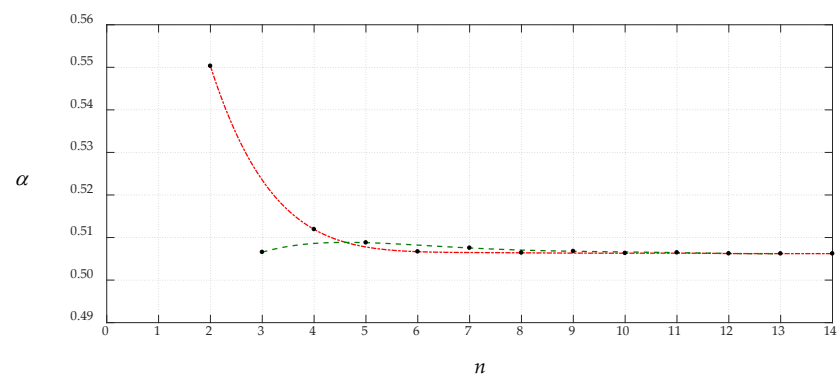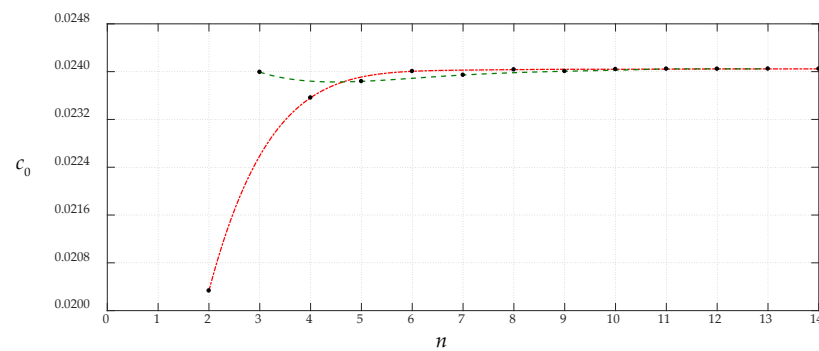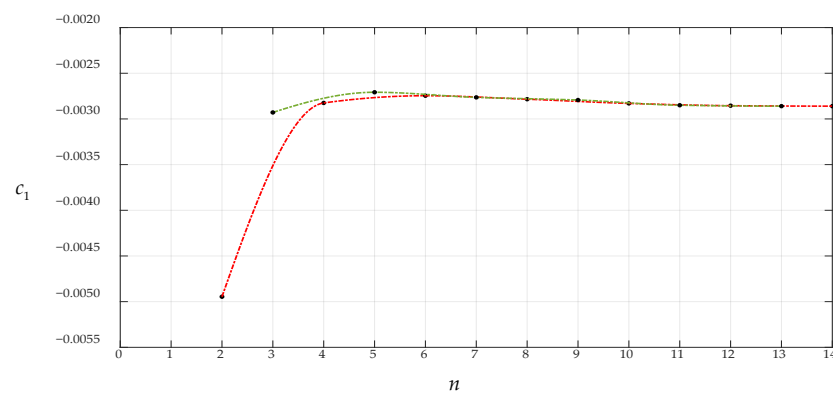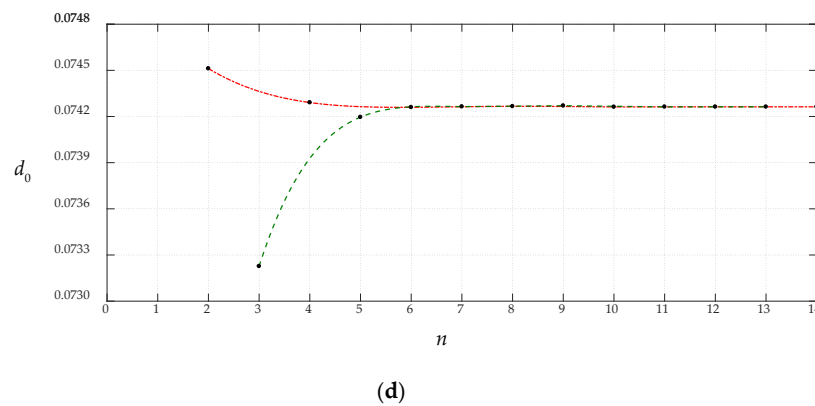
Figure 3. The variations of c_0, c_1, α, and d_0 with terms n, where the dash-dotted lines show the convergence trend of the data points of even terms ($n = 2, 4, 6 \ldots$), the dashed lines show that of odd terms ($n = 3, 5, 7 \ldots$), and $q = 1.8 \times 10^{-3}$ MPa: (**a**) the variation of α with n, (**b**) the variation of c_0 with n, (**c**) the variation of c_1 with n, and (**d**) the variation of d_0 with n.

It can be seen from Figure 3 that the undetermined constants c_0, c_1, α, and d_0 when $q = 0.0018$ MPa should take the numerical values calculated by $n \geq 10$ or 11. Here, the numerical values at $n = 14$ in Table 1 are taken as the convergence values of the undetermined constants c_0, c_1, α, and d_0 when $q = 0.0018$ MPa to investigate the convergence of the power series particular solutions of stress and deflection, that is, $c_0 = 0.024047$, $c_1 = -0.002860$, $\alpha = 0.506210$, and $d_0 = 0.074263$. Obviously, if the particular solutions of stress and deflection converge at the two ends of the closed interval [0.506210, 1], then they converge in the whole closed interval [0.506210, 1]. The numerical calculation results of stress and deflection at the two ends of the closed interval [0.506210, 1] are listed in Table 2, which are calculated by using Equations (37) and (38), where the coefficients c_i ($i = 2, 3, 4, \ldots$) and d_i ($i = 1, 2, 3, \ldots$) are listed in Appendices A and B, and $\beta = (1 + \alpha)/2 = (1 + 0.506210)/2 = 0.753105$. Figures 4 and 5 show the variations of $c_i(1 - \beta)^i$, $c_i(\alpha - \beta)^i$, $d_i(1 - \beta)^i$ and $d_i(\alpha - \beta)^i$ with i, indicating that the particular solutions of stress and deflection converge very well at the two ends of the closed interval [0.506210, 1]. Therefore, the particular solutions of stress and deflection converge in the closed interval [0.506210, 1].

Table 2. The numerical calculation results of $c_i(\alpha - \beta)^i$, $d_i(\alpha - \beta)^i$, $c_i(1 - \beta)^i$ and $d_i(1 - \beta)^i$, where $q = 1.8 \times 10^{-3}$ MPa.

i	$c_i(\alpha - \beta)^i$	$d_i(\alpha - \beta)^i$	$c_i(1 - \beta)^i$	$d_i(1 - \beta)^i$
0	0.024047	0.074263	0.024047	0.074263
1	7.0612×10^{-4}	4.8669×10^{-3}	-7.0612×10^{-4}	-4.8669×10^{-3}
2	3.3694×10^{-4}	-2.1851×10^{-3}	3.3694×10^{-4}	-2.1851×10^{-3}
3	1.5232×10^{-4}	-1.2296×10^{-4}	-1.5232×10^{-4}	1.2296×10^{-4}
4	6.2122×10^{-5}	-2.5098×10^{-5}	6.2122×10^{-5}	-2.5098×10^{-5}
5	2.4282×10^{-5}	-4.6319×10^{-6}	-2.4282×10^{-5}	4.6319×10^{-6}
6	9.2305×10^{-6}	-7.3651×10^{-7}	9.2305×10^{-6}	-7.3651×10^{-7}
7	3.4402×10^{-6}	-5.7636×10^{-8}	-3.4402×10^{-6}	5.7636×10^{-8}
8	1.2634×10^{-6}	2.4572×10^{-8}	1.2634×10^{-6}	2.4572×10^{-8}
9	4.5869×10^{-7}	1.8160×10^{-8}	-4.5869×10^{-7}	-1.8160×10^{-8}

Table 2. *Cont.*

i	$c_i(\alpha - \beta)^i$	$d_i(\alpha - \beta)^i$	$c_i(1 - \beta)^i$	$d_i(1 - \beta)^i$
10	1.6500×10^{-7}	8.1933×10^{-9}	1.6500×10^{-7}	8.1933×10^{-9}
11	5.8903×10^{-8}	3.1359×10^{-9}	-5.8903×10^{-8}	-3.1359×10^{-9}
12	2.0894×10^{-8}	1.0994×10^{-9}	2.0894×10^{-8}	1.0994×10^{-9}
13	7.3714×10^{-9}	3.6352×10^{-10}	-7.3714×10^{-9}	-3.6352×10^{-10}
14	2.5883×10^{-9}	1.1475×10^{-10}	2.5883×10^{-9}	1.1475×10^{-10}
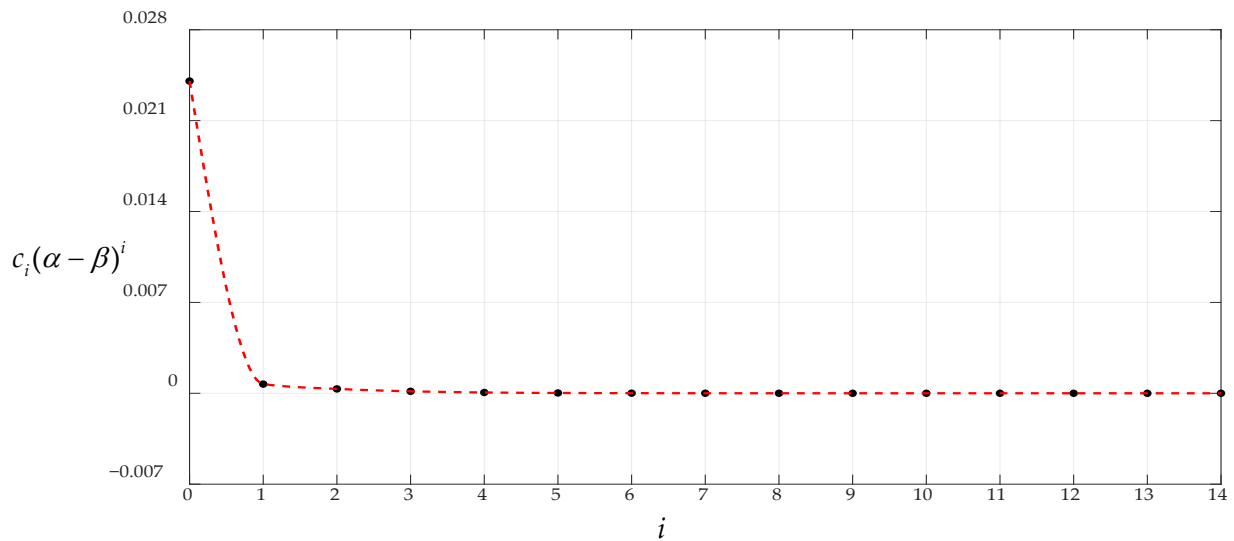
(**a**)
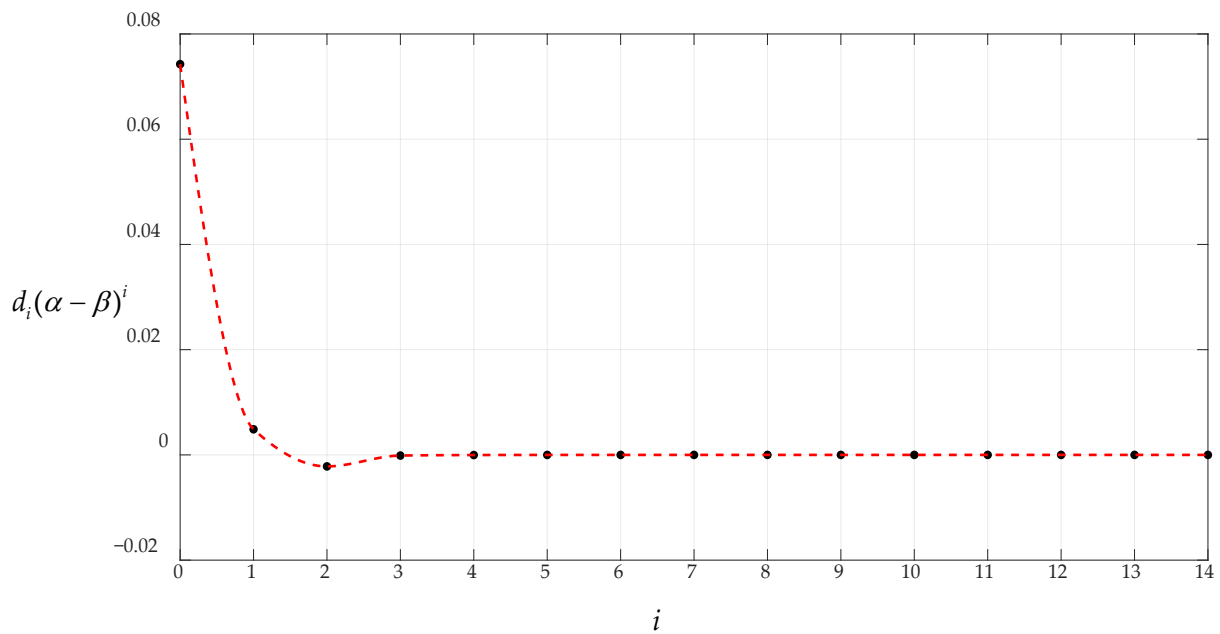
(**b**)

Figure 4. The variations of $c_i(\alpha - \beta)^i$ and $d_i(\alpha - \beta)^i$ with terms i, where $q = 1.8 \times 10^{-3}$ MPa: (**a**) the variation of $c_i(\alpha - \beta)^i$ with i, and (**b**) the variation of $d_i(\alpha - \beta)^i$ with i.

(a)

(b)
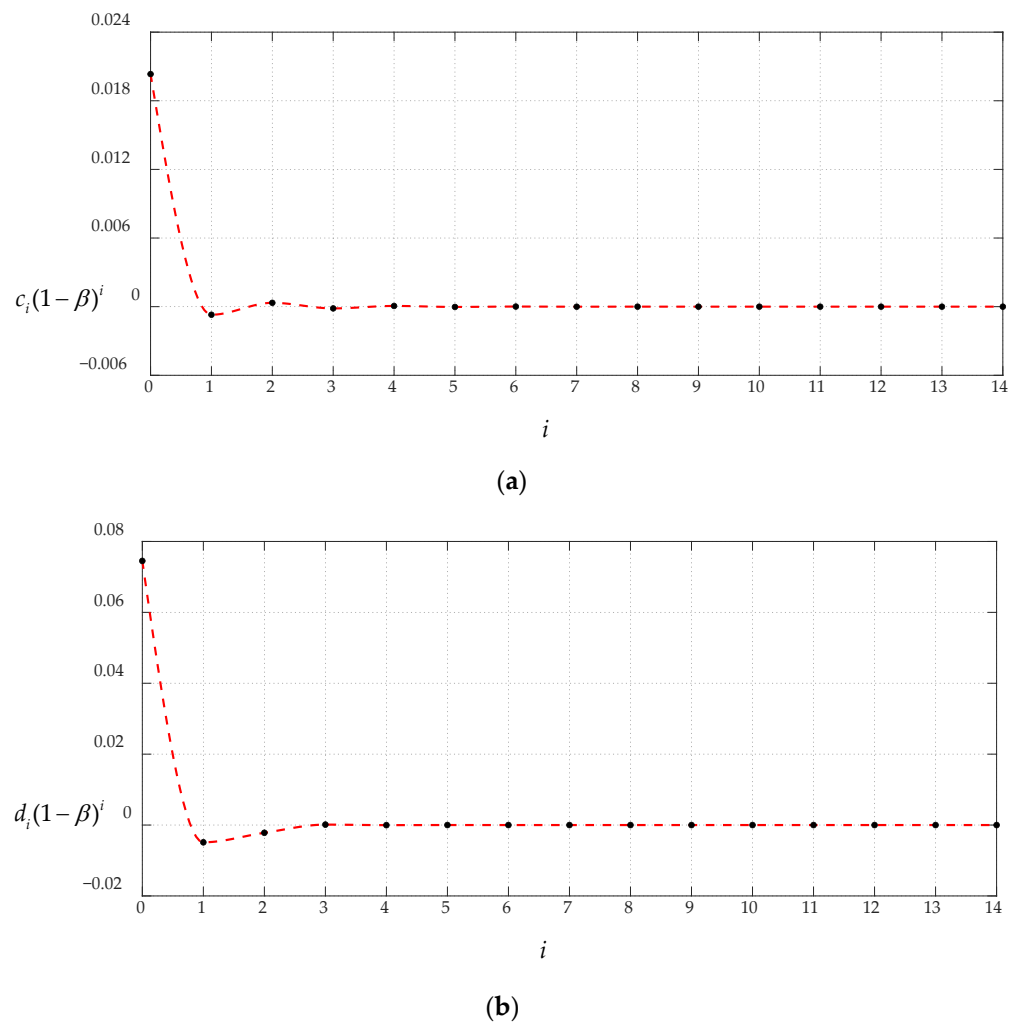
Figure 5. The variations of $c_i(1 - \beta)^i$ and $d_i(1 - \beta)^i$ with terms i, where $q = 1.8 \times 10^{-3}$ MPa: (**a**) the variation of $c_i(1 - \beta)^i$ with i, and (**b**) the variation of $d_i(1 - \beta)^i$ with i.

Table 3 shows the results of numerical calculation of c_0, c_1, α, and d_0 when $q = 1.725 \times 10^{-6}$ MPa. The variations of c_0, c_1, α, and d_0 with n are shown in Figure 6, where the dash-dotted lines show the convergence trends of the data points of even terms ($n = 2, 4, 6 \ldots$) and the dashed lines show that of odd terms ($n = 3, 5, 7 \ldots$). From Figure 6, it can be seen that the data sequences for c_0, c_1, α, and d_0 have a very good convergence trend and show a very good saturation when the parameter n takes 9 or 10, which indicates that the undetermined constants c_0, c_1, α, and d_0 when $q = 1.725 \times 10^{-6}$ MPa can take the numerical values calculated by $n = 9$ or 10. By comparing Figures 3 and 6, it can be seen that the convergence of the undetermined constants c_0, c_1, α, and d_0 becomes better when the loads q is reduced from 1.8×10^{-3} MPa to 1.725×10^{-6} MPa.

Table 3. The numerical calculation results of the undetermined constants c_0, c_1, α, and d_0, where $q = 1.725 \times 10^{-6}$ MPa.

n	α	c_0	c_1	d_0
2	0.538654	1.9856×10^{-4}	-4.8200×10^{-5}	7.3324×10^{-3}
3	0.489766	2.3466×10^{-4}	-3.1514×10^{-5}	7.2671×10^{-3}
4	0.501960	2.2515×10^{-4}	-2.9399×10^{-5}	7.3553×10^{-3}

Table 3. *Cont.*

n	α	c_0	c_1	d_0
5	0.497930	2.2814×10^{-4}	-2.8463×10^{-5}	7.3522×10^{-3}
6	0.496600	2.2917×10^{-4}	-2.8560×10^{-5}	7.3556×10^{-3}
7	0.497174	2.2817×10^{-4}	-2.8024×10^{-5}	7.3549×10^{-3}
8	0.496810	2.2905×10^{-4}	-2.8150×10^{-5}	7.3554×10^{-3}
9	0.496670	2.2880×10^{-4}	-2.7950×10^{-5}	7.3553×10^{-3}
10	0.496704	2.2885×10^{-4}	-2.8010×10^{-5}	7.3554×10^{-3}
11	0.496710	2.2886×10^{-4}	-2.7980×10^{-5}	7.3553×10^{-3}
12	0.496708	2.2885×10^{-4}	-2.7990×10^{-5}	7.3554×10^{-3}
13	0.496708	2.2886×10^{-4}	-2.7980×10^{-5}	7.3553×10^{-3}
14	0.496708	2.2885×10^{-4}	-2.7990×10^{-5}	7.3554×10^{-3}

(**a**)

(**b**)

(**c**)

Figure 6. *Cont.*

(**d**)
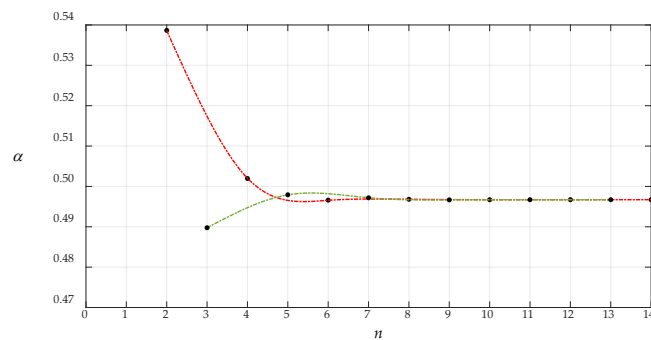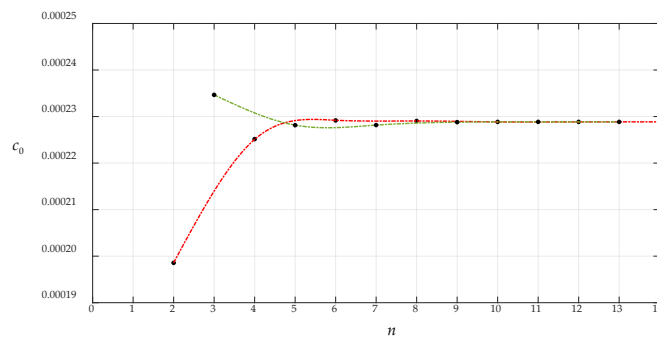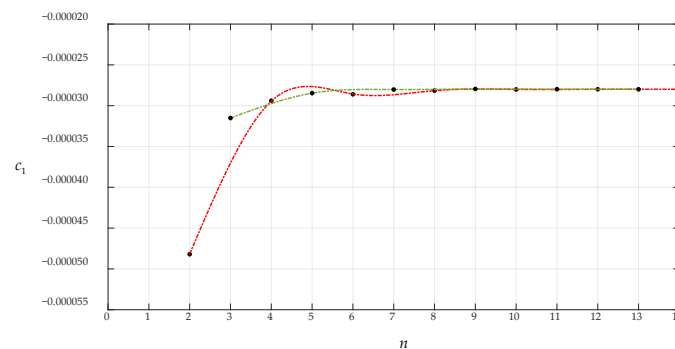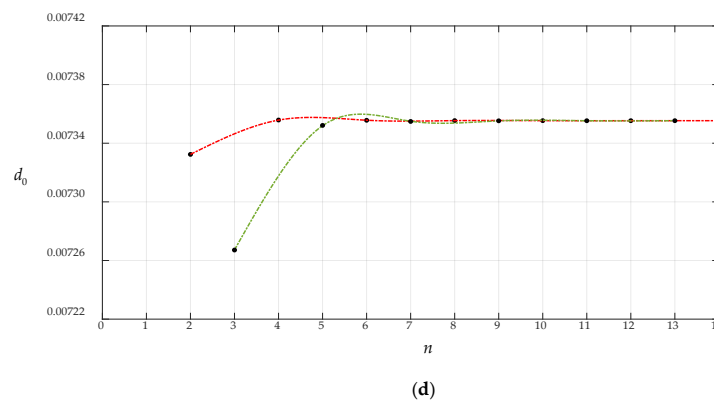
Figure 6. The variations of c_0, c_1, α, and d_0 with terms n, where the dash-dotted lines show the convergence trend of the data points of even terms (n = 2, 4, 6 . . .), the dashed lines show that of odd terms (n = 3, 5, 7 . . .), and where $q = 1.725 \times 10^{-6}$ MPa: (**a**) the variation of α with n, (**b**) the variation of c_0 with n, (**c**) the variation of c_1 with n, and (**d**) the variation of d_0 with n.

It can be seen from Figure 6 that the undetermined constants c_0, c_1, α, and d_0 when $q = 1.725 \times 10^{-6}$ MPa should take the numerical values calculated by $n \geq 9$ or 10. Here, the numerical values at n = 14 in Table 3 are taken as the convergence values of the undetermined constants c_0, c_1, α, and d_0 when $q = 1.725 \times 10^{-6}$ MPa to investigate the convergence of the power series particular solutions of stress and deflection, that is, $c_0 = 2.2885 \times 10^{-4}$, $c_1 = -2.7990 \times 10^{-5}$, $\alpha = 0.496708$, and $d_0 = 7.3554 \times 10^{-3}$. Table 4 shows the numerical calculation results of stress and deflection at the two ends of the closed interval [0.496708, 1]. Figures 7 and 8 show the variations of $c_i(1 - \beta)^i$, $c_i(\alpha - \beta)^i$, $d_i(1 - \beta)^i$ and $d_i(\alpha - \beta)^i$ with i, indicating that the particular solutions of stress and deflection converge very well at the two ends of the closed interval [0.496708, 1]. Therefore, the particular solutions of stress and deflection also converge in the closed interval [0.496708, 1].

Table 4. The numerical calculation results of $c_i(\alpha - \beta)^i$, $d_i(\alpha - \beta)^i$, $c_i(1 - \beta)^i$ and $d_i(1 - \beta)^i$, when $q = 1.725 \times 10^{-6}$ MPa.

| i	$c_i(\alpha - \beta)^i$	$d_i(\alpha - \beta)^i$	$c_i(1 - \beta)^i$	$d_i(1 - \beta)^i$
0	2.2885×10^{-4}	7.3554×10^{-3}	2.2885×10^{-4}	7.3554×10^{-3}
1	7.0436×10^{-6}	5.0657×10^{-3}	-7.0436×10^{-6}	-5.0657×10^{-3}
2	-7.9021×10^{-6}	-2.2719×10^{-3}	-7.9021×10^{-6}	-2.2720×10^{-3}
3	2.0236×10^{-6}	-4.4641×10^{-5}	-2.0236×10^{-6}	4.4641×10^{-5}
4	3.5072×10^{-7}	-8.7459×10^{-5}	3.5072×10^{-7}	-8.7459×10^{-5}
5	1.4484×10^{-7}	-2.4508×10^{-6}	-1.4484×10^{-7}	2.4508×10^{-6}
6	-3.3957×10^{-8}	-4.0025×10^{-6}	-3.3958×10^{-8}	-4.0025×10^{-6}
7	-3.4012×10^{-8}	2.1156×10^{-7}	3.4012×10^{-8}	-2.1156×10^{-7}
8	-2.3883×10^{-8}	-2.5281×10^{-7}	-2.3883×10^{-8}	-2.5281×10^{-7}
9	-1.1568×10^{-8}	-2.8124×10^{-8}	1.1568×10^{-8}	2.8124×10^{-8}
10	-5.3121×10^{-9}	-5.4178×10^{-8}	-5.3121×10^{-9}	-5.4178×10^{-8}
11	-2.2077×10^{-9}	-1.9538×10^{-8}	2.2077×10^{-9}	1.9538×10^{-8}
12	-9.0917×10^{-10}	-1.1500×10^{-8}	-9.0917×10^{-10}	-1.1499×10^{-8}
13	-3.6399×10^{-10}	-4.1701×10^{-9}	3.6399×10^{-10}	4.1702×10^{-9}
14	-1.4728×10^{-10}	-1.8333×10^{-9}	-1.4728×10^{-10}	1.8333×10^{-9}
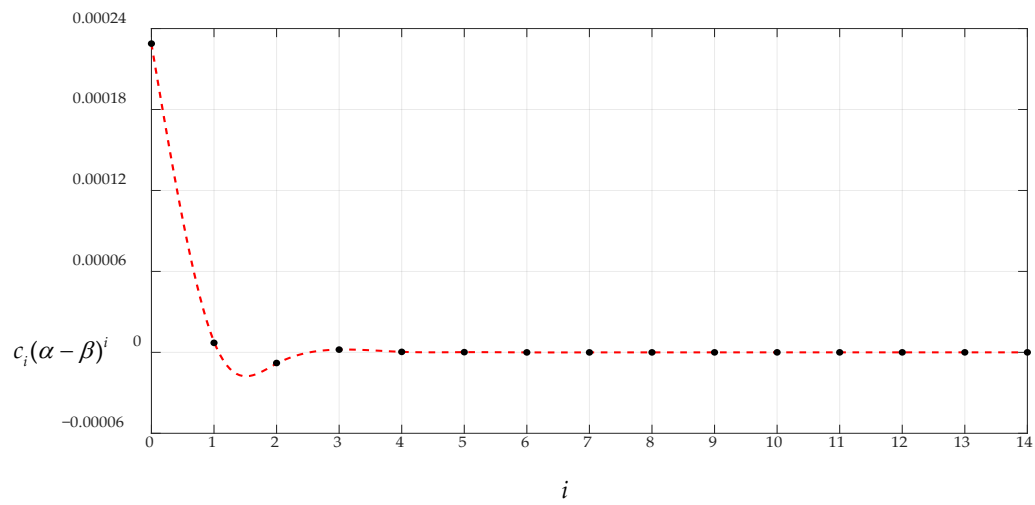
(**a**)
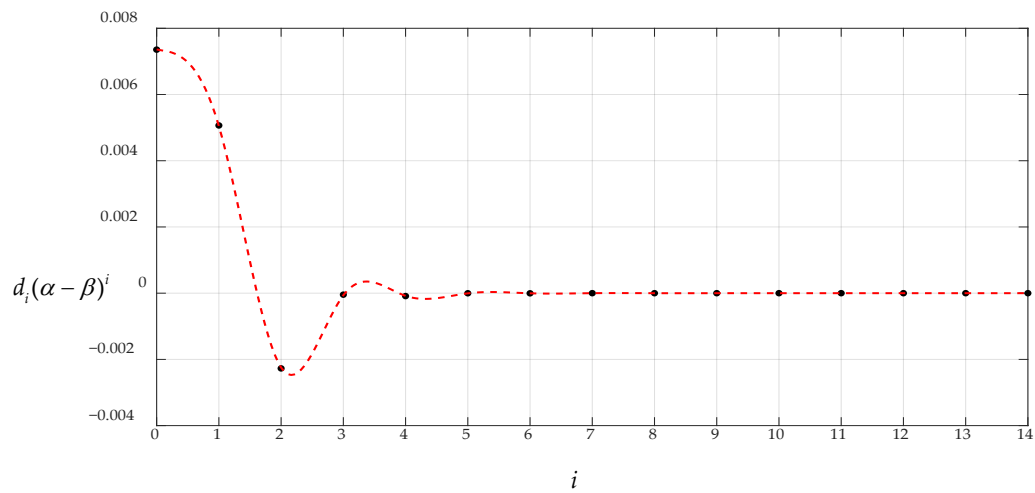
(**b**)

Figure 7. The variations of $c_i(\alpha - \beta)^i$ and $d_i(\alpha - \beta)^i$ with terms i, where $q = 1.725 \times 10^{-6}$ MPa: (**a**) the variation of $c_i(\alpha - \beta)^i$ with i, and (**b**) the variation of $d_i(\alpha - \beta)^i$ with i.
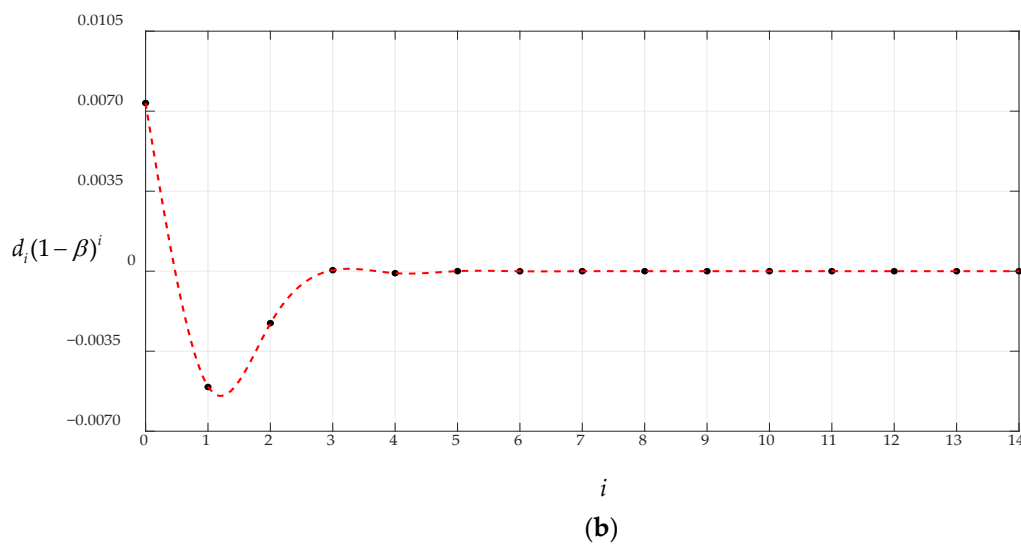

(**a**)

Figure 8. *Cont.*

(b)
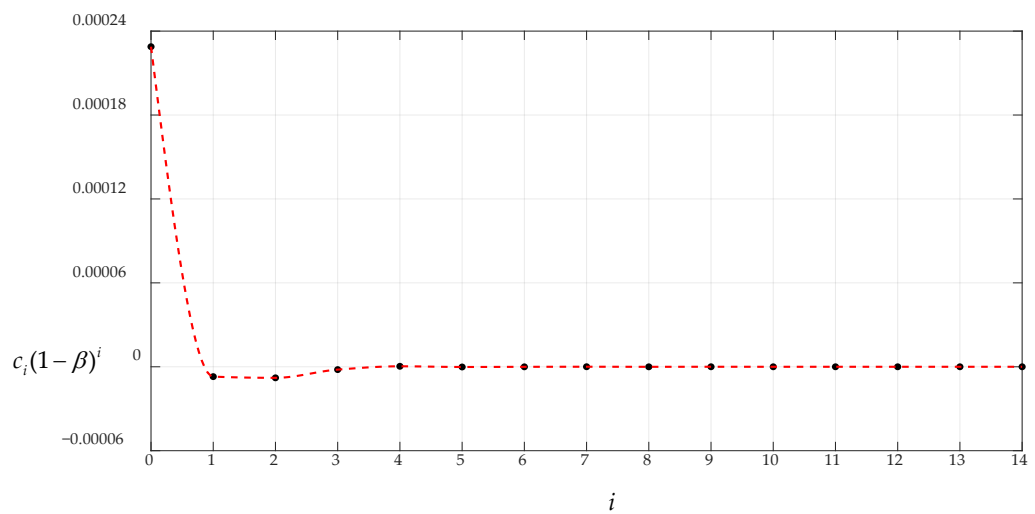
Figure 8. The variations of $c_i(1 - \beta)^i$ and $d_i(1 - \beta)^i$ with terms i, where $q = 1.725 \times 10^{-6}$ MPa: (**a**) the variation of $c_i(1 - \beta)^i$ with i, and (**b**) the variation of $d_i(1 - \beta)^i$ with i.

3.2. Regression of the Solution after Contact to the Solution before Contact

In this section, we shall prove that the closed-form solution of the plate/membrane contact problem, which is given in Section 2, can return to the closed-form solution of circular membrane problems when the plate/membrane contact area approaches zero. We are going to prove it from two perspectives. One is to fix the size of the parallel gap g between the initially flat circular membrane and the frictionless rigid plate and change the size of the uniformly-distributed transverse loads q, to observe whether the shape of the deflection curve of the circular membrane in contact with the frictionless rigid plate can gradually approach the shape of the deflection curve of a circular membrane as the uniformly-distributed transverse loads q gradually decreases (the contact radius b gradually approaches zero). The second is to fix the size of the uniformly distributed transverse loads q and change the size of the parallel gap g, to observe whether the shape of the deflection curve of the circular membrane in contact with the frictionless rigid plate can gradually approach the shape of the deflection curve of a circular membrane as the parallel gap g gradually increases (the contact radius b gradually approaches zero).

To this end, an initially flat, peripherally fixed circular membrane with radius $a = 100$ mm, thickness $h = 1$ mm, Young's modulus $E = 7.84$ MPa, Poisson's ratio $v = 0.47$ is used for numerical calculations. In the first case, the frictionless rigid plate keeps a parallel gap of $g = 10$ mm from the initially flat circular membrane, and the uniformly distributed transverse loads q decreases from 1.8×10^{-3} MPa to 8.3843×10^{-4} MPa, then to 4.9431×10^{-4} MPa, and finally to 3.5216×10^{-4} MPa, while the corresponding contact radius b decreases from 50.72 mm to 35.00 mm, then to 20.00 mm, and finally to 0.01 mm, as shown in Figure 9. In the second case, the circular membrane is always subjected to the uniformly distributed transverse loads of $q = 3.5216 \times 10^{-4}$ MPa, and the parallel gap g between plate and membrane increases from 2 mm to 5 mm, then to 8 mm, then to 9.5 mm, and finally to 10 mm, while the corresponding contact radius b decreases from 83.40 mm to 57.71 mm, then to 29.90 mm, then to 12.58 mm, and finally to 0.01 mm, as shown in Figure 10. In Figures 9 and 10, the "Solution after contact" refers to the closed-form solution of plate/membrane contact problems which is given in Section 2, and the "Solution before contact" refers to the closed-form solution of circular membrane problems which was given in reference [18]. When the circular membrane is freely deflecting under the action of $q = 3.5216 \times 10^{-4}$ MPa, as shown in Figures 9 and 10, the corresponding undetermined constants are $c_0 = 0.100003871$ and $b_0 = 0.01251267355$, and the corresponding deflection expression is $w(r) = 10.0003871 - 0.8990541942 \times 10^{-3} r^2 - 7.938281317 \times 10^{-9} r^4 - 1.593670115 \times 10^{-13} r^6 - 4.019220774 \times 10^{-18} r^8 - 1.136680135 \times 10^{-22} r^{10} - 3.448101848$

$\times\ 10^{-27}r^{12} - 1.097048702 \times 10^{-31}r^{14} - 3.613480399 \times 10^{-36}r^{16} - 1.222061190 \times 10^{-40}r^{18}$
$- 4.219889721 \times 10^{-45}r^{20} - 1.481932061 \times 10^{-49}r^{22} - 5.277237532 \times 10^{-54}r^{24}$, which are calculated by using the "Solution before contact".
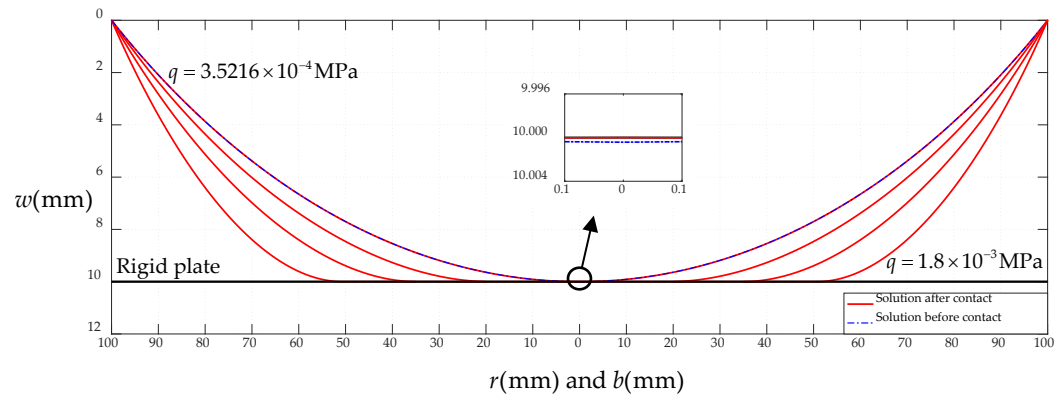
Figure 9. Sketch from contact deflection to free deflection, where the parallel gap g keeps 10 mm and the loads q decreases from 1.8×10^{-3} MPa to 8.3843×10^{-4} MPa, then to 4.9431×10^{-4} MPa, and finally to 3.5216×10^{-4} MPa.
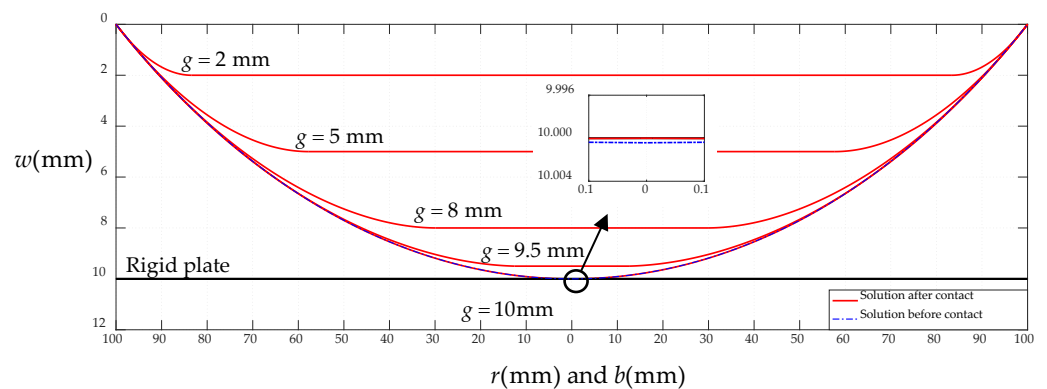
Figure 10. Sketch from contact deflection to free deflection, where the loads q keeps 3.5216×10^{-4} MPa and the parallel gap g increases from 2 mm to 5 mm, then to 8 mm, then to 9.5 mm, and finally to 10 mm.

It can be seen from Figures 9 and 10 that whether the parallel gap g is fixed and the loads q is changed or the loads q is fixed and the parallel gap g is changed, the shape of the deflection curve of the circular membrane in contact with the frictionless rigid plate can gradually approach the shape of the deflection curve of the circular membrane. This means, to some extent, that the closed-form solution given in Section 2 is basically reliable without derivation errors.

3.3. Comparison between Present Solution and Previous Solution

In this section, the circular membrane of radius $a = 100$ mm, thickness $h = 1$ mm, Young's modulus $E = 7.84$ MPa, Poisson's ratio $v = 0.47$, which is used in Section 3.2, is still used for numerical calculations in order to quantitatively analyze the improvement effect of the closed-form solution given in Section 2, that is, the quantitative difference between the present closed-form solution given in Section 2 and the previous closed-form solutions given in references [33–35]. The circular membrane is still initially flat and peripherally fixed, keeps the parallel gap of $g = 1$ mm, 5 mm, and 10 mm from the frictionless rigid plate, and is subjected to the loads $q = 1.725 \times 10^{-6}$ MPa, 2.2×10^{-4} MPa and 1.8×10^{-3} MPa (corresponding to $g = 1$ mm, 5 mm, and 10 mm, respectively). The contact radius b between plate/membrane under different parallel gap g and the maximum stress σ_m of the circular membrane under different loads q are list in Table 5. The distributions of deflection and

stress of the circular membrane under different loads q are shown in Figures 11 and 12. In Table 5 and Figures 11 and 12, the "Solution 1" refers to the results obtained by using the closed-form solution given in Section 2, the "Solution 2" refers to the results by using the closed-form solution given in reference [35], the "Solution 3" refers to the results by using the closed-form solution given in reference [34], and the "Solution 4" refers to the results by using the closed-form solution given in reference [33].

Table 5. The contact radius b and maximum stress σ_m under different loads q.

q (MPa)	g (mm)	b (mm)				σ_m (MPa)			
		Solution 1	Solution 2	Solution 3	Solution 4	Solution 1	Solution 2	Solution 3	Solution 4
1.725×10^{-6}	1	49.66	47.97	47.01	46.66	1.82×10^{-3}	1.75×10^{-3}	1.67×10^{-3}	1.66×10^{-3}
2.2×10^{-4}	5	50.12	41.47	36.72	34.87	4.60×10^{-2}	3.88×10^{-2}	3.57×10^{-2}	2.96×10^{-2}
1.8×10^{-3}	10	50.72	37.55	28.34	23.04	1.90×10^{-1}	1.46×10^{-1}	1.26×10^{-1}	9.61×10^{-2}
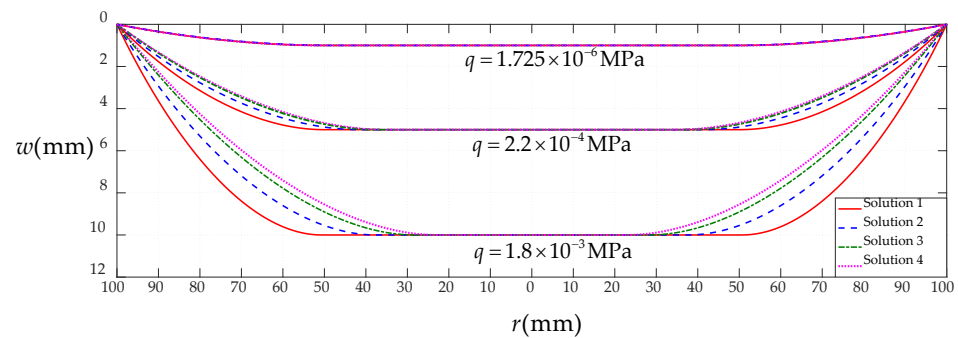
Figure 11. The variations of deflection w with radial coordinate r.
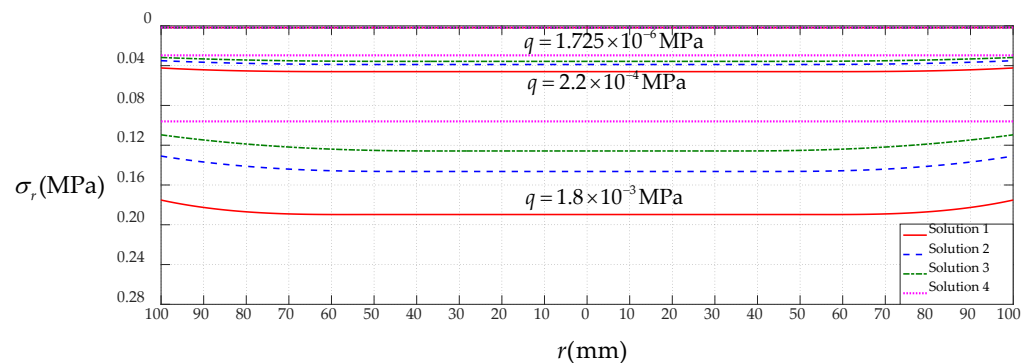
Figure 12. The variations of radial stress σ_r with radial coordinate r.

It can be calculated from Table 5 that for the contact radius b, the relative error of Solution 2 to Solution 1 is about 3.52% for $q = 1.725 \times 10^{-6}$ MPa, 20.86% for $q = 2.2 \times 10^{-4}$ MPa and 35.07% for $q = 1.8 \times 10^{-3}$ MPa, the relative error of Solution 3 to Solution 1 is about 5.34% for $q = 1.725 \times 10^{-6}$ MPa, 26.74% for $q = 2.2 \times 10^{-4}$ MPa and 44.12% for $q = 1.8 \times 10^{-3}$ MPa, and the relative error of Solution 4 to Solution 1 is about 6.04% for $q = 1.725 \times 10^{-6}$ MPa, 30.43% for $q = 2.2 \times 10^{-4}$ MPa and 54.57% for $q = 1.8 \times 10^{-3}$ MPa, while for the maximum stress σ_m, the relative error of Solution 2 to Solution 1 is about 4% for $q = 1.725 \times 10^{-6}$ MPa, 8.56% for $q = 2.2 \times 10^{-4}$ MPa and 30.14% for $q = 1.8 \times 10^{-3}$ MPa, the relative error of Solution 3 to Solution 1 is about 8.24% for $q = 1.725 \times 10^{-6}$ MPa, 22.39% for $q = 2.2 \times 10^{-4}$ MPa and 33.68% for $q = 1.8 \times 10^{-3}$ MPa, and the relative error of Solution 4 to Solution 1 is about 8.79% for $q = 1.725 \times 10^{-6}$ MPa, 35.65% for $q = 2.2 \times 10^{-4}$ MPa and 49.42% for $q = 1.8 \times 10^{-3}$ MPa. Therefore, the minimum relative error is the relative error of Solution 2 to Solution 1, but for the case of $q = 1.8 \times 10^{-3}$ MPa and $g = 10$ mm, may be as high as 35%

for the contact radius b and 30% for the maximum stress σ_m. Moreover, from Figure 11, it can also be seen that for the case of $q = 1.8 \times 10^{-3}$ MPa and $g = 10$ mm, the shape of the deflection curves in non-contact region also has great difference.

The choice of the elastic membranes of contact mode capacitive pressure sensors is highly dependent on the magnitude of maximum stress, so such a large maximum stress error will undoubtedly affect the correctness of the selection of elastic membranes. The total capacitance of a capacitive pressure sensor consists of two parts: one is the capacitance in the plate/membrane contact region, which is proportional to the square of the contact radius b, and the other is the capacitance in the plate/membrane non-contact region, which is affected by the shape of the deflection curves in the plate/membrane non-contact region.

All in all, Table 5 and Figures 11 and 12 show that the closed-form solution given in Section 2 has achieved a very significant and beneficial improvement.

4. Concluding Remarks

In this paper, the plate/membrane contact problem is investigated again, an initially flat, peripherally fixed circular membrane, which elastically deflects under uniformly distributed transverse loads, comes into contact with a concentric circular rigid flat plate that keeps a certain parallel gap from the initially flat circular membrane. In comparison with our previous works [34,35], the main improvements made here are that the assumption of small rotation angle of membrane is given up synchronously in the establishments of out-of-plane equilibrium equation and geometric equations. The resulting new and more refined closed-form solution has higher computational accuracy and can play a better role if further incorporated into the design of contact mode capacitive pressure sensors.

Further research on this plate/membrane contact problem should be focused on the consideration of plate/membrane friction. Since the larger the contact radius b, the greater the friction, the solution without considering plate/membrane friction is not suitable for the case of a too large contact radius b. Therefore, the solution considering plate/membrane friction will make the pressure measurement range of capacitive pressure sensors wider, since a large contact radius corresponds to a large pressure.

Author Contributions: Conceptualization, J.-Y.S.; methodology, F.-Y.L., X.L. and J.-Y.S.; validation, X.L. and X.-T.H.; writing—original draft preparation, F.-Y.L. and Q.Z.; writing—review and editing, X.L. and X.-T.H.; visualization, F.-Y.L. and Q.Z.; funding acquisition, J.-Y.S. All authors have read and agreed to the published version of the manuscript.

Institutional Review Board Statement: Not applicable.

Informed Consent Statement: Not applicable.

Data Availability Statement: Not applicable.

Conflicts of Interest: The authors declare no conflict of interest.

Nomenclature

a	Radius of the circular membrane
b	Radius of the circular contact area
h	Thickness of the circular membrane
ν	Poisson's ratio
E	Young's modulus
q	Uniformly distributed transverse loads

g	Certain parallel gap between rigid flat plate and circular membrane
r	Radial coordinate
φ	Circumferential coordinate
w	Transverse coordinate or displacement of the deflected membrane
o	Coordinate origin
π	Pi (ratio of circumference to diameter)
σ_r	Radial stress
θ	Rotation angle of the deflected membrane
σ_t	Circumferential stress
e_r	Radial strain
e_t	Circumferential strain
u	Radial displacement of the deflected membrane
Q	Dimensionless loads (aq/hE)
W	Dimensionless transverse displacement (w/a)
S_r	Dimensionless radial stress (σ_r/E)
S_t	Dimensionless circumferential stress (σ_t/E)
α	Dimensionless variable $(\alpha = b/a)$
x	Dimensionless radial coordinate (r/a)
β	Dimensionless variable $(\beta = (1+\alpha)/2)$
c_i	Coefficients of the power series for S_r
d_i	Coefficients of the power series for W

Appendix A

$$c_2 = \frac{1}{2\beta^2}(\beta\nu c_1 - 3\beta c_1 + \nu c_0 - c_0 - 1 + (\beta^2\nu^2 c_1{}^2 + 2\beta\nu^2 c_0 c_1 - 2\beta\nu c_0 c_1 + \nu^2 c_0{}^2 - 2\beta\nu c_1 - 2\nu c_0{}^2 - 2\nu c_0 + c_0{}^2 - d_1{}^2 + 2c_0 + 1)^{1/2}),$$

$$c_3 = -\frac{1}{6\beta^2(2\beta^2 c_2 - \beta\nu c_1 + 3\beta c_1 - \nu c_0 + c_0 + 1)}(20\,\beta^3 c_2{}^2 - 4\beta^3\nu c_2{}^2 - 20\beta^2\nu c_1 c_2 + 38\beta^2 c_1 c_2 - 10\beta\nu c_0 c_2 - 9\beta\nu c_1{}^2 + 10\beta c_0 c_2 + 12\beta c_1{}^2 - 3\nu c_0 c_1 + 10\beta c_2 + 3c_0 c_1 + 2d_1 d_2 + 3c_1)$$

$$c_4 = -\frac{1}{24\beta^2(2\beta^2 c_2 - \beta\nu c_1 + 3\beta c_1 - \nu c_0 + c_0 + 1)}(36\,\beta^4 c_3{}^2 - 36\beta^3\nu c_2 c_3 + 204\beta^3 c_2 c_3 - 84\beta^2\nu c_1 c_3 - 52\beta^2\nu c_2{}^2 + 174\beta^2 c_1 c_3 + 136\beta^2 c_2{}^2 - 42\beta\nu c_0 c_3 - 86\beta\nu c_1 c_2 + 42\beta c_0 c_3 + 134\beta c_1 c_2 - 16\nu c_0 c_2 - 12\nu c_1{}^2 + 42\beta c_3 + 16c_0 c_2 + 15c_1{}^2 + 6d_1 d_3 + 4d_2{}^2 + 16c_2)$$

$$c_5 = -\frac{1}{20\beta^2(2\beta^2 c_2 - \beta\nu c_1 + 3\beta c_1 - \nu c_0 + c_0 + 1)}(72\,\beta^4 c_3 c_4 - 32\beta^3\nu c_2 c_4 - 18\beta^3\nu c_3{}^2 + 192\beta^3 c_2 c_4 + 126\beta^3 c_3{}^2 - 72\beta^2\nu c_1 c_4 - 98\beta^2\nu c_2 c_3 + 156\beta^2 c_1 c_4 + 296\beta^2 c_2 c_3 - 36\beta\nu c_0 c_4 - 78\beta\nu c_1 c_3 - 46\beta\nu c_2{}^2 + 36\beta c_0 c_4 + 132\beta c_1 c_3 + 90\beta c_2{}^2 - 15\nu c_0 c_3 - 25\nu c_1 c_2 + 36\beta c_4 + 15c_0 c_3 + 35c_1 c_2 + 4d_1 d_4 + 6d_2 d_3 + 15c_3)$$

$$c_6 = -\frac{1}{60\beta^2(2\beta^2 c_2 - \beta\nu c_1 + 3\beta c_1 - \nu c_0 + c_0 + 1)}(240\,\beta^4 c_3 c_5 + 144\beta^4 c_4{}^2 - 100\beta^3\nu c_2 c_5 - 120\beta^3\nu c_3 c_4 + 620\beta^3 c_2 c_5 + 936\beta^3 c_3 c_4 - 220\beta^2\nu c_1 c_5 - 316\beta^2\nu c_2 c_4 - 174\beta^2\nu c_3{}^2 + 490\beta^2 c_1 c_5 + 1036\beta^2 c_2 c_4 + 633\beta^2 c_3{}^2 - 110\beta\nu c_0 c_5 - 246\beta\nu c_1 c_4 - 314\beta\nu c_2 c_3 + 110\beta c_0 c_5 + 438\beta c_1 c_4 + 698\beta c_2 c_3 - 48\nu c_0 c_4 - 84\nu c_1 c_3 - 48\nu c_2{}^2 + 110\beta c_5 + 48c_0 c_4 + 126c_1 c_3 + 80c_2{}^2 + 10d_1 d_5 + 16d_2 d_4 + 9d_3{}^2 + 48c_4)$$

$$c_7 = -\frac{1}{42\beta^2(2\,\beta^2 c_2 - \beta\nu c_1 + 3\beta c_1 - \nu c_0 + c_0 + 1)}(180\,\beta^4 c_3 c_6 + 240\beta^4 c_4 c_5 - 72\beta^3\nu c_2 c_6 - 90\beta^3\nu c_3 c_5 - 48\beta^3\nu c_4{}^2 + 456\beta^3 c_2 c_6 + 750\beta^3 c_3 c_5 + 432\beta^3 c_4{}^2 - 156\beta^2\nu c_1 c_6 - 78\beta\nu c_0 c_6 - 232\beta^2\nu c_2 c_5 - 270\beta^2\nu c_3 c_4 + 354\beta^2 c_1 c_6 + 802\beta^2 c_2 c_5 + 1098\beta^2 c_3 c_4 + 12d_3 d_4 - 35\nu c_0 c_5 - 178\beta\nu c_1 c_5 - 238\beta\nu c_2 c_4 - 129\beta\nu c_3{}^2 + 78\beta c_0 c_6 + 328\beta c_1 c_5 + 574\beta c_2 c_4 + 336\beta c_3{}^2 - 63\nu c_1 c_4 - 77\nu c_2 c_3 + 78\beta c_6 + 35c_0 c_5 + 99c_1 c_4 + 143c_2 c_3 + 6d_1 d_6 + 10d_2 d_5 + 35c_5)$$

$$c_8 = -\frac{1}{112\beta^2(2\beta^2c_2-\beta\nu c_1+3\beta c_1-\nu c_0+c_0+1)}(504\,\beta^4 c_3 c_7 + 720\beta^4 c_4 c_6 + 400\beta^4 c_5{}^2$$
$$-196\beta^3\nu c_2 c_7 - 252\beta^3\nu c_3 c_6 - 280\beta^3\nu c_4 c_5 + 1260\beta^3 c_2 c_7 + 2196\beta^3 c_3 c_6 + 2760\beta^3 c_4 c_5$$
$$-420\beta^2\nu c_1 c_7 - 640\beta^2\nu c_2 c_6 - 772\beta^2\nu c_3 c_5 - 408\beta^2\nu c_4{}^2 + 966\beta^2 c_1 c_7 + 2296\beta^2 c_2 c_6$$
$$+3382\beta^2 c_3 c_5 + 1896\beta^2 c_4{}^2 - 210\beta\nu c_0 c_7 - 486\beta\nu c_1 c_6 - 670\beta\nu c_2 c_5 - 762\beta\nu c_3 c_4 \qquad ,$$
$$+210\beta c_0 c_7 + 918\beta c_1 c_6 + 1710\beta c_2 c_5 + 2202\beta c_3 c_4 - 96\nu c_0 c_6 - 176\nu c_1 c_5 - 224\nu c_2 c_4$$
$$-120\nu c_3{}^2 + 210\beta c_7 + 96 c_0 c_6 + 286 c_1 c_5 + 448 c_2 c_4 + 255 c_3{}^2 + 14 d_1 d_7 + 24 d_2 d_6$$
$$+30 d_3 d_5 + 16 d_4{}^2 + 96 c_6)$$

$$c_9 = -\frac{1}{72\beta^2(2\beta^2c_2-\beta\nu c_1+3\beta c_1-\nu c_0+c_0+1)}(336\,\beta^4 c_3 c_8 + 504\beta^4 c_4 c_7 + 600\beta^4 c_5 c_6$$
$$-128\beta^3\nu c_2 c_8 - 168\beta^3\nu c_3 c_7 - 192\beta^3\nu c_4 c_6 - 100\beta^3\nu c_5{}^2 + 832\beta^3 c_2 c_8 + 1512\beta^3 c_3 c_7$$
$$+2016\beta^3 c_4 c_6 + 1100\beta^3 c_5{}^2 - 272\beta^2\nu c_1 c_8 - 422\beta^2\nu c_2 c_7 - 522\beta^2\nu c_3 c_6 - 572\beta^2\nu c_4 c_5$$
$$+632\beta^2 c_1 c_8 + 1556\beta^2 c_2 c_7 + 2412\beta^2 c_3 c_6 + 2912\beta^2 c_4 c_5 - 136\beta\nu c_0 c_8 - 318\beta\nu c_1 c_7 \qquad ,$$
$$-448\beta\nu c_2 c_6 - 526\beta\nu c_3 c_5 - 276\beta\nu c_4{}^2 + 136\beta c_0 c_8 + 612\beta c_1 c_7 + 1192\beta c_2 c_6$$
$$+1636\beta c_3 c_5 + 900\beta c_4{}^2 - 63\nu c_0 c_7 - 117\nu c_1 c_6 - 153\nu c_2 c_5 - 171\nu c_3 c_4 + 136\beta c_8$$
$$+63 c_0 c_7 + 195 c_1 c_6 + 323 c_2 c_5 + 399 c_3 c_4 + 8 d_1 d_8 + 14 d_2 d_7 + 18 d_3 d_6 + 20 d_4 d_5 + 63 c_7)$$

$$c_{10} = -\frac{1}{180\beta^2(2\beta^2c_2-\beta\nu c_1+3\beta c_1-\nu c_0+c_0+1)}(25\,d_5{}^2 + 18 d_1 d_9 + 32 d_2 d_8 + 42 d_3 d_7$$
$$+48 d_4 d_6 + 510 c_1 c_7 + 880 c_2 c_6 + 1150 c_3 c_5 + 160 c_0 c_8 - 240\nu c_4{}^2 + 4465\beta^2 c_5{}^2 + 900\beta^4 c_6{}^2$$
$$+342\beta c_9 - 1386\beta\nu c_3 c_6 - 1502\beta\nu c_4 c_5 - 324\beta^3\nu c_2 c_9 - 684\beta^2\nu c_1 c_9 - 1076\beta^2\nu c_2 c_8$$
$$-432\beta^3\nu c_3 c_8 - 1356\beta^2\nu c_3 c_7 - 504\beta^3\nu c_4 c_7 - 1524\beta^2\nu c_4 c_6 - 540\beta^3\nu c_5 c_6 - 342\beta\nu c_0 c_9$$
$$-806\beta\nu c_1 c_8 - 1154\beta\nu c_2 c_7 + 160 c_8 + 5342\beta c_4 c_5 + 8292\beta^2 c_4 c_6 + 1680\beta^4 c_5 c_7 \qquad ,$$
$$-160\nu c_0 c_8 + 3170\beta c_2 c_7 + 5544\beta^3 c_4 c_7 + 6522\beta^2 c_3 c_7 + 624 c_4{}^2 + 342\beta c_0 c_9 + 4554\beta c_3 c_6$$
$$+864\beta^4 c_3 c_9 + 2124\beta^3 c_2 c_9 - 300\nu c_1 c_7 + 6420\beta^3 c_5 c_6 + 1344\beta^4 c_4 c_8 + 1602\beta^2 c_1 c_9$$
$$-400\nu c_2 c_6 - 790\beta^2\nu c_5{}^2 - 460\nu c_3 c_5 + 1574\beta c_1 c_8 + 3984\beta^3 c_3 c_8 + 4052\beta^2 c_2 c_8)$$

$$c_{11} = -\frac{1}{110\beta^2(2\beta^2c_2-\beta\nu c_1+3\beta c_1-\nu c_0+c_0+1)}(-187\nu\,c_1 c_8 - 253\nu c_2 c_7 + 210\beta c_{10}$$
$$+10 d_1 d_{10} + 18 d_2 d_9 + 24 d_3 d_8 + 28 d_4 d_7 + 30 d_5 d_6 + 99 c_0 c_9 + 323 c_1 c_8 + 575 c_2 c_7 + 783 c_3 c_6$$
$$+899 c_4 c_5 + 2340\beta^3 c_6{}^2 + 1980\beta c_5{}^2 + 99 c_9 - 180\beta^3\nu c_6{}^2 - 99\nu c_0 c_9 + 3714\beta c_4 c_6 + 1260\beta^4 c_6 c_7$$
$$+1120\beta^4 c_5 c_8 + 6350\beta^2 c_5 c_6 + 4410\beta^3 c_5 c_7 + 3024\beta c_3 c_7 + 2034\beta c_2 c_8 + 4238\beta^2 c_3 c_8$$
$$+5598\beta^2 c_4 c_7 + 864\beta^4 c_4 c_9 + 3648\beta^3 c_4 c_8 + 210\beta c_0 c_{10} + 984\beta c_1 c_9 + 540\beta^4 c_3 c_{10} - 319\nu c_4 c_5 \qquad ,$$
$$+2558\beta^2 c_2 c_9 + 990\beta^2 c_1 c_{10} + 2538\beta^3 c_3 c_9 - 505\beta\nu c_5{}^2 + 1320\beta^3 c_2 c_{10} - 297\nu c_3 c_6$$
$$-200\beta^3\nu c_2 c_{10} - 270\beta^3\nu c_3 c_9 - 320\beta^3\nu c_4 c_8 - 350\beta^3\nu c_5 c_7 - 420\beta^2\nu c_1 c_{10} - 668\beta^2\nu c_2 c_9$$
$$-854\beta^2\nu c_3 c_8 - 978\beta^2\nu c_4 c_7 - 1040\beta^2\nu c_5 c_6 - 210\beta\nu c_0 c_{10} - 498\beta\nu c_1 c_9 - 722\beta\nu c_2 c_8$$
$$-882\beta\nu c_3 c_7 - 978\beta\nu c_4 c_6)$$

$$c_{12} = -\frac{1}{264\beta^2(2\beta^2c_2-\beta\nu c_1+3\beta c_1-\nu c_0+c_0+1)}(1320\,\beta^4 c_3 c_{11} + 1764\beta^4 c_7{}^2 - 484\beta^3\nu c_2 c_{11}$$
$$-660\beta^3\nu c_3 c_{10} - 792\beta^3\nu c_4 c_9 + 3212\beta^3 c_2 c_{11} + 6300\beta^3 c_3 c_{10} - 1012\beta^2\nu c_1 c_{11} - 1624\beta^2\nu c_2 c_{10}$$
$$-2100\beta^2\nu c_3 c_9 + 2398\beta^2 c_1 c_{11} + 6304\beta^2 c_2 c_{10} + 9024\beta^2 c_6{}^2 - 506\beta\nu c_0 c_{11} - 1206\beta\nu c_1 c_{10}$$
$$-1766\beta\nu c_2 c_9 - 2186\beta\nu c_3 c_8 - 2466\beta\nu c_4 c_7 - 2606\beta\nu c_5 c_6 + 506\beta c_0 c_{11} + 2406\beta c_1 c_{10}$$
$$+5078\beta c_2 c_9 - 240\nu c_0 c_{10} - 624\nu c_2 c_8 - 744\nu c_3 c_7 - 816\nu c_4 c_6 - 420\nu c_5{}^2 + 240 c_0 c_{10} + 798 c_1 c_9$$
$$+1456 c_2 c_8 + 2046 c_3 c_7 + 2448 c_4 c_6 + 10686\beta^2 c_3 c_9 - 456\nu c_1 c_9 + 7754\beta c_3 c_8 + 2160\beta^4 c_4 c_{10} \qquad ,$$
$$+9288\beta^3 c_4 c_9 + 14536\beta^2 c_4 c_8 + 11600\beta^3 c_5 c_8 + 17134\beta^2 c_5 c_7 + 2880\beta^4 c_5 c_9 + 3360\beta^4 c_6 c_8$$
$$+9858\beta c_4 c_7 - 1356\beta^2\nu c_6{}^2 + 12852\beta^3 c_6 c_7 + 11006\beta c_5 c_6 + 506\beta c_{11} + 22 d_1 d_{11} + 40 d_2 d_{10}$$
$$+54 d_3 d_9 + 64 d_4 d_8 + 70 d_5 d_7 + 240 c_{10} - 924\beta^3\nu c_6 c_7 - 2440\beta^2\nu c_4 c_8 - 880\beta^3\nu c_5 c_8$$
$$-2644\beta^2\nu c_5 c_7 + 36 d_6{}^2 + 1295 c_5{}^2)$$

$$c_{13} = -\frac{1}{156\beta^2(2\beta^2 c_2 - \beta \nu c_1 + 3\beta c_1 - \nu c_0 + c_0 + 1)}(792\beta^4 c_3 c_{12} + 1320\beta^4 c_4 c_{11} + 1800\beta^4 c_5 c_{10}$$
$$+2160\beta^4 c_6 c_9 + 2352\beta^4 c_7 c_8 + 1920\beta^3 c_2 c_{12} + 3828\beta^3 c_3 c_{11} + 5760\beta^3 c_4 c_{10} + 7380\beta^3 c_5 c_9$$
$$+8448\beta^3 c_6 c_8 + 1428\beta^2 c_1 c_{12} + 3808\beta^2 c_2 c_{11} + 6576\beta^2 c_3 c_{10} + 9156\beta^2 c_4 c_9 + 11116\beta^2 c_5 c_8$$
$$+12168\beta^2 c_6 c_7 - 834\beta \nu c_6^2 + 300\beta c_0 c_{12} + 1444\beta c_1 c_{11} + 3100\beta c_2 c_{10} + 4836\beta c_3 c_9 + 6316\beta c_4 c_8$$
$$+7300\beta c_5 c_7 - 143\nu c_0 c_{11} - 273\nu c_1 c_{10} - 377\nu c_2 c_9 - 455\nu c_3 c_8 - 507\nu c_4 c_7 - 533\nu c_5 c_6$$
$$-288\beta^3 \nu c_2 c_{12} - 396\beta^3 \nu c_3 c_{11} - 480\beta^3 \nu c_4 c_{10} - 540\beta^3 \nu c_5 c_9 - 576\beta^3 \nu c_6 c_8 - 294\beta^3 \nu c_7^2$$
$$+4410\beta^3 c_7^2 - 600\beta^2 \nu c_1 c_{12} - 970\beta^2 \nu c_2 c_{11} - 1266\beta^2 \nu c_3 c_{10} - 1488\beta^2 \nu c_4 c_9 - 1636\beta^2 \nu c_5 c_8$$
$$-1710\beta^2 \nu c_6 c_7 - 300\beta \nu c_0 c_{12} - 718\beta \nu c_1 c_{11} - 1060\beta \nu c_2 c_{10} - 1326\beta \nu c_3 c_9 - 1516\beta \nu c_4 c_8$$
$$-1630\beta \nu c_5 c_7 + 3822\beta c_6^2 + 300\beta c_{12} + 143 c_0 c_{11} + 483 c_1 c_{10} + 899 c_2 c_9 + 1295 c_3 c_8 + 1599 c_4 c_7$$
$$+1763 c_5 c_6 + 12 d_1 d_{12} + 22 d_2 d_{11} + 30 d_3 d_{10} + 36 d_4 d_9 + 40 d_5 d_8 + 42 d_6 d_7 + 143 c_{11}),$$

$$c_{14} = -\frac{1}{364\beta^2(2\beta^2 c_2 - \beta \nu c_1 + 3\beta c_1 - \nu c_0 + c_0 + 1)}(1872\beta^4 c_3 c_{13} + 3168\beta^4 c_4 c_{12} + 4400\beta^4 c_5 c_{11}$$
$$+5400\beta^4 c_6 c_{10} + 6048\beta^4 c_7 c_9 + 4524\beta^3 c_2 c_{13} + 9144\beta^3 c_3 c_{12} + 13992\beta^3 c_4 c_{11} + 18300\beta^3 c_5 c_{10}$$
$$+21492\beta^3 c_6 c_9 + 23184\beta^3 c_7 c_8 - 2142\beta^2 \nu c_7^2 + 3354\beta^2 c_1 c_{13} + 9052\beta^2 c_2 c_{12} + 15874\beta^2 c_3 c_{11}$$
$$+22524\beta^2 c_4 c_{10} + 27994\beta^2 c_5 c_9 + 31564\beta^2 c_6 c_8 + 702\beta c_0 c_{13} + 3414\beta c_1 c_{12} + 7434\beta c_2 c_{11}$$
$$+11802\beta c_3 c_{10} + 15750\beta c_4 c_9 + 18702\beta c_5 c_8 + 20274\beta c_6 c_7 - 336\nu c_0 c_{12} - 644\nu c_1 c_{11} - 896\nu c_2 c_{10}$$
$$-1092\nu c_3 c_9 - 1232\nu c_4 c_8 - 1316\nu c_5 c_7 + 702\beta c_{13} + 26 d_1 d_{13} - 1404\beta^3 \nu c_6 c_9 - 1144\beta^3 \nu c_4 c_{11}$$
$$-3564\beta^2 \nu c_4 c_{10} - 936\beta^3 \nu c_3 c_{12} - 3004\beta^2 \nu c_3 c_{11} - 676\beta^3 \nu c_2 c_{13} - 1404\beta^2 \nu c_1 c_{13} - 2284\beta^2 \nu c_2 c_{12}$$
$$-702\beta \nu c_0 c_{13} - 1686\beta \nu c_1 c_{12} - 2506\beta \nu c_2 c_{11} - 3162\beta \nu c_3 c_{10} - 3654\beta \nu c_4 c_9 - 3982\beta \nu c_5 c_8$$
$$-4146\beta \nu c_6 c_7 + 96 d_6 d_8 + 48 d_2 d_{12} + 66 d_3 d_{11} + 80 d_4 d_{10} + 90 d_5 d_9 - 1456\beta^3 \nu c_7 c_8 - 4204\beta^2 \nu c_6 c_8$$
$$+336 c_0 c_{12} + 1150 c_1 c_{11} + 16401\beta^2 c_7^2 + 3136\beta^4 c_8^2 - 672\nu c_6^2 + 4048 c_4 c_8 + 4606 c_5 c_7 + 2400 c_6^2$$
$$+49 d_7^2 + 2176 c_2 c_{10} + 3198 c_3 c_9 - 1300\beta^3 \nu c_5 c_{10} - 3964\beta^2 \nu c_5 c_9 + 336 c_{12}),$$

where $\beta = (1+\alpha)/2$ and $\eta = (1 + 2\alpha - 3\alpha^2)/4$.

Appendix B

$$d_1 = -\frac{\eta Q}{\sqrt{-Q^2 \eta^2 + 4\beta^2 c_0^2}}$$
$$d_2 = -\frac{1}{d_1(Q^2 \eta^2 - 4\beta^2 c_0^2)}\beta\left(Q^2 \eta d_1^2 - 2\beta c_0 c_1 d_1^2 - 2 c_0^2 d_1^2 + Q^2 \eta\right),$$

$$d_3 = -\frac{1}{3 d_1(Q^2 \eta^2 - 4\beta^2 c_0^2)}(2Q^2 \beta^2 d_1^2 + 8 Q^2 \beta \eta d_1 d_2 + 2 Q^2 \eta^2 d_2^2 - 8\beta^2 c_0^2 d_2^2 - 16\beta^2 c_0 c_1 d_1 d_2$$
$$-4\beta^2 c_0 c_2 d_1^2 - 2\beta^2 c_1^2 d_1^2 + Q^2 \eta d_1^2 - 16\beta c_0^2 d_1 d_2 - 8\beta c_0 c_1 d_1^2 + 2 Q^2 \beta^2 - 2 c_0^2 d_1^2 + Q^2 \eta),$$

$$d_4 = -\frac{1}{2 d_1(Q^2 \eta^2 - 4\beta^2 c_0^2)}(4 Q^2 \beta^2 d_1 d_2 + 6 Q^2 \beta \eta d_1 d_3 + 4 Q^2 \beta \eta d_2^2 + 3 Q^2 \eta^2 d_2 d_3 - 12\beta^2 c_0^2 d_2 d_3$$
$$-12\beta^2 c_0 c_1 d_1 d_3 - 8\beta^2 c_0 c_1 d_2^2 - 8\beta^2 c_0 c_2 d_1 d_2 - 2\beta^2 c_0 c_3 d_1^2 - 4\beta^2 c_1^2 d_1 d_2 - 2\beta^2 c_1 c_2 d_1^2 + Q^2 \beta d_1^2$$
$$+2 Q^2 \eta d_1 d_2 - 12\beta c_0^2 d_1 d_3 - 8\beta c_0^2 d_2^2 - 16\beta c_0 c_1 d_1 d_2 - 4\beta c_0 c_2 d_1^2 - 2\beta c_1^2 d_1^2 - 4 c_0^2 d_1 d_2$$
$$-2 c_0 c_1 d_1^2 + Q^2 \beta),$$

$$d_5 = -\frac{1}{10 d_1(Q^2 \eta^2 - 4\beta^2 c_0^2)}(24 Q^2 \beta^2 d_1 d_3 + 16 Q^2 \beta^2 d_2^2 + 32 Q^2 \beta \eta d_1 d_4 + 48 Q^2 \beta \eta d_2 d_3$$
$$+16 Q^2 \eta^2 d_2 d_4 + 9 Q^2 \eta^2 d_3^2 - 64\beta^2 c_0^2 d_2 d_4 - 36\beta^2 c_0^2 d_3^2 - 64\beta^2 c_0 c_1 d_1 d_4 - 96\beta^2 c_0 c_1 d_2 d_3$$
$$-48\beta^2 c_0 c_2 d_1 d_3 - 32\beta^2 c_0 c_2 d_2^2 - 32\beta^2 c_0 c_3 d_1 d_2 - 8\beta^2 c_0 c_4 d_1^2 - 24\beta^2 c_1^2 d_1 d_3 - 16\beta^2 c_1^2 d_2^2$$
$$-32\beta^2 c_1 c_2 d_1 d_2 - 8\beta^2 c_1 c_3 d_1^2 - 4\beta^2 c_2^2 d_1^2 + 16 Q^2 \beta d_1 d_2 + 12 Q^2 \eta d_1 d_3 + 8 Q^2 \eta d_2^2 - 4 c_1^2 d_1^2$$
$$-64\beta c_0^2 d_1 d_4 - 96\beta c_0^2 d_2 d_3 - 96\beta c_0 c_1 d_1 d_3 - 64\beta c_0 c_1 d_2^2 - 64\beta c_0 c_2 d_1 d_2 - 16\beta c_0 c_3 d_1^2$$
$$-32\beta c_1^2 d_1 d_2 - 16\beta c_1 c_2 d_1^2 + Q^2 d_1^2 - 24 c_0^2 d_1 d_3 - 16 c_0^2 d_2^2 - 32 c_0 c_1 d_1 d_2 - 8 c_0 c_2 d_1^2 + Q^2),$$

$$
\begin{aligned}
d_6 = & -\frac{1}{3d_1(Q^2\eta^2-4\beta^2c_0^2)}(8\,Q^2\beta^2d_1d_4 + 12Q^2\beta^2d_2d_3 + 10Q^2\beta\eta d_1d_5 + 16Q^2\beta\eta d_2d_4 \\
& +9Q^2\beta\eta d_3{}^2 + 5Q^2\eta^2d_2d_5 + 6Q^2\eta^2d_3d_4 - 20\beta^2c_0{}^2d_2d_5 - 24\beta^2c_0{}^2d_3d_4 - 20\beta^2c_0c_1d_1d_5 \\
& -32\beta^2c_0c_1d_2d_4 - 18\beta^2c_0c_1d_3{}^2 - 16\beta^2c_0c_2d_1d_4 - 24\beta^2c_0c_2d_2d_3 - 12\beta^2c_0c_3d_1d_3 \\
& -8\beta^2c_0c_3d_2{}^2 - 8\beta^2c_0c_4d_1d_2 - 2\beta^2c_0c_5d_1{}^2 - 8\beta^2c_1{}^2d_1d_4 - 12\beta^2c_1{}^2d_2d_3 - 12\beta^2c_1c_2d_1d_3 \\
& -8\beta^2c_1c_2d_2{}^2 - 8\beta^2c_1c_3d_1d_2 - 2\beta^2c_1c_4d_1{}^2 - 4\beta^2c_2{}^2d_1d_2 - 2\beta^2c_2c_3d_1{}^2 + 6Q^2\beta d_1d_3 \\
& +4Q^2\beta d_2{}^2 + 4Q^2\eta d_1d_4 + 6Q^2\eta d_2d_3 - 20\beta c_0{}^2d_1d_5 - 32\beta c_0{}^2d_2d_4 - 18\beta c_0{}^2d_3{}^2 \\
& -32\beta c_0c_1d_1d_4 - 48\beta c_0c_1d_2d_3 - 24\beta c_0c_2d_1d_3 - 16\beta c_0c_2d_2{}^2 - 16\beta c_0c_3d_1d_2 - 4\beta c_0c_4d_1{}^2 \\
& -12\beta c_1{}^2d_1d_3 - 8\beta c_1{}^2d_2{}^2 - 16\beta c_1c_2d_1d_2 - 4\beta c_1c_3d_1{}^2 - 2\beta c_2{}^2d_1{}^2 + Q^2d_1d_2 - 8c_0{}^2d_1d_4 \\
& -12c_0{}^2d_2d_3 - 12c_0c_1d_1d_3 - 8c_0c_1d_2{}^2 - 8c_0c_2d_1d_2 - 2c_0c_3d_1{}^2 - 4c_1{}^2d_1d_2 - 2c_1c_2d_1{}^2),
\end{aligned}
$$

$$
\begin{aligned}
d_7 = & -\frac{1}{7d_1(Q^2\eta^2-4\beta^2c_0^2)}(20\,Q^2\beta^2d_1d_5 + 32Q^2\beta^2d_2d_4 + 18Q^2\beta^2d_3{}^2 + 24Q^2\beta\eta d_1d_6 \\
& +40Q^2\beta\eta d_2d_5 + 48Q^2\beta\eta d_3d_4 + 12Q^2\eta^2d_2d_6 + 15Q^2\eta^2d_3d_5 + 8Q^2\eta^2d_4{}^2 - 48\beta^2c_0{}^2d_2d_6 \\
& -60\beta^2c_0{}^2d_3d_5 - 32\beta^2c_0{}^2d_4{}^2 - 48\beta^2c_0c_1d_1d_6 - 80\beta^2c_0c_1d_2d_5 - 96\beta^2c_0c_1d_3d_4 - 16c_1c_2d_1d_2 \\
& -40\beta^2c_0c_2d_1d_5 - 64\beta^2c_0c_2d_2d_4 - 36\beta^2c_0c_2d_3{}^2 - 32\beta^2c_0c_3d_1d_4 - 4\beta^2c_0c_6d_1{}^2 - 4c_1c_3d_1{}^2 \\
& -24\beta^2c_0c_4d_1d_3 - 16\beta^2c_0c_4d_2{}^2 - 16\beta^2c_0c_5d_1d_2 - 20\beta^2c_1{}^2d_1d_5 + 9Q^2\eta d_3{}^2 - 48\beta^2c_0c_3d_2d_3 \\
& -32\beta^2c_1{}^2d_2d_4 - 18\beta^2c_1{}^2d_3{}^2 - 32\beta^2c_1c_2d_1d_4 - 48\beta^2c_1c_2d_2d_3 - 24\beta^2c_1c_3d_1d_3 + 2Q^2d_2{}^2 \\
& -16\beta^2c_1c_3d_2{}^2 - 16\beta^2c_1c_4d_1d_2 + 16Q^2\beta d_1d_4 - 12\beta^2c_2{}^2d_1d_3 - 8\beta^2c_2{}^2d_2{}^2 - 16\beta^2c_2c_3d_1d_2 \\
& -4\beta^2c_2c_4d_1{}^2 - 2\beta^2c_3{}^2d_1{}^2 + 24Q^2\beta d_2d_3 + 10Q^2\eta d_1d_5 - 4\beta^2c_1c_5d_1{}^2 - 2c_2{}^2d_1{}^2 - 8\beta c_1c_4d_1{}^2 \\
& -48\beta c_0{}^2d_1d_6 - 80\beta c_0{}^2d_2d_5 - 96\beta c_0{}^2d_3d_4 - 80\beta c_0c_1d_1d_5 - 128\beta c_0c_1d_2d_4 - 72\beta c_0c_1d_3{}^2 \\
& -64\beta c_0c_2d_1d_4 - 96\beta c_0c_2d_2d_3 - 48\beta c_0c_3d_1d_3 - 32\beta c_0c_3d_2{}^2 - 32\beta c_0c_4d_1d_2 - 8\beta c_0c_5d_1{}^2 \\
& -32\beta c_1{}^2d_1d_4 - 48\beta c_1{}^2d_2d_3 - 48\beta c_1c_2d_1d_3 - 32\beta c_1c_2d_2{}^2 - 32\beta c_1c_3d_1d_2 + 16Q^2\eta d_2d_4 \\
& -16\beta c_2{}^2d_1d_2 - 8\beta c_2c_3d_1{}^2 + 3Q^2d_1d_3 - 20c_0{}^2d_1d_5 - 32c_0{}^2d_2d_4 - 18c_0{}^2d_3{}^2 - 32c_0c_1d_1d_4 \\
& -48c_0c_1d_2d_3 - 24c_0c_2d_1d_3 - 16c_0c_2d_2{}^2 - 16c_0c_3d_1d_2 - 4c_0c_4d_1{}^2 - 12c_1{}^2d_1d_3 - 8c_1{}^2d_2{}^2),
\end{aligned}
$$

$$
\begin{aligned}
d_8 = & -\frac{1}{4d_1(Q^2\eta^2-4\beta^2c_0^2)}(12\,Q^2\beta^2d_1d_6 + 20Q^2\beta^2d_2d_5 + 24Q^2\beta^2d_3d_4 + 14Q^2\beta\eta d_1d_7 \\
& +24Q^2\beta\eta d_2d_6 + 30Q^2\beta\eta d_3d_5 + 16Q^2\beta\eta d_4{}^2 + 7Q^2\eta^2d_2d_7 + 9Q^2\eta^2d_3d_6 + 10Q^2\eta^2d_4d_5 \\
& -28\beta^2c_0{}^2d_2d_7 - 36\beta^2c_0{}^2d_3d_6 - 40\beta^2c_0{}^2d_4d_5 - 28\beta^2c_0c_1d_1d_7 - 48\beta^2c_0c_1d_2d_6 \\
& -60\beta^2c_0c_1d_3d_5 - 32\beta^2c_0c_1d_4{}^2 - 24\beta^2c_0c_2d_1d_6 - 40\beta^2c_0c_2d_2d_5 - 48\beta^2c_0c_2d_3d_4 \\
& -20\beta^2c_0c_3d_1d_5 - 32\beta^2c_0c_3d_2d_4 - 18\beta^2c_0c_3d_3{}^2 - 16\beta^2c_0c_4d_1d_4 - 24\beta^2c_0c_4d_2d_3 \\
& -12\beta^2c_0c_5d_1d_3 - 8\beta^2c_0c_5d_2{}^2 - 8\beta^2c_0c_6d_1d_2 - 2\beta^2c_0c_7d_1{}^2 - 12\beta^2c_1{}^2d_1d_6 - 20\beta^2 \\
& -24\beta^2c_1{}^2d_3d_4 - 20\beta^2c_1c_2d_1d_5 - 32\beta^2c_1c_2d_2d_4 - 18\beta^2c_1c_2d_3{}^2 - 16\beta^2c_1c_3d_1d_4 \\
& -24\beta^2c_1c_3d_2d_3 - 12\beta^2c_1c_4d_1d_3 - 8\beta^2c_1c_4d_2{}^2 - 8\beta^2c_1c_5d_1d_2 - 2\beta^2c_1c_6d_1{}^2 - 8\beta^2c_2{}^2d_1d_4 \\
& -12\beta^2c_2{}^2d_2d_3 - 12\beta^2c_2c_3d_1d_3 - 8\beta^2c_2c_3d_2{}^2 - 8\beta^2c_2c_4d_1d_2 - 2\beta^2c_2c_5d_1{}^2 - 4\beta^2c_3{}^2d_1d_2 \\
& -2\beta^2c_3c_4d_1{}^2 + 10Q^2\beta d_1d_5 + 16Q^2\beta d_2d_4 + 9Q^2\beta d_3{}^2 + 6Q^2\eta d_1d_6 + 10Q^2\eta d_2d_5 \\
& +12Q^2\eta d_3d_4 - 28\beta c_0{}^2d_1d_7 - 48\beta c_0{}^2d_2d_6 - 60\beta c_0{}^2d_3d_5 - 32\beta c_0{}^2d_4{}^2 - 48\beta c_0c_1d_1d_6 \\
& -80\beta c_0c_1d_2d_5 - 96\beta c_0c_1d_3d_4 - 40\beta c_0c_2d_1d_5 - 64\beta c_0c_2d_2d_4 - 36\beta c_0c_2d_3{}^2 + c_1{}^2d_2d_5 \\
& -32\beta c_0c_3d_1d_4 - 48\beta c_0c_3d_2d_3 - 24\beta c_0c_4d_1d_3 - 16\beta c_0c_4d_2{}^2 - 16\beta c_0c_5d_1d_2 - 4\beta c_0c_6d_1{}^2 \\
& -20\beta c_1{}^2d_1d_5 - 32\beta c_1{}^2d_2d_4 - 18\beta c_1{}^2d_3{}^2 - 32\beta c_1c_2d_1d_4 - 48\beta c_1c_2d_2d_3 - 24\beta c_1c_3d_1d_3 \\
& -16\beta c_1c_3d_2{}^2 - 16\beta c_1c_4d_1d_2 - 4\beta c_1c_5d_1{}^2 - 12\beta c_2{}^2d_1d_3 - 8\beta c_2{}^2d_2{}^2 - 16\beta c_2c_3d_1d_2 \\
& -4\beta c_2c_4d_1{}^2 - 2\beta c_3{}^2d_1{}^2 + 2Q^2d_1d_4 + 3Q^2d_2d_3 - 12c_0{}^2d_1d_6 - 20c_0{}^2d_2d_5 - 24c_0{}^2d_3d_4 \\
& -20c_0c_1d_1d_5 - 32c_0c_1d_2d_4 - 18c_0c_1d_3{}^2 - 16c_0c_2d_1d_4 - 24c_0c_2d_2d_3 - 12c_0c_3d_1d_3 - 8c_0c_3d_2{}^2 \\
& -8c_0c_4d_1d_2 - 2c_0c_5d_1{}^2 - 8c_1{}^2d_1d_4 - 12c_1{}^2d_2d_3 - 12c_1c_2d_1d_3 - 8c_1c_2d_2{}^2 - 8c_1c_3d_1d_2 \\
& -2c_1c_4d_1{}^2 - 4c_2{}^2d_1d_2 - 2c_2c_3d_1),
\end{aligned}
$$

$$d_9 = -\frac{1}{18d_1(Q^2\eta^2 - 4\beta^2c_0^2)}(56\,Q^2 - ta^2d_1d_7 + 96Q^2\beta^2d_2d_6 + 120Q^2\beta^2d_3d_5 + 64Q^2\beta^2d_4{}^2$$
$$+64Q^2\beta\eta d_1d_8 + 112Q^2\beta\eta d_2d_7 + 144Q^2\beta\eta d_3d_6 + 160Q^2\beta\eta d_4d_5 + 32Q^2\eta^2d_2d_8$$
$$+42Q^2\eta^2d_3d_7 + 48Q^2\eta^2d_4d_6 + 25Q^2\eta^2d_5{}^2 - 128\beta^2c_0^2d_2d_8 - 168\beta^2c_0^2d_3d_7$$
$$-192\beta^2c_0^2d_4d_6 - 100\beta^2c_0^2d_5{}^2 - 128\beta^2c_0c_1d_1d_8 - 224\beta^2c_0c_1d_2d_7 - 288\beta^2c_0c_1d_3d_6$$
$$-320\beta^2c_0c_1d_4d_5 - 112\beta^2c_0c_2d_1d_7 - 192\beta^2c_0c_2d_2d_6 - 240\beta^2c_0c_2d_3d_5 - 128\beta^2c_0c_2d_4{}^2$$
$$-96\beta^2c_0c_3d_1d_6 - 160\beta^2c_0c_3d_2d_5 - 192\beta^2c_0c_3d_3d_4 - 80\beta^2c_0c_4d_1d_5 - 128\beta^2c_0c_4d_2d_4$$
$$-72\beta^2c_0c_4d_3{}^2 - 64\beta^2c_0c_5d_1d_4 - 96\beta^2c_0c_5d_2d_3 - 48\beta^2c_0c_6d_1d_3 - 32\beta^2c_0c_6d_2{}^2$$
$$-32\beta^2c_0c_7d_1d_2 - 8\beta^2c_0c_8d_1{}^2 - 56\beta^2 - 96\beta^2c_1{}^2d_2d_6 - 120\beta^2c_1{}^2d_3d_5 - 64\beta^2c_1{}^2d_4{}^2$$
$$-96\beta^2c_1c_2d_1d_6 - 160\beta^2c_1c_2d_2d_5 - 192\beta^2c_1c_2d_3d_4 - 80\beta^2c_1c_3d_1d_5 - 128\beta^2c_1c_3d_2d_4$$
$$-72\beta^2c_1c_3d_3{}^2 - 64\beta^2c_1c_4d_1d_4 - 96\beta^2c_1c_4d_2d_3 - 48\beta^2c_1c_5d_1d_3 - 32\beta^2c_1c_5d_2{}^2$$
$$-32\beta^2c_1c_6d_1d_2 - 8\beta^2c_1c_7d_1{}^2 - 40\beta^2c_2{}^2d_1d_5 - 64\beta^2c_2{}^2d_2d_4 - 36\beta^2c_2{}^2d_3{}^2$$
$$-96\beta^2c_2c_3d_2d_3 - 48\beta^2c_2c_4d_1d_3 - 32\beta^2c_2c_4d_2{}^2 - 32\beta^2c_2c_5d_1d_2 - 32\beta^2c_3c_4d_1d_2$$
$$-8\beta^2c_2c_6d_1{}^2 - 24\beta^2c_3{}^2d_1d_3 - 16 - ta^2c_3{}^2d_2{}^2 - 8\beta^2c_3c_5d_1{}^2 - 4\beta^2c_4{}^2d_1{}^2 + 32Q^2\eta d_4{}^2$$
$$+48Q^2\beta d_1d_6 + 80Q^2\beta d_2d_5 + 96Q^2\beta d_3d_4 + 28Q^2\eta d_1d_7 + c_1{}^2d_1d_7 + 48Q^2\eta d_2d_6$$
$$+60Q^2\eta d_3d_5 - 64\beta^2c_2c_3d_1d_4 - 128\beta c_0^2d_1d_8 - 224\beta c_0^2d_2d_7 - 288\beta c_0^2d_3d_6$$
$$-320\beta c_0^2d_4d_5 - 224\beta c_0c_1d_1d_7 - 384\beta c_0c_1d_2d_6 - 480\beta c_0c_1d_3d_5 - 256\beta c_0c_1d_4{}^2$$
$$-192\beta c_0c_2d_1d_6 - 320\beta c_0c_2d_2d_5 - 384\beta c_0c_2d_3d_4 - 160\beta c_0c_3d_1d_5 - 256\beta c_0c_3d_2d_4$$
$$-144\beta c_0c_3d_3{}^2 - 128\beta c_0c_4d_1d_4 - 192\beta c_0c_4d_2d_3 - 96\beta c_0c_5d_1d_3 - 64\beta c_0c_5d_2{}^2$$
$$-64\beta c_0c_6d_1d_2 - 16\beta c_0c_7d_1{}^2 - 96\beta c_1{}^2d_1d_6 - 160\beta c_1{}^2d_2d_5 - 192\beta c_1{}^2d_3d_4$$
$$-160\beta c_1c_2d_1d_5 - 256\beta c_1c_2d_2d_4 - 144\beta c_1c_2d_3{}^2 - 128\beta c_1c_3d_1d_4 - 192\beta c_1c_3d_2d_3$$
$$-96\beta c_1c_4d_1d_3 - 64\beta c_1c_4d_2{}^2 - 64\beta c_1c_5d_1d_2 - 16\beta c_1c_6d_1{}^2 - 64\beta c_2{}^2d_1d_4 - 32c_2c_3d_1d_2$$
$$-96\beta c_2{}^2d_2d_3 - 96\beta c_2c_3d_1d_3 - 64\beta c_2c_3d_2{}^2 - 64\beta c_2c_4d_1d_2 - 16\beta c_2c_5d_1{}^2 - 8c_2c_4d_1{}^2$$
$$-32\beta c_3{}^2d_1d_2 - 16\beta c_3c_4d_1{}^2 + 10Q^2d_1d_5 + 16Q^2d_2d_4 + 9Q^2d_3{}^2 - 56c_0^2d_1d_7 - 4c_3{}^2d_1{}^2$$
$$-96c_0^2d_2d_6 - 120c_0^2d_3d_5 - 64c_0^2d_4{}^2 - 96c_0c_1d_1d_6 - 160c_0c_1d_2d_5 - 192c_0c_1d_3d_4$$
$$-80c_0c_2d_1d_5 - 128c_0c_2d_2d_4 - 72c_0c_2d_3{}^2 - 64c_0c_3d_1d_4 - 96c_0c_3d_2d_3 - 48c_0c_4d_1d_3$$
$$-32c_0c_4d_2{}^2 - 32c_0c_5d_1d_2 - 8c_0c_6d_1{}^2 - 40c_1{}^2d_1d_5 - 64c_1{}^2d_2d_4 - 36c_1{}^2d_3{}^2 - 64c_1c_2d_1d_4$$
$$-96c_1c_2d_2d_3 - 48c_1c_3d_1d_3 - 32c_1c_3d_2{}^2 - 32c_1c_4d_1d_2 - 8c_1c_5d_1{}^2 - 24c_2{}^2d_1d_3 - 16c_2{}^2d_2{}^2)$$

$$d_{10} = -\frac{1}{5d_1(Q^2\eta^2 - 4\beta^2c_0^2)}(16Q^2 - ta^2d_1d_8 + 28Q^2\beta^2d_2d_7 + 36Q^2\beta^2d_3d_6 + 40Q^2\beta^2d_4d_5$$
$$+18Q^2\beta\eta d_1d_9 + 32Q^2\beta\eta d_2d_8 + 42Q^2\beta\eta d_3d_7 + 48Q^2\beta\eta d_4d_6 + 25Q^2\beta\eta d_5{}^2$$
$$+9Q^2\eta^2d_2d_9 + 12Q^2\eta^2d_3d_8 + 14Q^2\eta^2d_4d_7 + 15Q^2\eta^2d_5d_6 - 36\beta^2c_0^2d_2d_9 - 48\beta^2c_0^2d_3d_8$$
$$-56\beta^2c_0^2d_4d_7 - 60\beta^2c_0^2d_5d_6 - 36\beta^2c_0c_1d_1d_9 - 64\beta^2c_0c_1d_2d_8 - 84\beta^2c_0c_1d_3d_7$$
$$-96\beta^2c_0c_1d_4d_6 - 50\beta^2c_0c_1d_5{}^2 - 32\beta^2c_0c_2d_1d_8 - 56\beta^2c_0c_2d_2d_7 - 72\beta^2c_0c_2d_3d_6$$
$$-80\beta^2c_0c_2d_4d_5 - 28\beta^2c_0c_3d_1d_7 - 48\beta^2c_0c_3d_2d_6 - 60\beta^2c_0c_3d_3d_5 - 32\beta^2c_0c_3d_4{}^2$$
$$-24\beta^2c_0c_4d_1d_6 - 40\beta^2c_0c_4d_2d_5 - 48\beta^2c_0c_4d_3d_4 - 20\beta^2c_0c_5d_1d_5 - 32\beta^2c_0c_5d_2d_4$$
$$-18\beta^2c_0c_5d_3{}^2 - 16\beta^2c_0c_6d_1d_4 - 24\beta^2c_0c_6d_2d_3 - 12\beta^2c_0c_7d_1d_3 - 40\beta^2c_1{}^2d_4d_5$$
$$-8\beta^2c_0c_8d_1d_2 - 2\beta^2c_0c_9d_1{}^2 - 16\beta^2c_1{}^2d_1d_8 - 28\beta^2c_1{}^2d_2d_7 - 36\beta^2c_1{}^2d_3d_6 - 8\beta^2c_0c_7d_2{}^2$$
$$-28\beta^2c_1c_2d_1d_7 - 48\beta^2c_1c_2d_2d_6 - 60\beta^2c_1c_2d_3d_5 - 32\beta^2c_1c_2d_4{}^2 - 24\beta^2c_1c_3d_1d_6$$
$$-40\beta^2c_1c_3d_2d_5 - 48\beta^2c_1c_3d_3d_4 - 20\beta^2c_1c_4d_1d_5 - 32\beta^2c_1c_4d_2d_4 - 18\beta^2c_1c_4d_3{}^2$$
$$-16\beta^2c_1c_5d_1d_4 - 24\beta^2c_1c_5d_2d_3 - 12\beta^2c_1c_6d_1d_3 - 8\beta^2c_1c_6d_2{}^2 - 8\beta^2c_1c_7d_1d_2 - 2\beta^2c_1c_8d_1{}^2$$
$$-12\beta^2c_2{}^2d_1d_6 - 20\beta^2c_2{}^2d_2d_5 - 24\beta^2c_2{}^2d_3d_4 - 20\beta^2c_2c_3d_1d_5 - 32\beta^2c_2c_3d_2d_4$$
$$-18\beta^2c_2c_3d_3{}^2 - 16\beta^2c_2c_4d_1d_4 - 24\beta^2c_2c_4d_2d_3 - 12\beta^2c_2c_5d_1d_3 - 8\beta^2c_2c_5d_2{}^2$$
$$-8\beta^2c_2c_6d_1d_2 - 2\beta^2c_2c_7d_1{}^2 - 8\beta^2c_3{}^2d_1d_4 - 12\beta^2c_3{}^2d_2d_3 - 12\beta^2c_3c_4d_1d_3 - 8\beta^2c_3c_4d_2{}^2$$
$$-8\beta^2c_3c_5d_1d_2 - 2\beta^2c_3c_6d_1{}^2 - 4\beta^2c_4{}^2d_1d_2 - 2\beta^2c_4c_5d_1{}^2 + 14Q^2\beta d_1d_7 + 24Q^2\beta d_2d_6$$
$$+30Q^2\beta d_3d_5 + 16Q^2\beta d_4{}^2 + 8Q^2\eta d_1d_8 + 14Q^2\eta d_2d_7 + 18Q^2\eta d_3d_6 + 20Q^2\eta d_4d_5$$
$$-36\beta c_0^2d_1d_9 - 64\beta c_0^2d_2d_8 - 84\beta c_0^2d_3d_7 - 96\beta c_0^2d_4d_6 - 50\beta c_0^2d_5{}^2 - 64\beta c_0c_1d_1d_8$$
$$-112\beta c_0c_1d_2d_7 - 144\beta c_0c_1d_3d_6 - 160\beta c_0c_1d_4d_5 - 56\beta c_0c_2d_1d_7 - 96\beta c_0c_2d_2d_6$$

$$-120\beta c_0c_2d_3d_5 - 64\beta c_0c_2d_4{}^2 - 48\beta c_0c_3d_1d_6 - 80\beta c_0c_3d_2d_5 - 96\beta c_0c_3d_3d_4$$
$$-40\beta c_0c_4d_1d_5 - 64\beta c_0c_4d_2d_4 - 36\beta c_0c_4d_3{}^2 - 32\beta c_0c_5d_1d_4 - 48\beta c_0c_5d_2d_3 - 8\beta c_3{}^2d_2{}^2$$
$$-24\beta c_0c_6d_1d_3 - 16\beta c_0c_6d_2{}^2 - 16\beta c_0c_7d_1d_2 - 4\beta c_0c_8d_1{}^2 - 28\beta c_1{}^2d_1d_7 - 48\beta c_1{}^2d_2d_6$$
$$-60\beta c_1{}^2d_3d_5 - 32\beta c_1{}^2d_4{}^2 - 48\beta c_1c_2d_1d_6 - 80\beta c_1c_2d_2d_5 - 96\beta c_1c_2d_3d_4 - 40\beta c_1c_3d_1d_5$$
$$-64\beta c_1c_3d_2d_4 - 36\beta c_1c_3d_3{}^2 - 32\beta c_1c_4d_1d_4 - 48\beta c_1c_4d_2d_3 - 24\beta c_1c_5d_1d_3 - 16\beta c_1c_5d_2{}^2$$
$$-16\beta c_1c_6d_1d_2 - 4\beta c_1c_7d_1{}^2 - 20\beta c_2{}^2d_1d_5 - 32\beta c_2{}^2d_2d_4 - 18\beta c_2{}^2d_3{}^2 - 32\beta c_2c_3d_1d_4$$
$$-48\beta c_2c_3d_2d_3 - 24\beta c_2c_4d_1d_3 - 16\beta c_2c_4d_2{}^2 - 16\beta c_2c_5d_1d_2 - 4\beta c_2c_6d_1{}^2 - 12\beta c_3{}^2d_1d_3$$
$$-16\beta c_3c_4d_1d_2 - 4\beta c_3c_5d_1{}^2 - 2\beta c_4{}^2d_1{}^2 + 3Q^2d_1d_6 + 5Q^2d_2d_5 + 6Q^2d_3d_4 - 16c_0{}^2d_1d_8$$
$$-28c_0{}^2d_2d_7 - 36c_0{}^2d_3d_6 - 40c_0{}^2d_4d_5 - 28c_0c_1d_1d_7 - 48c_0c_1d_2d_6 - 60c_0c_1d_3d_5 - 32c_0c_1d_4{}^2$$
$$-24c_0c_2d_1d_6 - 40c_0c_2d_2d_5 - 48c_0c_2d_3d_4 - 20c_0c_3d_1d_5 - 32c_0c_3d_2d_4 - 18c_0c_3d_3{}^2$$
$$-16c_0c_4d_1d_4 - 24c_0c_4d_2d_3 - 12c_0c_5d_1d_3 - 8c_0c_5d_2{}^2 - 8c_0c_6d_1d_2 - 2c_0c_7d_1{}^2 - 12c_1{}^2d_1d_6$$
$$-20c_1{}^2d_2d_5 - 24c_1{}^2d_3d_4 - 20c_1c_2d_1d_5 - 32c_1c_2d_2d_4 - 18c_1c_2d_3{}^2 - 16c_1c_3d_1d_4 - 24c_1c_3d_2d_3$$
$$-12c_1c_4d_1d_3 - 8c_1c_4d_2{}^2 - 8c_1c_5d_1d_2 - 2c_1c_6d_1{}^2 - 8c_2{}^2d_1d_4 - 12c_2{}^2d_2d_3 - 12c_2c_3d_1d_3$$
$$-8c_2c_3d_2{}^2 - 8c_2c_4d_1d_2 - 2c_2c_5d_1{}^2 - 4c_3{}^2d_1d_2 - 2c_3c_4d_1{}^2),$$

$$d_{11} = -\frac{1}{11d_1(Q^2\eta^2 - 4\beta^2c_0{}^2)}(36Q^2\beta^2d_1d_9 + 64Q^2\beta^2d_2d_8 + 84Q^2\beta^2d_3d_7 + 96Q^2\beta^2d_4d_6$$
$$+50Q^2\beta^2d_5{}^2 + 40Q^2\beta\eta d_1d_{10} + 72Q^2\beta\eta d_2d_9 + 96Q^2\beta\eta d_3d_8 + 112Q^2\beta\eta d_4d_7 + 120Q^2\beta\eta d_5d_6$$
$$+20Q^2\eta^2d_2d_{10} + 27Q^2\eta^2d_3d_9 + 32Q^2\eta^2d_4d_8 + 35Q^2\eta^2d_5d_7 + 18Q^2\eta^2d_6{}^2 - 80\beta^2c_0{}^2d_2d_{10}$$
$$-108\beta^2c_0{}^2d_3d_9 - 128\beta^2c_0{}^2d_4d_8 - 140\beta^2c_0{}^2d_5d_7 - 72\beta^2c_0{}^2d_6{}^2 - 80\beta^2c_0c_1d_1d_{10} - 144\beta^2c_0c_1d_2d_9$$
$$-192\beta^2c_0c_1d_3d_8 - 224\beta^2c_0c_1d_4d_7 - 240\beta^2c_0c_1d_5d_6 - 72\beta^2c_0c_2d_1d_9 - 128\beta^2c_0c_2d_2d_8$$
$$-168\beta^2c_0c_2d_3d_7 - 192\beta^2c_0c_2d_4d_6 - 100\beta^2c_0c_2d_5{}^2 - 64\beta^2c_0c_3d_1d_8 - 112\beta^2c_0c_3d_2d_7$$
$$-144\beta^2c_0c_3d_3d_6 - 160\beta^2c_0c_3d_4d_5 - 56\beta^2c_0c_4d_1d_7 - 96\beta^2c_0c_4d_2d_6 - 120\beta^2c_0c_4d_3d_5$$
$$-64\beta^2c_0c_4d_4{}^2 - 48\beta^2c_0c_5d_1d_6 - 80\beta^2c_0c_5d_2d_5 - 96\beta^2c_0c_5d_3d_4 - 40\beta^2c_0c_6d_1d_5 - 64\beta^2c_0c_6d_2d_4$$
$$-36\beta^2c_0c_6d_3{}^2 - 32\beta^2c_0c_7d_1d_4 - 48\beta^2c_0c_7d_2d_3 - 24\beta^2c_0c_8d_1d_3 - 16\beta^2c_0c_8d_2{}^2 - 16\beta^2c_0c_9d_1d_2$$
$$-4\beta^2c_0c_{10}d_1{}^2 - 36\beta^2c_1{}^2d_1d_9 - 64\beta^2c_1{}^2d_2d_8 - 84\beta^2c_1{}^2d_3d_7 - 96\beta^2c_1{}^2d_4d_6 - 50\beta^2c_1{}^2d_5{}^2$$
$$-64\beta^2c_1c_2d_1d_8 - 112\beta^2c_1c_2d_2d_7 - 144\beta^2c_1c_2d_3d_6 - 160\beta^2c_1c_2d_4d_5 - 56\beta^2c_1c_3d_1d_7$$
$$-120\beta^2c_1c_3d_3d_5 - 64\beta^2c_1c_3d_4{}^2 - 48\beta^2c_1c_4d_1d_6 - 80\beta^2c_1c_4d_2d_5 - 96\beta^2c_1c_4d_3d_4 - 40\beta^2c_1c_5d_1d_5$$
$$-64\beta^2c_1c_5d_2d_4 - 36\beta^2c_1c_5d_3{}^2 - 32\beta^2c_1c_6d_1d_4 - 48\beta^2c_1c_6d_2d_3 - 24\beta^2c_1c_7d_1d_3 - 16\beta^2c_1c_7d_2{}^2$$
$$-16\beta^2c_1c_8d_1d_2 - 4\beta^2c_1c_9d_1{}^2 - 28\beta^2c_2{}^2d_1d_7 - 48\beta^2c_2{}^2d_2d_6 - 60\beta^2c_2{}^2d_3d_5 - 32\beta^2c_2{}^2d_4{}^2$$
$$-48\beta^2c_2c_3d_1d_6 - 80\beta^2c_2c_3d_2d_5 - 96\beta^2c_2c_3d_3d_4 - 40\beta^2c_2c_4d_1d_5 - 64\beta^2c_2c_4d_2d_4 - 36\beta^2c_2c_4d_3{}^2$$
$$-32\beta^2c_2c_5d_1d_4 - 48\beta^2c_2c_5d_2d_3 - 24\beta^2c_2c_6d_1d_3 - 16\beta^2c_2c_6d_2{}^2 - 16\beta^2c_2c_7d_1d_2 - 4\beta^2c_2c_8d_1{}^2$$
$$-20\beta^2c_3{}^2d_1d_5 - 32\beta^2c_3{}^2d_2d_4 - 18\beta^2c_3{}^2d_3{}^2 - 32\beta^2c_3c_4d_1d_4 - 48\beta^2c_3c_4d_2d_3 - 24\beta^2c_3c_5d_1d_3$$
$$-16\beta^2c_3c_5d_2{}^2 - 16\beta^2c_3c_6d_1d_2 - 4\beta^2c_3c_7d_1{}^2 - 12\beta^2c_4{}^2d_1d_3 - 8\beta^2c_4{}^2d_2{}^2 - 16\beta^2c_4c_5d_1d_2$$
$$-4\beta^2c_4c_6d_1{}^2 - 2\beta^2c_5{}^2d_1{}^2 + 32Q^2\beta d_1d_8 + 56Q^2\beta d_2d_7 + 72Q^2\beta d_3d_6 + 80Q^2\beta d_4d_5 + 18Q^2\eta d_1d_9$$
$$+32Q^2\eta d_2d_8 + 42Q^2\eta d_3d_7 + 48Q^2\eta d_4d_6 + 25Q^2\eta d_5{}^2 - 80\beta c_0{}^2d_1d_{10} - 144\beta c_0{}^2d_2d_9 + 15Q^2d_3d_5$$
$$-224\beta c_0{}^2d_4d_7 - 240\beta c_0{}^2d_5d_6 - 144\beta c_0c_1d_1d_9 - 256\beta c_0c_1d_2d_8 - 336\beta c_0c_1d_3d_7 - 384\beta c_0c_1d_4d_6$$
$$-200\beta c_0c_1d_5{}^2 - 128\beta c_0c_2d_1d_8 - 224\beta c_0c_2d_2d_7 - 288\beta c_0c_2d_3d_6 - 320\beta c_0c_2d_4d_5 - 112\beta c_0c_3d_1d_7$$
$$-192\beta c_0c_3d_2d_6 - 240\beta c_0c_3d_3d_5 - 128\beta c_0c_3d_4{}^2 - 96\beta c_0c_4d_1d_6 - 160\beta c_0c_4d_2d_5 - 192\beta c_0c_4d_3d_4$$
$$-80\beta c_0c_5d_1d_5 - 128\beta c_0c_5d_2d_4 - 72\beta c_0c_5d_3{}^2 - 64\beta c_0c_6d_1d_4 - 96\beta c_0c_6d_2d_3 - 48\beta c_0c_7d_1d_3$$
$$-32\beta c_0c_7d_2{}^2 - 32\beta c_0c_8d_1d_2 - 8\beta c_0c_9d_1{}^2 - 64\beta c_1{}^2d_1d_8 - 112\beta c_1{}^2d_2d_7 - 144\beta c_1{}^2d_3d_6$$
$$-112\beta c_1c_2d_1d_7 - 192\beta c_1c_2d_2d_6 - 240\beta c_1c_2d_3d_5 - 128\beta c_1c_2d_4{}^2 - 96\beta c_1c_3d_1d_6 - 160\beta c_1c_3d_2d_5$$
$$-192\beta c_1c_3d_3d_4 - 80\beta c_1c_4d_1d_5 - 128\beta c_1c_4d_2d_4 - 72\beta c_1c_4d_3{}^2 - 64\beta c_1c_5d_1d_4 - 96\beta c_1c_5d_2d_3$$
$$-48\beta c_1c_6d_1d_3 - 32\beta c_1c_6d_2{}^2 - 32\beta c_1c_7d_1d_2 - 8\beta c_1c_8d_1{}^2 - 48\beta c_2{}^2d_1d_6 - 80\beta c_2{}^2d_2d_5$$
$$-80\beta c_2c_3d_1d_5 - 128\beta c_2c_3d_2d_4 - 72\beta c_2c_3d_3{}^2 - 64\beta c_2c_4d_1d_4 - 96\beta c_2c_4d_2d_3 - 48\beta c_2c_5d_1d_3$$
$$-32\beta c_2c_5d_2{}^2 - 32\beta c_2c_6d_1d_2 - 8\beta c_2c_7d_1{}^2 - 32\beta c_3{}^2d_1d_4 - 48\beta c_3{}^2d_2d_3 - 48\beta c_3c_4d_1d_3 + 8Q^2d_4{}^2$$
$$-32\beta c_3c_5d_1d_2 - 8\beta c_3c_6d_1{}^2 - 16\beta c_4{}^2d_1d_2 - 8\beta c_4c_5d_1{}^2 + 7Q^2d_1d_7 + 12Q^2d_2d_6 - 96\beta c_2{}^2d_3d_4$$
$$-36c_0{}^2d_1d_9 - 64c_0{}^2d_2d_8 - 84c_0{}^2d_3d_7 - 96c_0{}^2d_4d_6 - 50c_0{}^2d_5{}^2 - 64c_0c_1d_1d_8 - 112c_0c_1d_2d_7$$
$$-160c_0c_1d_4d_5 - 56c_0c_2d_1d_7 - 96c_0c_2d_2d_6 - 120c_0c_2d_3d_5 - 64c_0c_2d_4{}^2 - 48c_0c_3d_1d_6 - 80c_0c_3d_2d_5$$
$$-96c_0c_3d_3d_4 - 40c_0c_4d_1d_5 - 64c_0c_4d_2d_4 - 36c_0c_4d_3{}^2 - 32c_0c_5d_1d_4 - 48c_0c_5d_2d_3 - 24c_0c_6d_1d_3$$
$$-16c_0c_6d_2{}^2 - 16c_0c_7d_1d_2 - 4c_0c_8d_1{}^2 - 28c_1{}^2d_1d_7 - 48c_1{}^2d_2d_6 - 60c_1{}^2d_3d_5 - 32c_1{}^2d_4{}^2 - 48c_1c_2d_1d_6$$
$$-80c_1c_2d_2d_5 - 96c_1c_2d_3d_4 - 40c_1c_3d_1d_5 - 64c_1c_3d_2d_4 - 36c_1c_3d_3{}^2 - 32c_1c_4d_1d_4 - 48c_1c_4d_2d_3$$

$$-24c_1c_5d_1d_3 - 16c_1c_5d_2{}^2 - 16c_1c_6d_1d_2 - 4c_1c_7d_1{}^2 - 20c_2{}^2d_1d_5 - 32c_2{}^2d_2d_4 - 18c_2{}^2d_3{}^2 - 32c_2c_3d_1d_4$$
$$-48c_2c_3d_2d_3 - 24c_2c_4d_1d_3 - 16c_2c_4d_2{}^2 - 16c_2c_5d_1d_2 - 4c_2c_6d_1{}^2 - 12c_3{}^2d_1d_3 - 8c_3{}^2d_2{}^2 - 16c_3c_4d_1d_2 \quad,$$
$$-32\beta c_3c_4d_2{}^2 - 144c_0c_1d_3d_6 - 160\beta c_1{}^2d_4d_5 - 192\beta c_0{}^2d_3d_8 - 96\beta^2c_1c_3d_2d_6 - 4c_3c_5d_1{}^2 - 2c_4{}^2d_1{}^2)$$

$$d_{12} = -\frac{1}{6d_1(Q^2\eta^2 - 4\beta^2c_0{}^2)}(20\,Q^2\beta^2d_1d_{10} + 36Q^2\beta^2d_2d_9 + 48Q^2\beta^2d_3d_8 + 56Q^2\beta^2d_4d_7$$
$$+60Q^2\beta^2d_5d_6 + 22Q^2\beta\eta d_1d_{11} + 40Q^2\beta\eta d_2d_{10} + 54Q^2\beta\eta d_3d_9 + 64Q^2\beta\eta d_4d_8 + 70Q^2\beta\eta d_5d_7$$
$$+36Q^2\beta\eta d_6{}^2 + 11Q^2\eta^2d_2d_{11} + 15Q^2\eta^2d_3d_{10} + 18Q^2\eta^2d_4d_9 + 20Q^2\eta^2d_5d_8 + 21Q^2\eta^2d_6d_7$$
$$-44\beta^2c_0{}^2d_2d_{11} - 60\beta^2c_0{}^2d_3d_{10} - 72\beta^2c_0{}^2d_4d_9 - 80\beta^2c_0{}^2d_5d_8 - 84\beta^2c_0{}^2d_6d_7 - 44\beta^2c_0c_1d_1d_{11}$$
$$-80\beta^2c_0c_1d_2d_{10} - 108\beta^2c_0c_1d_3d_9 - 128\beta^2c_0c_1d_4d_8 - 140\beta^2c_0c_1d_5d_7 - 72\beta^2c_0c_1d_6{}^2 + 32Q^2\beta d_2d_8$$
$$-40\beta^2c_0c_2d_1d_{10} - 72\beta^2c_0c_2d_2d_9 - 96\beta^2c_0c_2d_3d_8 - 112\beta^2c_0c_2d_4d_7 - 120\beta^2c_0c_2d_5d_6$$
$$-36\beta^2c_0c_3d_1d_9 - 64\beta^2c_0c_3d_2d_8 - 84\beta^2c_0c_3d_3d_7 - 96\beta^2c_0c_3d_4d_6 - 50\beta^2c_0c_3d_5{}^2 - 32\beta^2c_0c_4d_1d_8$$
$$-56\beta^2c_0c_4d_2d_7 - 72\beta^2c_0c_4d_3d_6 - 80\beta^2c_0c_4d_4d_5 - 28\beta^2c_0c_5d_1d_7 - 48\beta^2c_0c_5d_2d_6 - 60\beta^2c_0c_5d_3d_5$$
$$-32\beta^2c_0c_5d_4{}^2 - 24\beta^2c_0c_6d_1d_6 - 40\beta^2c_0c_6d_2d_5 - 48\beta^2c_0c_6d_3d_4 - 20\beta^2c_0c_7d_1d_5 - 32\beta^2c_0c_7d_2d_4$$
$$-18\beta^2c_0c_7d_3{}^2 - 16\beta^2c_0c_8d_1d_4 - 24\beta^2c_0c_8d_2d_3 - 12\beta^2c_0c_9d_1d_3 - 8\beta^2c_0c_9d_2{}^2 - 8\beta^2c_0c_{10}d_1d_2$$
$$-2\beta^2c_0c_{11}d_1{}^2 - 20\beta^2c_1{}^2d_1d_{10} - 36\beta^2c_1{}^2d_2d_9 - 48\beta^2c_1{}^2d_3d_8 - 56\beta^2c_1{}^2d_4d_7 - 60\beta^2c_1{}^2d_5d_6$$
$$-36\beta^2c_1c_2d_1d_9 - 64\beta^2c_1c_2d_2d_8 - 84\beta^2c_1c_2d_3d_7 - 96\beta^2c_1c_2d_4d_6 - 50\beta^2c_1c_2d_5{}^2 - 32\beta^2c_1c_3d_1d_8$$
$$-56\beta^2c_1c_3d_2d_7 - 72\beta^2c_1c_3d_3d_6 - 80\beta^2c_1c_3d_4d_5 - 28\beta^2c_1c_4d_1d_7 - 48\beta^2c_1c_4d_2d_6 - 60\beta^2c_1c_4d_3d_5$$
$$-32\beta^2c_1c_4d_4{}^2 - 24\beta^2c_1c_5d_1d_6 - 40\beta^2c_1c_5d_2d_5 - 48\beta^2c_1c_5d_3d_4 - 20\beta^2c_1c_6d_1d_5 - 32\beta^2c_1c_6d_2d_4$$
$$-18\beta^2c_1c_6d_3{}^2 - 16\beta^2c_1c_7d_1d_4 - 24\beta^2c_1c_7d_2d_3 - 12\beta^2c_1c_8d_1d_3 - 8\beta^2c_1c_8d_2{}^2 - 8\beta^2c_1c_9d_1d_2$$
$$-2\beta^2c_1c_{10}d_1{}^2 - 16\beta^2c_2{}^2d_1d_8 - 28\beta^2c_2{}^2d_2d_7 - 36\beta^2c_2{}^2d_3d_6 - 40\beta^2c_2{}^2d_4d_5 - 28\beta^2c_2c_3d_1d_7$$
$$-48\beta^2c_2c_3d_2d_6 - 60\beta^2c_2c_3d_3d_5 - 32\beta^2c_2c_3d_4{}^2 - 24\beta^2c_2c_4d_1d_6 - 40\beta^2c_2c_4d_2d_5 - 48\beta^2c_2c_4d_3d_4$$
$$-20\beta^2c_2c_5d_1d_5 - 32\beta^2c_2c_5d_2d_4 - 18\beta^2c_2c_5d_3{}^2 - 16\beta^2c_2c_6d_1d_4 - 24\beta^2c_2c_6d_2d_3 - 12\beta^2c_2c_7d_1d_3$$
$$-8\beta^2c_2c_7d_2{}^2 - 8\beta^2c_2c_8d_1d_2 - 2\beta^2c_2c_9d_1{}^2 - 12\beta^2c_3{}^2d_1d_6 - 20\beta^2c_3{}^2d_2d_5 - 24\beta^2c_3{}^2d_3d_4$$
$$-20\beta^2c_3c_4d_1d_5 - 32\beta^2c_3c_4d_2d_4 - 18\beta^2c_3c_4d_3{}^2 - 16\beta^2c_3c_5d_1d_4 - 24\beta^2c_3c_5d_2d_3 - 12\beta^2c_3c_6d_1d_3$$
$$-8\beta^2c_3c_6d_2{}^2 - 8\beta^2c_3c_7d_1d_2 - 2\beta^2c_3c_8d_1{}^2 - 8\beta^2c_4{}^2d_1d_4 - 12\beta^2c_4{}^2d_2d_3 - 12\beta^2c_4c_5d_1d_3$$
$$-8\beta^2c_4c_5d_2{}^2 - 8\beta^2c_4c_6d_1d_2 - 2\beta^2c_4c_7d_1{}^2 - 4\beta^2c_5{}^2d_1d_2 - 2\beta^2c_5c_6d_1{}^2 + 18Q^2\beta d_1d_9 + 42Q^2\beta d_3d_7$$
$$+48Q^2\beta d_4d_6 + 25Q^2\beta d_5{}^2 + 10Q^2\eta d_1d_{10} + 18Q^2\eta d_2d_9 + 24Q^2\eta d_3d_8 + 28Q^2\eta d_4d_7 + 30Q^2\eta d_5d_6 \quad,$$
$$-44\beta c_0{}^2d_1d_{11} - 80\beta c_0{}^2d_2d_{10} - 108\beta c_0{}^2d_3d_9 - 128\beta c_0{}^2d_4d_8 - 140\beta c_0{}^2d_5d_7 - 72\beta c_0{}^2d_6{}^2$$
$$-80\beta c_0c_1d_1d_{10} - 144\beta c_0c_1d_2d_9 - 192\beta c_0c_1d_3d_8 - 224\beta c_0c_1d_4d_7 - 240\beta c_0c_1d_5d_6 - 72\beta c_0c_2d_1d_9$$
$$-128\beta c_0c_2d_2d_8 - 168\beta c_0c_2d_3d_7 - 192\beta c_0c_2d_4d_6 - 100\beta c_0c_2d_5{}^2 - 64\beta c_0c_3d_1d_8 - 112\beta c_0c_3d_2d_7$$
$$-144\beta c_0c_3d_3d_6 - 160\beta c_0c_3d_4d_5 - 56\beta c_0c_4d_1d_7 - 96\beta c_0c_4d_2d_6 - 120\beta c_0c_4d_3d_5 - 64\beta c_0c_4d_4{}^2$$
$$-48\beta c_0c_5d_1d_6 - 80\beta c_0c_5d_2d_5 - 96\beta c_0c_5d_3d_4 - 40\beta c_0c_6d_1d_5 - 64\beta c_0c_6d_2d_4 - 36\beta c_0c_6d_3{}^2$$
$$-32\beta c_0c_7d_1d_4 - 48\beta c_0c_7d_2d_3 - 24\beta c_0c_8d_1d_3 - 16\beta c_0c_8d_2{}^2 - 16\beta c_0c_9d_1d_2 - 4\beta c_0c_{10}d_1{}^2$$
$$-36\beta c_1{}^2d_1d_9 - 64\beta c_1{}^2d_2d_8 - 84\beta c_1{}^2d_3d_7 - 96\beta c_1{}^2d_4d_6 - 50\beta c_1{}^2d_5{}^2 - 64\beta c_1c_2d_1d_8$$
$$-112\beta c_1c_2d_2d_7 - 144\beta c_1c_2d_3d_6 - 160\beta c_1c_2d_4d_5 - 56\beta c_1c_3d_1d_7 - 120\beta c_1c_3d_3d_5 - 64\beta c_1c_3d_4{}^2$$
$$-48\beta c_1c_4d_1d_6 - 80\beta c_1c_4d_2d_5 - 96\beta c_1c_4d_3d_4 - 40\beta c_1c_5d_1d_5 - 64\beta c_1c_5d_2d_4 - 36\beta c_1c_5d_3{}^2$$
$$-32\beta c_1c_6d_1d_4 - 48\beta c_1c_6d_2d_3 - 24\beta c_1c_7d_1d_3 - 16\beta c_1c_7d_2{}^2 - 16\beta c_1c_8d_1d_2 - 4\beta c_1c_9d_1{}^2$$
$$-28\beta c_2{}^2d_1d_7 - 48\beta c_2{}^2d_2d_6 - 60\beta c_2{}^2d_3d_5 - 32\beta c_2{}^2d_4{}^2 - 48\beta c_2c_3d_1d_6 - 80\beta c_2c_3d_2d_5$$
$$-96\beta c_2c_3d_3d_4 - 40\beta c_2c_4d_1d_5 - 64\beta c_2c_4d_2d_4 - 36\beta c_2c_4d_3{}^2 - 32\beta c_2c_5d_1d_4 - 48\beta c_2c_5d_2d_3$$
$$-24\beta c_2c_6d_1d_3 - 16\beta c_2c_6d_2{}^2 - 16\beta c_2c_7d_1d_2 - 4\beta c_2c_8d_1{}^2 - 20\beta c_3{}^2d_1d_5 - 32\beta c_3{}^2d_2d_4$$
$$-18\beta c_3{}^2d_3{}^2 - 32\beta c_3c_4d_1d_4 - 48\beta c_3c_4d_2d_3 - 24\beta c_3c_5d_1d_3 - 16\beta c_3c_5d_2{}^2 - 16\beta c_3c_6d_1d_2$$
$$-4\beta c_3c_7d_1{}^2 - 12\beta c_4{}^2d_1d_3 - 8\beta c_4{}^2d_2{}^2 - 16\beta c_4c_5d_1d_2 - 4\beta c_4c_6d_1{}^2 - 2\beta c_5{}^2d_1{}^2 + 4Q^2d_1d_8$$
$$+7Q^2d_2d_7 + 9Q^2d_3d_6 + 10Q^2d_4d_5 - 20c_0{}^2d_1d_{10} - 36c_0{}^2d_2d_9 - 48c_0{}^2d_3d_8 - 56c_0{}^2d_4d_7 - 60c_0{}^2d_5d_6$$
$$-36c_0c_1d_1d_9 - 64c_0c_1d_2d_8 - 84c_0c_1d_3d_7 - 96c_0c_1d_4d_6 - 50c_0c_1d_5{}^2 - 32c_0c_2d_1d_8 - 56c_0c_2d_2d_7$$
$$-96\beta c_1c_3d_2d_6 - 72c_0c_2d_3d_6 - 80c_0c_2d_4d_5 - 28c_0c_3d_1d_7 - 48c_0c_3d_2d_6 - 60c_0c_3d_3d_5 - 32c_0c_3d_4{}^2$$
$$-24c_0c_4d_1d_6 - 40c_0c_4d_2d_5 - 48c_0c_4d_3d_4 - 20c_0c_5d_1d_5 - 32c_0c_5d_2d_4 - 18c_0c_5d_3{}^2 - 16c_0c_6d_1d_4$$
$$-24c_0c_6d_2d_3 - 12c_0c_7d_1d_3 - 8c_0c_7d_2{}^2 - 8c_0c_8d_1d_2 - 2c_0c_9d_1{}^2 - 16c_1{}^2d_1d_8 - 28c_1{}^2d_2d_7 - 36c_1{}^2d_3d_6$$
$$-40c_1{}^2d_4d_5 - 28c_1c_2d_1d_7 - 48c_1c_2d_2d_6 - 60c_1c_2d_3d_5 - 32c_1c_2d_4{}^2 - 24c_1c_3d_1d_6 - 40c_1c_3d_2d_5$$
$$-48c_1c_3d_3d_4 - 20c_1c_4d_1d_5 - 32c_1c_4d_2d_4 - 18c_1c_4d_3{}^2 - 16c_1c_5d_1d_4 - 24c_1c_5d_2d_3 - 12c_1c_6d_1d_3$$
$$-8c_1c_6d_2{}^2 - 8c_1c_7d_1d_2 - 2c_1c_8d_1{}^2 - 12c_2{}^2d_1d_6 - 20c_2{}^2d_2d_5 - 24c_2{}^2d_3d_4 - 20c_2c_3d_1d_5 - 32c_2c_3d_2d_4$$

$$-18c_2c_3{d_3}^2 - 16c_2c_4d_1d_4 - 24c_2c_4d_2d_3 - 12c_2c_5d_1d_3 - 8c_2c_5{d_2}^2 - 8c_2c_6d_1d_2 - 2c_2c_7{d_1}^2 - 8{c_3}^2d_1d_4$$
$$-12{c_3}^2d_2d_3 - 12c_3c_4d_1d_3 - 8c_3c_4{d_2}^2 - 8c_3c_5d_1d_2 - 2c_3c_6{d_1}^2 - 4{c_4}^2d_1d_2 - 2c_4c_5{d_1}^2),$$

$$d_{13} = -\frac{1}{26d_1(Q^2\eta^2-4\beta^2{c_0}^2)}(88\,Q^2\beta^2d_1d_{11} + 160Q^2\beta^2d_2d_{10} + 216Q^2\beta^2d_3d_9 + 256Q^2\beta^2d_4d_8$$
$$+280Q^2\beta^2d_5d_7 + 144Q^2\beta^2{d_6}^2 + 96Q^2\beta\eta d_1d_{12} + 176Q^2\beta\eta d_2d_{11} + 240Q^2\beta\eta d_3d_{10}$$
$$+288Q^2\beta\eta d_4d_9 + 320Q^2\beta\eta d_5d_8 + 336Q^2\beta\eta d_6d_7 + 48Q^2\eta^2d_2d_{12} + 66Q^2\eta^2d_3d_{11} + 80Q^2\eta^2d_4d_{10}$$
$$+90Q^2\eta^2d_5d_9 + 96Q^2\eta^2d_6d_8 + 49Q^2\eta^2{d_7}^2 - 192\beta^2{c_0}^2d_2d_{12} - 264\beta^2{c_0}^2d_3d_{11} - 320\beta^2{c_0}^2d_4d_{10}$$
$$-360\beta^2{c_0}^2d_5d_9 - 384\beta^2{c_0}^2d_6d_8 - 196\beta^2{c_0}^2{d_7}^2 - 192\beta^2c_0c_1d_1d_{12} - 352\beta^2c_0c_1d_2d_{11}$$
$$-480\beta^2c_0c_1d_3d_{10} - 576\beta^2c_0c_1d_4d_9 - 640\beta^2c_0c_1d_5d_8 - 672\beta^2c_0c_1d_6d_7 - 176\beta^2c_0c_2d_1d_{11}$$
$$-320\beta^2c_0c_2d_2d_{10} - 432\beta^2c_0c_2d_3d_9 - 512\beta^2c_0c_2d_4d_8 - 560\beta^2c_0c_2d_5d_7 - 288\beta^2c_0c_2{d_6}^2$$
$$-160\beta^2c_0c_3d_1d_{10} - 288\beta^2c_0c_3d_2d_9 - 384\beta^2c_0c_3d_3d_8 - 448\beta^2c_0c_3d_4d_7 - 480\beta^2c_0c_3d_5d_6$$
$$-144\beta^2c_0c_4d_1d_9 - 256\beta^2c_0c_4d_2d_8 - 336\beta^2c_0c_4d_3d_7 - 384\beta^2c_0c_4d_4d_6 - 200\beta^2c_0c_4{d_5}^2$$
$$-128\beta^2c_0c_5d_1d_8 - 224\beta^2c_0c_5d_2d_7 - 288\beta^2c_0c_5d_3d_6 - 320\beta^2c_0c_5d_4d_5 - 112\beta^2c_0c_6d_1d_7$$
$$-192\beta^2c_0c_6d_2d_6 - 240\beta^2c_0c_6d_3d_5 - 128\beta^2c_0c_6{d_4}^2 - 96\beta^2c_0c_7d_1d_6 - 160\beta^2c_0c_7d_2d_5$$
$$-192\beta^2c_0c_7d_3d_4 - 80\beta^2c_0c_8d_1d_5 - 128\beta^2c_0c_8d_2d_4 - 72\beta^2c_0c_8{d_3}^2 - 64\beta^2c_0c_9d_1d_4$$
$$-96\beta^2c_0c_9d_2d_3 - 48\beta^2c_0c_{10}d_1d_3 - 32\beta^2c_0c_{10}{d_2}^2 - 32\beta^2c_0c_{11}d_1d_2 - 8\beta^2c_0c_{12}{d_1}^2 - 88\beta^2{c_1}^2d_1d_{11}$$
$$-160\beta^2{c_1}^2d_2d_{10} - 216\beta^2{c_1}^2d_3d_9 - 256\beta^2{c_1}^2d_4d_8 - 280\beta^2{c_1}^2d_5d_7 - 144\beta^2{c_1}^2{d_6}^2$$
$$-160\beta^2c_1c_2d_1d_{10} - 288\beta^2c_1c_2d_2d_9 - 384\beta^2c_1c_2d_3d_8 - 448\beta^2c_1c_2d_4d_7 - 480\beta^2c_1c_2d_5d_6$$
$$-144\beta^2c_1c_3d_1d_9 - 256\beta^2c_1c_3d_2d_8 - 336\beta^2c_1c_3d_3d_7 - 384\beta^2c_1c_3d_4d_6 - 200\beta^2c_1c_3{d_5}^2$$
$$-128\beta^2c_1c_4d_1d_8 - 224\beta^2c_1c_4d_2d_7 - 288\beta^2c_1c_4d_3d_6 - 320\beta^2c_1c_4d_4d_5 - 112\beta^2c_1c_5d_1d_7$$
$$-192\beta^2c_1c_5d_2d_6 - 240\beta^2c_1c_5d_3d_5 - 128\beta^2c_1c_5{d_4}^2 - 96\beta^2c_1c_6d_1d_6 - 160\beta^2c_1c_6d_2d_5$$
$$-192\beta^2c_1c_6d_3d_4 - 80\beta^2c_1c_7d_1d_5 - 128\beta^2c_1c_7d_2d_4 - 72\beta^2c_1c_7{d_3}^2 - 64\beta^2c_1c_8d_1d_4 - 96\beta^2c_1c_8d_2d_3$$
$$-48\beta^2c_1c_9d_1d_3 - 32\beta^2c_1c_9{d_2}^2 - 32\beta^2c_1c_{10}d_1d_2 - 8\beta^2c_1c_{11}{d_1}^2 - 72\beta^2{c_2}^2d_1d_9 - 128\beta^2{c_2}^2d_2d_8$$
$$-168\beta^2{c_2}^2d_3d_7 - 192\beta^2{c_2}^2d_4d_6 - 100\beta^2{c_2}^2{d_5}^2 - 128\beta^2c_2c_3d_1d_8 - 224\beta^2c_2c_3d_2d_7$$
$$-288\beta^2c_2c_3d_3d_6 - 320\beta^2c_2c_3d_4d_5 - 112\beta^2c_2c_4d_1d_7 - 192\beta^2c_2c_4d_2d_6 - 240\beta^2c_2c_4d_3d_5$$
$$-128\beta^2c_2c_4{d_4}^2 - 96\beta^2c_2c_5d_1d_6 - 160\beta^2c_2c_5d_2d_5 - 192\beta^2c_2c_5d_3d_4 - 80\beta^2c_2c_6d_1d_5$$
$$-128\beta^2c_2c_6d_2d_4 - 72\beta^2c_2c_6{d_3}^2 - 64\beta^2c_2c_7d_1d_4 - 96\beta^2c_2c_7d_2d_3 - 48\beta^2c_2c_8d_1d_3 - 32\beta^2c_2c_8{d_2}^2$$
$$-32\beta^2c_2c_9d_1d_2 - 8\beta^2c_2c_{10}{d_1}^2 - 56\beta^2{c_3}^2d_1d_7 - 96\beta^2{c_3}^2d_2d_6 - 120\beta^2{c_3}^2d_3d_5 - 64\beta^2{c_3}^2{d_4}^2$$
$$-96\beta^2c_3c_4d_1d_6 - 160\beta^2c_3c_4d_2d_5 - 192\beta^2c_3c_4d_3d_4 - 80\beta^2c_3c_5d_1d_5 - 128\beta^2c_3c_5d_2d_4$$
$$-72\beta^2c_3c_5{d_3}^2 - 64\beta^2c_3c_6d_1d_4 - 96\beta^2c_3c_6d_2d_3 - 48\beta^2c_3c_7d_1d_3 - 32\beta^2c_3c_7{d_2}^2 - 32\beta^2c_3c_8d_1d_2$$
$$-8\beta^2c_3c_9{d_1}^2 - 40\beta^2{c_4}^2d_1d_5 - 64 - ta^2{c_4}^2d_2d_4 - 36\beta^2{c_4}^2{d_3}^2 - 64\beta^2c_4c_5d_1d_4 - 96\beta^2c_4c_5d_2d_3$$
$$-48\beta^2c_4c_6d_1d_3 - 32\beta^2c_4c_6{d_2}^2 - 32\beta^2c_4c_7d_1d_2 - 8\beta^2c_4c_8{d_1}^2 - 24\beta^2{c_5}^2d_1d_3 - 16\beta^2{c_5}^2{d_2}^2$$
$$-32\beta^2c_5c_6d_1d_2 - 8\beta^2c_5c_7{d_1}^2 - 4\beta^2{c_6}^2{d_1}^2 + 80Q^2\beta d_1d_{10} + 144Q^2\beta d_2d_9 + 192Q^2\beta d_3d_8$$
$$+224Q^2\beta d_4d_7 + 240Q^2\beta d_5d_6 + 44Q^2\eta d_1d_{11} + 80Q^2\eta d_2d_{10} + 108Q^2\eta d_3d_9 + 128Q^2\eta d_4d_8$$
$$+140Q^2\eta d_5d_7 + 72Q^2\eta{d_6}^2 - 192\beta{c_0}^2d_1d_{12} - 352\beta{c_0}^2d_2d_{11} - 480\beta{c_0}^2d_3d_{10} - 576\beta{c_0}^2d_4d_9$$
$$-640\beta{c_0}^2d_5d_8 - 672\beta{c_0}^2d_6d_7 - 352\beta c_0c_1d_1d_{11} - 640\beta c_0c_1d_2d_{10} - 864\beta c_0c_1d_3d_9 - 1024\beta c_0c_1d_4d_8$$
$$-1120\beta c_0c_1d_5d_7 - 576\beta c_0c_1{d_6}^2 - 320\beta c_0c_2d_1d_{10} - 576\beta c_0c_2d_2d_9 - 768\beta c_0c_2d_3d_8$$
$$-896\beta c_0c_2d_4d_7 - 960\beta c_0c_2d_5d_6 - 288\beta c_0c_3d_1d_9 - 512\beta c_0c_3d_2d_8 - 672\beta c_0c_3d_3d_7$$
$$-768\beta c_0c_3d_4d_6 - 400\beta c_0c_3{d_5}^2 - 256\beta c_0c_4d_1d_8 - 448\beta c_0c_4d_2d_7 - 576\beta c_0c_4d_3d_6$$
$$-640\beta c_0c_4d_4d_5 - 224\beta c_0c_5d_1d_7 - 384\beta c_0c_5d_2d_6 - 480\beta c_0c_5d_3d_5 - 256\beta c_0c_5{d_4}^2$$
$$-192\beta c_0c_6d_1d_6 - 320\beta c_0c_6d_2d_5 - 384\beta c_0c_6d_3d_4 - 160\beta c_0c_7d_1d_5 - 256\beta c_0c_7d_2d_4$$
$$-144\beta c_0c_7{d_3}^2 - 128\beta c_0c_8d_1d_4 - 192\beta c_0c_8d_2d_3 - 96\beta c_0c_9d_1d_3 - 64\beta c_0c_9{d_2}^2 - 64\beta c_0c_{10}d_1d_2$$
$$-16\beta c_0c_{11}{d_1}^2 - 160\beta{c_1}^2d_1d_{10} - 288\beta{c_1}^2d_2d_9 - 384\beta{c_1}^2d_3d_8 - 448\beta{c_1}^2d_4d_7 - 480\beta{c_1}^2d_5d_6$$
$$-288\beta c_1c_2d_1d_9 - 512\beta c_1c_2d_2d_8 - 672\beta c_1c_2d_3d_7 - 768\beta c_1c_2d_4d_6 - 400\beta c_1c_2{d_5}^2$$
$$-256\beta c_1c_3d_1d_8 - 448\beta c_1c_3d_2d_7 - 576\beta c_1c_3d_3d_6 - 640\beta c_1c_3d_4d_5 - 224\beta c_1c_4d_1d_7$$
$$-384\beta c_1c_4d_2d_6 - 480\beta c_1c_4d_3d_5 - 256\beta c_1c_4{d_4}^2 - 192\beta c_1c_5d_1d_6 - 320\beta c_1c_5d_2d_5$$
$$-384\beta c_1c_5d_3d_4 - 160\beta c_1c_6d_1d_5 - 256\beta c_1c_6d_2d_4 - 144\beta c_1c_6{d_3}^2 - 128\beta c_1c_7d_1d_4$$

$$-192\beta c_1 c_7 d_2 d_3 - 96\beta c_1 c_8 d_1 d_3 - 64\beta c_1 c_8 d_2{}^2 - 64\beta c_1 c_9 d_1 d_2 - 16\beta c_1 c_{10} d_1{}^2 - 128\beta c_2{}^2 d_1 d_8$$
$$-224\beta c_2{}^2 d_2 d_7 - 288\beta c_2{}^2 d_3 d_6 - 320\beta c_2{}^2 d_4 d_5 - 224\beta c_2 c_3 d_1 d_7 - 384\beta c_2 c_3 d_2 d_6$$
$$-480\beta c_2 c_3 d_3 d_5 - 256\beta c_2 c_3 d_4{}^2 - 192\beta c_2 c_4 d_1 d_6 - 320\beta c_2 c_4 d_2 d_5 - 384\beta c_2 c_4 d_3 d_4$$
$$-160\beta c_2 c_5 d_1 d_5 - 256\beta c_2 c_5 d_2 d_4 - 144\beta c_2 c_5 d_3{}^2 - 128\beta c_2 c_6 d_1 d_4 - 192\beta c_2 c_6 d_2 d_3$$
$$-96\beta c_2 c_7 d_1 d_3 - 64\beta c_2 c_7 d_2{}^2 - 64\beta c_2 c_8 d_1 d_2 - 16\beta c_2 c_9 d_1{}^2 - 96\beta c_3{}^2 d_1 d_6 - 160\beta c_3{}^2 d_2 d_5$$
$$-192\beta c_3{}^2 d_3 d_4 - 160\beta c_3 c_4 d_1 d_5 - 256\beta c_3 c_4 d_2 d_4 - 144\beta c_3 c_4 d_3{}^2 - 128\beta c_3 c_5 d_1 d_4 - 192\beta c_3 c_5 d_2 d_3$$
$$-96\beta c_3 c_6 d_1 d_3 - 64\beta c_3 c_6 d_2{}^2 - 64\beta c_3 c_7 d_1 d_2 - 16\beta c_3 c_8 d_1{}^2 - 64\beta c_4{}^2 d_1 d_4 - 96\beta c_4{}^2 d_2 d_3$$
$$-96\beta c_4 c_5 d_1 d_3 - 64\beta c_4 c_5 d_2{}^2 - 64\beta c_4 c_6 d_1 d_2 - 16\beta c_4 c_7 d_1{}^2 - 32\beta c_5{}^2 d_1 d_2 - 16\beta c_5 c_6 d_1{}^2$$
$$+18Q^2 d_1 d_9 + 32Q^2 d_2 d_8 + 42Q^2 d_3 d_7 + 48Q^2 d_4 d_6 + 25Q^2 d_5{}^2 - 88c_0{}^2 d_1 d_{11} - 160c_0{}^2 d_2 d_{10}$$
$$-216c_0{}^2 d_3 d_9 - 256c_0{}^2 d_4 d_8 - 280c_0{}^2 d_5 d_7 - 144c_0{}^2 d_6{}^2 - 160c_0 c_1 d_1 d_{10} - 288c_0 c_1 d_2 d_9 - 192c_2 c_3 d_3 d_4$$
$$-384c_0 c_1 d_3 d_8 - 448c_0 c_1 d_4 d_7 - 480c_0 c_1 d_5 d_6 - 144c_0 c_2 d_1 d_9 - 256c_0 c_2 d_2 d_8 - 336c_0 c_2 d_3 d_7$$
$$-384c_0 c_2 d_4 d_6 - 200c_0 c_2 d_5{}^2 - 128c_0 c_3 d_1 d_8 - 224c_0 c_3 d_2 d_7 - 288c_0 c_3 d_3 d_6 - 320c_0 c_3 d_4 d_5$$
$$-112c_0 c_4 d_1 d_7 - 192c_0 c_4 d_2 d_6 - 240c_0 c_4 d_3 d_5 - 128c_0 c_4 d_4{}^2 - 96c_0 c_5 d_1 d_6 - 160c_0 c_5 d_2 d_5$$
$$-192c_0 c_5 d_3 d_4 - 80c_0 c_6 d_1 d_5 - 128c_0 c_6 d_2 d_4 - 72c_0 c_6 d_3{}^2 - 64c_0 c_7 d_1 d_4 - 96c_0 c_7 d_2 d_3 - 48c_0 c_8 d_1 d_3$$
$$-32c_0 c_8 d_2{}^2 - 32c_0 c_9 d_1 d_2 - 8c_0 c_{10} d_1{}^2 - 72c_1{}^2 d_1 d_9 - 128c_1{}^2 d_2 d_8 - 168c_1{}^2 d_3 d_7 - 192c_1{}^2 d_4 d_6$$
$$-100c_1{}^2 d_5{}^2 - 128c_1 c_2 d_1 d_8 - 224c_1 c_2 d_2 d_7 - 288c_1 c_2 d_3 d_6 - 320c_1 c_2 d_4 d_5 - 112c_1 c_3 d_1 d_7 - 32c_2 c_7 d_1 d_2$$
$$-192c_1 c_3 d_2 d_6 - 240c_1 c_3 d_3 d_5 - 128c_1 c_3 d_4{}^2 - 96c_1 c_4 d_1 d_6 - 160c_1 c_4 d_2 d_5 - 192c_1 c_4 d_3 d_4 - 80c_1 c_5 d_1 d_5$$
$$-128c_1 c_5 d_2 d_4 - 72c_1 c_5 d_3{}^2 - 64c_1 c_6 d_1 d_4 - 96c_1 c_6 d_2 d_3 - 48c_1 c_7 d_1 d_3 - 32c_1 c_7 d_2{}^2 - 32c_1 c_8 d_1 d_2$$
$$-8c_1 c_9 d_1{}^2 - 56c_2{}^2 d_1 d_7 - 96c_2{}^2 d_2 d_6 - 120c_2{}^2 d_3 d_5 - 64c_2{}^2 d_4{}^2 - 96c_2 c_3 d_1 d_6 - 160c_2 c_3 d_2 d_5$$
$$-80c_2 c_4 d_1 d_5 - 128c_2 c_4 d_2 d_4 - 72c_2 c_4 d_3{}^2 - 64c_2 c_5 d_1 d_4 - 96c_2 c_5 d_2 d_3 - 48c_2 c_6 d_1 d_3 - 32c_2 c_6 d_2{}^2$$
$$-8c_2 c_8 d_1{}^2 - 40c_3{}^2 d_1 d_5 - 64c_3{}^2 d_2 d_4 - 36c_3{}^2 d_3{}^2 - 64c_3 c_4 d_1 d_4 - 96c_3 c_4 d_2 d_3 - 48c_3 c_5 d_1 d_3$$
$$-32c_3 c_5 d_2{}^2 - 32c_3 c_6 d_1 d_2 - 8c_3 c_7 d_1{}^2 - 24c_4{}^2 d_1 d_3 - 16c_4{}^2 d_2{}^2 - 32c_4 c_5 d_1 d_2 - 8c_4 c_6 d_1{}^2 - 4c_5{}^2 d_1{}^2)$$

$$d_{14} = -\frac{1}{7 d_1 (Q^2 \eta^2 - 4\beta^2 c_0{}^2)} (24 Q^2 \beta^2 d_1 d_{12} + 44 Q^2 \beta^2 d_2 d_{11} + 60 Q^2 \beta^2 d_3 d_{10} + 72 Q^2 \beta^2 d_4 d_9$$
$$+80 Q^2 \beta^2 d_5 d_8 + 84 Q^2 \beta^2 d_6 d_7 + 26 Q^2 \beta\eta d_1 d_{13} + 48 Q^2 \beta\eta d_2 d_{12} + 66 Q^2 \beta\eta d_3 d_{11} + 80 Q^2 \beta\eta d_4 d_{10}$$
$$+90 Q^2 \beta\eta d_5 d_9 + 96 Q^2 \beta\eta d_6 d_8 + 49 Q^2 \beta\eta d_7{}^2 + 13 Q^2 \eta^2 d_2 d_{13} + 18 Q^2 \eta^2 d_3 d_{12} + 22 Q^2 \eta^2 d_4 d_{11}$$
$$+25 Q^2 \eta^2 d_5 d_{10} + 27 Q^2 \eta^2 d_6 d_9 + 28 Q^2 \eta^2 d_7 d_8 - 52\beta^2 c_0{}^2 d_2 d_{13} - 72\beta^2 c_0{}^2 d_3 d_{12} - 88\beta^2 c_0{}^2 d_4 d_{11}$$
$$-100\beta^2 c_0{}^2 d_5 d_{10} - 108\beta^2 c_0{}^2 d_6 d_9 - 112\beta^2 c_0{}^2 d_7 d_8 - 52\beta^2 c_0 c_1 d_1 d_{13} - 96\beta^2 c_0 c_1 d_2 d_{12}$$
$$-132\beta^2 c_0 c_1 d_3 d_{11} - 160\beta^2 c_0 c_1 d_4 d_{10} - 180\beta^2 c_0 c_1 d_5 d_9 - 192\beta^2 c_0 c_1 d_6 d_8 - 98\beta^2 c_0 c_1 d_7{}^2$$
$$-48\beta^2 c_0 c_2 d_1 d_{12} - 88\beta^2 c_0 c_2 d_2 d_{11} - 120\beta^2 c_0 c_2 d_3 d_{10} - 144\beta^2 c_0 c_2 d_4 d_9 - 160\beta^2 c_0 c_2 d_5 d_8$$
$$-168\beta^2 c_0 c_2 d_6 d_7 - 44\beta^2 c_0 c_3 d_1 d_{11} - 80\beta^2 c_0 c_3 d_2 d_{10} - 108\beta^2 c_0 c_3 d_3 d_9 - 128\beta^2 c_0 c_3 d_4 d_8$$
$$-140\beta^2 c_0 c_3 d_5 d_7 - 72\beta^2 c_0 c_3 d_6{}^2 - 40\beta^2 c_0 c_4 d_1 d_{10} - 72\beta^2 c_0 c_4 d_2 d_9 - 96\beta^2 c_0 c_4 d_3 d_8 - 112\beta^2 c_0 c_4 d_4 d_7$$
$$-120\beta^2 c_0 c_4 d_5 d_6 - 36\beta^2 c_0 c_5 d_1 d_9 - 64\beta^2 c_0 c_5 d_2 d_8 - 84\beta^2 c_0 c_5 d_3 d_7 - 96\beta^2 c_0 c_5 d_4 d_6 - 50\beta^2 c_0 c_5 d_5{}^2$$
$$-32\beta^2 c_0 c_6 d_1 d_8 - 56\beta^2 c_0 c_6 d_2 d_7 - 72\beta^2 c_0 c_6 d_3 d_6 - 80\beta^2 c_0 c_6 d_4 d_5 - 28\beta^2 c_0 c_7 d_1 d_7 - 48\beta^2 c_0 c_7 d_2 d_6$$
$$-60\beta^2 c_0 c_7 d_3 d_5 - 32\beta^2 c_0 c_7 d_4{}^2 - 24\beta^2 c_0 c_8 d_1 d_6 - 40\beta^2 c_0 c_8 d_2 d_5 - 48\beta^2 c_0 c_8 d_3 d_4 - 20\beta^2 c_0 c_9 d_1 d_5$$
$$-32\beta^2 c_0 c_9 d_2 d_4 - 18\beta^2 c_0 c_9 d_3{}^2 - 16\beta^2 c_0 c_{10} d_1 d_4 - 24\beta^2 c_0 c_{10} d_2 d_3 - 12\beta^2 c_0 c_{11} d_1 d_3 - 8\beta^2 c_0 c_{11} d_2{}^2$$
$$-8\beta^2 c_0 c_{12} d_1 d_2 - 2\beta^2 c_0 c_{13} d_1{}^2 - 24\beta^2 c_1{}^2 d_1 d_{12} - 44\beta^2 c_1{}^2 d_2 d_{11} - 60\beta^2 c_1{}^2 d_3 d_{10} - 72\beta^2 c_1{}^2 d_4 d_9$$
$$-80\beta^2 c_1{}^2 d_5 d_8 - 84\beta^2 c_1{}^2 d_6 d_7 - 44\beta^2 c_1 c_2 d_1 d_{11} - 80\beta^2 c_1 c_2 d_2 d_{10} - 108\beta^2 c_1 c_2 d_3 d_9 - 128\beta^2 c_1 c_2 d_4 d_8$$
$$-140\beta^2 c_1 c_2 d_5 d_7 - 72\beta^2 c_1 c_2 d_6{}^2 - 40\beta^2 c_1 c_3 d_1 d_{10} - 72\beta^2 c_1 c_3 d_2 d_9 - 96\beta^2 c_1 c_3 d_3 d_8 - 112\beta^2 c_1 c_3 d_4 d_7$$
$$-120\beta^2 c_1 c_3 d_5 d_6 - 36\beta^2 c_1 c_4 d_1 d_9 - 64\beta^2 c_1 c_4 d_2 d_8 - 84\beta^2 c_1 c_4 d_3 d_7 - 96\beta^2 c_1 c_4 d_4 d_6 - 50\beta^2 c_1 c_4 d_5{}^2$$
$$-32\beta^2 c_1 c_5 d_1 d_8 - 56\beta^2 c_1 c_5 d_2 d_7 - 72\beta^2 c_1 c_5 d_3 d_6 - 80\beta^2 c_1 c_5 d_4 d_5 - 28\beta^2 c_1 c_6 d_1 d_7 - 48\beta^2 c_1 c_6 d_2 d_6$$
$$-60\beta^2 c_1 c_6 d_3 d_5 - 32\beta^2 c_1 c_6 d_4{}^2 - 24\beta^2 c_1 c_7 d_1 d_6 - 40\beta^2 c_1 c_7 d_2 d_5 - 48\beta^2 c_1 c_7 d_3 d_4 - 20\beta^2 c_1 c_8 d_1 d_5$$
$$-32\beta^2 c_1 c_8 d_2 d_4 - 18\beta^2 c_1 c_8 d_3{}^2 - 16\beta^2 c_1 c_9 d_1 d_4 - 24\beta^2 c_1 c_9 d_2 d_3 - 12\beta^2 c_1 c_{10} d_1 d_3 - 8\beta^2 c_1 c_{10} d_2{}^2$$
$$-8\beta^2 c_1 c_{11} d_1 d_2 - 2\beta^2 c_1 c_{12} d_1{}^2 - 20\beta^2 c_2{}^2 d_1 d_{10} - 36\beta^2 c_2{}^2 d_2 d_9 - 48\beta^2 c_2{}^2 d_3 d_8 - 56\beta^2 c_2{}^2 d_4 d_7$$
$$-60\beta^2 c_2{}^2 d_5 d_6 - 36\beta^2 c_2 c_3 d_1 d_9 - 64\beta^2 c_2 c_3 d_2 d_8 - 84\beta^2 c_2 c_3 d_3 d_7 - 96\beta^2 c_2 c_3 d_4 d_6 - 32\beta^2 c_3 c_4 d_4{}^2$$
$$-50\beta^2 c_2 c_3 d_5{}^2 - 32\beta^2 c_2 c_4 d_1 d_8 - 56\beta^2 c_2 c_4 d_2 d_7 - 72\beta^2 c_2 c_4 d_3 d_6 - 80\beta^2 c_2 c_4 d_4 d_5 - 28\beta^2 c_2 c_5 d_1 d_7$$
$$-48\beta^2 c_2 c_5 d_2 d_6 - 60\beta^2 c_2 c_5 d_3 d_5 - 32\beta^2 c_2 c_5 d_4{}^2 - 24\beta^2 c_2 c_6 d_1 d_6 - 40\beta^2 c_2 c_6 d_2 d_5 - 48\beta^2 c_2 c_6 d_3 d_4$$
$$-20\beta^2 c_2 c_7 d_1 d_5 - 32\beta^2 c_2 c_7 d_2 d_4 - 18\beta^2 c_2 c_7 d_3{}^2 - 16\beta^2 c_2 c_8 d_1 d_4 - 24\beta^2 c_2 c_8 d_2 d_3 - 12\beta^2 c_2 c_9 d_1 d_3$$
$$-8\beta^2 c_2 c_9 d_2{}^2 - 8\beta^2 c_2 c_{10} d_1 d_2 - 2\beta^2 c_2 c_{11} d_1{}^2 - 16\beta^2 c_3{}^2 d_1 d_8 - 28\beta^2 c_3{}^2 d_2 d_7 - 36\beta^2 c_3{}^2 d_3 d_6$$

$$-40\beta^2 c_3^2 d_4 d_5 - 28\beta^2 c_3 c_4 d_1 d_7 - 48\beta^2 c_3 c_4 d_2 d_6 - 60\beta^2 c_3 c_4 d_3 d_5 - 24\beta^2 c_3 c_5 d_1 d_6 - 40\beta^2 c_3 c_5 d_2 d_5$$

$$-48\beta^2 c_3 c_5 d_3 d_4 - 20\beta^2 c_3 c_6 d_1 d_5 - 32\beta^2 c_3 c_6 d_2 d_4 - 18\beta^2 c_3 c_6 d_3^2 - 16\beta^2 c_3 c_7 d_1 d_4 - 24\beta^2 c_3 c_7 d_2 d_3$$

$$-12\beta^2 c_3 c_8 d_1 d_3 - 8\beta^2 c_3 c_8 d_2^2 - 8\beta^2 c_3 c_9 d_1 d_2 - 2\beta^2 c_3 c_{10} d_1^2 - 12\beta^2 c_4^2 d_1 d_6 - 20\beta^2 c_4^2 d_2 d_5$$

$$-24\beta^2 c_4^2 d_3 d_4 - 20\beta^2 c_4 c_5 d_1 d_5 - 32\beta^2 c_4 c_5 d_2 d_4 - 18\beta^2 c_4 c_5 d_3^2 - 16\beta^2 c_4 c_6 d_1 d_4 - 24\beta^2 c_4 c_6 d_2 d_3$$

$$-12\beta^2 c_4 c_7 d_1 d_3 - 8\beta^2 c_4 c_7 d_2^2 - 8\beta^2 c_4 c_8 d_1 d_2 - 2\beta^2 c_4 c_9 d_1^2 - 8\beta^2 c_5^2 d_1 d_4 - 12\beta^2 c_5^2 d_2 d_3$$

$$-12\beta^2 c_5 c_6 d_1 d_3 - 8\beta^2 c_5 c_6 d_2^2 - 8\beta^2 c_5 c_7 d_1 d_2 - 2\beta^2 c_5 c_8 d_1^2 - 4\beta^2 c_6^2 d_1 d_2 - 2\beta^2 c_6 c_7 d_1^2 + 22Q^2 \beta d_1 d_{11}$$

$$+40Q^2 \beta d_2 d_{10} + 54Q^2 \beta d_3 d_9 + 64Q^2 \beta d_4 d_8 + 70Q^2 \beta d_5 d_7 + 36Q^2 \beta d_6^2 + 12Q^2 \eta d_1 d_{12} + 22Q^2 \eta d_2 d_{11}$$

$$+30Q^2 \eta d_3 d_{10} + 36Q^2 \eta d_4 d_9 + 40Q^2 \eta d_5 d_8 + 42Q^2 \eta d_6 d_7 - 52\beta c_0^2 d_1 d_{13} - 96\beta c_0^2 d_2 d_{12} - 132\beta c_0^2 d_3 d_{11}$$

$$-160\beta c_0^2 d_4 d_{10} - 180\beta c_0^2 d_5 d_9 - 192\beta c_0^2 d_6 d_8 - 98\beta c_0^2 d_7^2 - 96\beta c_0 c_1 d_1 d_{12} - 176\beta c_0 c_1 d_2 d_{11}$$

$$-240\beta c_0 c_1 d_3 d_{10} - 288\beta c_0 c_1 d_4 d_9 - 320\beta c_0 c_1 d_5 d_8 - 336\beta c_0 c_1 d_6 d_7 - 88\beta c_0 c_2 d_1 d_{11} - 160\beta c_0 c_2 d_2 d_{10}$$

$$-216\beta c_0 c_2 d_3 d_9 - 256\beta c_0 c_2 d_4 d_8 - 280\beta c_0 c_2 d_5 d_7 - 144\beta c_0 c_2 d_6^2 - 80\beta c_0 c_3 d_1 d_{10} - 144\beta c_0 c_3 d_2 d_9$$

$$-192\beta c_0 c_3 d_3 d_8 - 224\beta c_0 c_3 d_4 d_7 - 240\beta c_0 c_3 d_5 d_6 - 72\beta c_0 c_4 d_1 d_9 - 128\beta c_0 c_4 d_2 d_8 - 168\beta c_0 c_4 d_3 d_7$$

$$-192\beta c_0 c_4 d_4 d_6 - 100\beta c_0 c_4 d_5^2 - 64\beta c_0 c_5 d_1 d_8 - 112\beta c_0 c_5 d_2 d_7 - 144\beta c_0 c_5 d_3 d_6 - 160\beta c_0 c_5 d_4 d_5$$

$$-56\beta c_0 c_6 d_1 d_7 - 96\beta c_0 c_6 d_2 d_6 - 120\beta c_0 c_6 d_3 d_5 - 64\beta c_0 c_6 d_4^2 - 48\beta c_0 c_7 d_1 d_6 - 80\beta c_0 c_7 d_2 d_5$$

$$-96\beta c_0 c_7 d_3 d_4 - 40\beta c_0 c_8 d_1 d_5 - 64\beta c_0 c_8 d_2 d_4 - 36\beta c_0 c_8 d_3^2 - 32\beta c_0 c_9 d_1 d_4 - 48\beta c_0 c_9 d_2 d_3$$

$$-24\beta c_0 c_{10} d_1 d_3 - 16\beta c_0 c_{10} d_2^2 - 16\beta c_0 c_{11} d_1 d_2 - 4\beta c_0 c_{12} d_1^2 - 44\beta c_1^2 d_1 d_{11} - 80\beta c_1^2 d_2 d_{10}$$

$$-108\beta c_1^2 d_3 d_9 - 128\beta c_1^2 d_4 d_8 - 140\beta c_1^2 d_5 d_7 - 72\beta c_1^2 d_6^2 - 80\beta c_1 c_2 d_1 d_{10} - 144\beta c_1 c_2 d_2 d_9$$

$$-192\beta c_1 c_2 d_3 d_8 - 224\beta c_1 c_2 d_4 d_7 - 240\beta c_1 c_2 d_5 d_6 - 72\beta c_1 c_3 d_1 d_9 - 128\beta c_1 c_3 d_2 d_8 - 168\beta c_1 c_3 d_3 d_7$$

$$-192\beta c_1 c_3 d_4 d_6 - 100\beta c_1 c_3 d_5^2 - 64\beta c_1 c_4 d_1 d_8 - 112\beta c_1 c_4 d_2 d_7 - 144\beta c_1 c_4 d_3 d_6 - 160\beta c_1 c_4 d_4 d_5$$

$$-56\beta c_1 c_5 d_1 d_7 - 96\beta c_1 c_5 d_2 d_6 - 120\beta c_1 c_5 d_3 d_5 - 64\beta c_1 c_5 d_4^2 - 48\beta c_1 c_6 d_1 d_6 - 80\beta c_1 c_6 d_2 d_5$$

$$-96\beta c_1 c_6 d_3 d_4 - 40\beta c_1 c_7 d_1 d_5 - 64\beta c_1 c_7 d_2 d_4 - 36\beta c_1 c_7 d_3^2 - 32\beta c_1 c_8 d_1 d_4 - 48\beta c_1 c_8 d_2 d_3$$

$$-24\beta c_1 c_9 d_1 d_3 - 16\beta c_1 c_9 d_2^2 - 16\beta c_1 c_{10} d_1 d_2 - 4\beta c_1 c_{11} d_1^2 - 36\beta c_2^2 d_1 d_9 - 64\beta c_2^2 d_2 d_8$$

$$-84\beta c_2^2 d_3 d_7 - 96\beta c_2^2 d_4 d_6 - 50\beta c_2^2 d_5^2 - 64\beta c_2 c_3 d_1 d_8 - 112\beta c_2 c_3 d_2 d_7 - 144\beta c_2 c_3 d_3 d_6$$

$$-160\beta c_2 c_3 d_4 d_5 - 56\beta c_2 c_4 d_1 d_7 - 96\beta c_2 c_4 d_2 d_6 - 120\beta c_2 c_4 d_3 d_5 - 64\beta c_2 c_4 d_4^2 - 48\beta c_2 c_5 d_1 d_6$$

$$-80\beta c_2 c_5 d_2 d_5 - 96\beta c_2 c_5 d_3 d_4 - 40\beta c_2 c_6 d_1 d_5 - 64\beta c_2 c_6 d_2 d_4 - 36\beta c_2 c_6 d_3^2 - 32\beta c_2 c_7 d_1 d_4$$

$$-48\beta c_2 c_7 d_2 d_3 - 24\beta c_2 c_8 d_1 d_3 - 16\beta c_2 c_8 d_2^2 - 16\beta c_2 c_9 d_1 d_2 - 4\beta c_2 c_{10} d_1^2 - 28\beta c_3^2 d_1 d_7$$

$$-48\beta c_3^2 d_2 d_6 - 60\beta c_3^2 d_3 d_5 - 32\beta c_3^2 d_4^2 - 48\beta c_3 c_4 d_1 d_6 - 80\beta c_3 c_4 d_2 d_5 - 96\beta c_3 c_4 d_3 d_4$$

$$-40\beta c_3 c_5 d_1 d_5 - 64\beta c_3 c_5 d_2 d_4 - 36\beta c_3 c_5 d_3^2 - 32\beta c_3 c_6 d_1 d_4 - 48\beta c_3 c_6 d_2 d_3 - 24\beta c_3 c_7 d_1 d_3$$

$$-16\beta c_3 c_7 d_2^2 - 16\beta c_3 c_8 d_1 d_2 - 4\beta c_3 c_9 d_1^2 - 20\beta c_4^2 d_1 d_5 - 32\beta c_4^2 d_2 d_4 - 18\beta c_4^2 d_3^2 - 12\beta c_5^2 d_1 d_3$$

$$-32\beta c_4 c_5 d_1 d_4 - 48\beta c_4 c_5 d_2 d_3 - 24\beta c_4 c_6 d_1 d_3 - 16\beta c_4 c_6 d_2^2 - 16\beta c_4 c_7 d_1 d_2 - 4\beta c_4 c_8 d_1^2$$

$$-8\beta c_5^2 d_2^2 - 16\beta c_5 c_6 d_1 d_2 - 4\beta c_5 c_7 d_1^2 - 2\beta c_6^2 d_1^2 + 5Q^2 d_1 d_{10} + 9Q^2 d_2 d_9 + 12Q^2 d_3 d_8$$

$$+14Q^2 d_4 d_7 + 15Q^2 d_5 d_6 - 24c_0^2 d_1 d_{12} - 44c_0^2 d_2 d_{11} - 60c_0^2 d_3 d_{10} - 72c_0^2 d_4 d_9 - 80c_0^2 d_5 d_8$$

$$-84c_0^2 d_6 d_7 - 44c_0 c_1 d_1 d_{11} - 80c_0 c_1 d_2 d_{10} - 108c_0 c_1 d_3 d_9 - 128c_0 c_1 d_4 d_8 - 140c_0 c_1 d_5 d_7 - 72c_0 c_1 d_6^2$$

$$-40c_0 c_2 d_1 d_{10} - 72c_0 c_2 d_2 d_9 - 96c_0 c_2 d_3 d_8 - 112c_0 c_2 d_4 d_7 - 120c_0 c_2 d_5 d_6 - 36c_0 c_3 d_1 d_9 - 64c_0 c_3 d_2 d_8$$

$$-84c_0 c_3 d_3 d_7 - 96c_0 c_3 d_4 d_6 - 50c_0 c_3 d_5^2 - 32c_0 c_4 d_1 d_8 - 56c_0 c_4 d_2 d_7 - 72c_0 c_4 d_3 d_6 - 80c_0 c_4 d_4 d_5$$

$$-28c_0 c_5 d_1 d_7 - 48c_0 c_5 d_2 d_6 - 60c_0 c_5 d_3 d_5 - 32c_0 c_5 d_4^2 - 24c_0 c_6 d_1 d_6 - 40c_0 c_6 d_2 d_5 - 48c_0 c_6 d_3 d_4$$

$$-20c_0 c_7 d_1 d_5 - 32c_0 c_7 d_2 d_4 - 18c_0 c_7 d_3^2 - 16c_0 c_8 d_1 d_4 - 24c_0 c_8 d_2 d_3 - 12c_0 c_9 d_1 d_3 - 8c_0 c_9 d_2^2$$

$$-8c_0 c_{10} d_1 d_2 - 2c_0 c_{11} d_1^2 - 20c_1^2 d_1 d_{10} - 36c_1^2 d_2 d_9 - 48c_1^2 d_3 d_8 - 56c_1^2 d_4 d_7 - 60c_1^2 d_5 d_6$$

$$-36c_1 c_2 d_1 d_9 - 64c_1 c_2 d_2 d_8 - 84c_1 c_2 d_3 d_7 - 96c_1 c_2 d_4 d_6 - 50c_1 c_2 d_5^2 - 32c_1 c_3 d_1 d_8 - 56c_1 c_3 d_2 d_7$$

$$-72c_1 c_3 d_3 d_6 - 80c_1 c_3 d_4 d_5 - 28c_1 c_4 d_1 d_7 - 48c_1 c_4 d_2 d_6 - 60c_1 c_4 d_3 d_5 - 32c_1 c_4 d_4^2 - 24c_1 c_5 d_1 d_6$$

$$-40c_1 c_5 d_2 d_5 - 48c_1 c_5 d_3 d_4 - 20c_1 c_6 d_1 d_5 - 32c_1 c_6 d_2 d_4 - 18c_1 c_6 d_3^2 - 16c_1 c_7 d_1 d_4 - 24c_1 c_7 d_2 d_3$$

$$-12c_1 c_8 d_1 d_3 - 8c_1 c_8 d_2^2 - 8c_1 c_9 d_1 d_2 - 2c_1 c_{10} d_1^2 - 16c_2^2 d_1 d_8 - 28c_2^2 d_2 d_7 - 36c_2^2 d_3 d_6 - 40c_2^2 d_4 d_5$$

$$-28c_2 c_3 d_1 d_7 - 48c_2 c_3 d_2 d_6 - 60c_2 c_3 d_3 d_5 - 32c_2 c_3 d_4^2 - 24c_2 c_4 d_1 d_6 - 40c_2 c_4 d_2 d_5 - 48c_2 c_4 d_3 d_4$$

$$-20c_2 c_5 d_1 d_5 - 32c_2 c_5 d_2 d_4 - 18c_2 c_5 d_3^2 - 16c_2 c_6 d_1 d_4 - 24c_2 c_6 d_2 d_3 - 12c_2 c_7 d_1 d_3 - 8c_2 c_7 d_2^2$$

$$-8c_2 c_8 d_1 d_2 - 2c_2 c_9 d_1^2 - 12c_3^2 d_1 d_6 - 20c_3^2 d_2 d_5 - 24c_3^2 d_3 d_4 - 20c_3 c_4 d_1 d_5 - 32c_3 c_4 d_2 d_4$$

$$-18c_3 c_4 d_3^2 - 16c_3 c_5 d_1 d_4 - 24c_3 c_5 d_2 d_3 - 12c_3 c_6 d_1 d_3 - 8c_3 c_6 d_2^2 - 8c_3 c_7 d_1 d_2 - 2c_3 c_8 d_1^2 - 8c_4^2 d_1 d_4$$

$$-12c_4^2 d_2 d_3 - 12c_4 c_5 d_1 d_3 - 8c_4 c_5 d_2^2 - 8c_4 c_6 d_1 d_2 - 2c_4 c_7 d_1^2 - 4c_5^2 d_1 d_2 - 2c_5 c_6 d_1^2)$$

where $\beta = (1 + \alpha)/2$ and $\eta = (1 + 2\alpha - 3\alpha^2)/4$.

References

1. Delfani, M.R. Nonlinear elasticity of monolayer hexagonal crystals: Theory and application to circular bulge test. *Eur. J. Mech. A-Solid.* **2018**, *68*, 117–132. [CrossRef]
2. Dai, Z.; Lu, N. Poking and bulging of suspended thin sheets: Slippage, instabilities, and metrology. *J. Mech. Phys. Solids* **2021**, *149*, 104320. [CrossRef]
3. Gutscher, G.; Wu, H.C.; Ngaile, G.; Altan, T. Determination of flow stress for sheet metal forming using the viscous pressure bulge (VPB) test. *J. Mater. Process. Tech.* **2004**, *146*, 1–7. [CrossRef]
4. Ma, Y.; Wang, G.R.; Chen, Y.L.; Long, D.; Guan, Y.C.; Liu, L.Q.; Zhang, Z. Extended Hencky solution for the blister test of nanomembrane. *Extreme Mech. Lett.* **2018**, *22*, 69–78. [CrossRef]
5. Sun, J.Y.; Qian, S.H.; Li, Y.M.; He, X.T.; Zheng, Z.L. Theoretical study of adhesion energy measurement for film/substrate interface using pressurized blister test: Energy release rate. *Measurement* **2013**, *46*, 2278–2287. [CrossRef]
6. Cao, Z.; Tao, L.; Akinwande, D.; Huang, R.; Liechti, K.M. Mixed-mode traction-separation relations between graphene and copper by blister tests. *Int. J. Solids Struct.* **2016**, *84*, 147–159. [CrossRef]
7. Napolitanno, M.J.; Chudnovsky, A.; Moet, A. The constrained blister test for the energy of interfacial adhesion. *J. Adhes. Sci. Technol.* **1988**, *2*, 311–323. [CrossRef]
8. Pervier, M.L.A.; Hammond, D.W. Measurement of the fracture energy in mode I of atmospheric ice accreted on different materials using a blister test. *Eng. Fract. Mech.* **2019**, *214*, 223–232. [CrossRef]
9. Zhu, T.T.; Li, G.X.; Müftü, S. Revisiting the constrained blister test to measure thin film adhesion. *J. Appl. Mech.-T ASME* **2017**, *84*, 071005. [CrossRef]
10. Zhu, T.T.; Müftü, S.; Wan, K.T. One-dimensional constrained blister test to measure thin film adhesion. *J. Appl. Mech.-T ASME* **2018**, *85*, 054501. [CrossRef]
11. Molla-Alipour, M.; Ganji, B.A. Analytical analysis of mems capacitive pressure sensor with circular diaphragm under dynamic load using differential transformation method (DTM). *Acta Mech. Solida Sin.* **2015**, *28*, 400–408. [CrossRef]
12. Lee, H.Y.; Choi, B. Theoretical and experimental investigation of the trapped air effect on air-sealed capacitive pressure sensor. *Sens. Actuat. A* **2015**, *221*, 104–114. [CrossRef]
13. Mishra, R.B.; Khan, S.M.; Shaikh, S.F. Low-cost foil/paper based touch mode pressure sensing element as artificial skin module for prosthetic hand. In Proceedings of the 2020 3rd IEEE International Conference on Soft Robotics (RoboSoft), New Haven, CT, USA, 15 May–15 July 2020; pp. 194–200.
14. Meng, G.Q.; Ko, W.H. Modeling of circular diaphragm and spreadsheet solution programming for touch mode capacitive sensors. *Sens. Actuat. A* **1999**, *75*, 45–52. [CrossRef]
15. Chien, W.Z.; Wang, Z.Z.; Xu, Y.G.; Chen, S.L. The symmetrical deformation of circular membrane under the action of uniformly distributed loads in its portion. *Appl. Math. Mech. Engl. Ed.* **1981**, *2*, 653–668.
16. Arthurs, A.M.; Clegg, J. On the solution of a boundary value problem for the nonlinear Föppl-Hencky equation. *Z. Angew. Math. Mech.* **1994**, *74*, 281–284. [CrossRef]
17. Plaut, R.H. Linearly elastic annular and circular membranes under radial, transverse, and torsional loading. Part I: Large unwrinkled axisymmetric deformations. *Acta Mech.* **2009**, *202*, 79–99. [CrossRef]
18. Lian, Y.S.; Sun, J.Y.; Zhao, Z.H.; He, X.T.; Zheng, Z.L. A revisit of the boundary value problem for Föppl–Hencky membranes: Improvement of geometric equations. *Mathematics* **2020**, *8*, 631. [CrossRef]
19. Rao, Y.; Qiao, S.; Dai, Z.; Lu, N. Elastic wetting: Substrate-supported droplets confined by soft elastic membranes. *J. Mech. Phys. Solids* **2021**, *151*, 104399. [CrossRef]
20. Alekseev, S.A. Elastic annular membranes with a stiff centre under the concentrated force. *Eng. Cor.* **1951**, *10*, 71–80.
21. Sun, J.Y.; Hu, J.L.; He, X.T.; Zheng, Z.L. A theoretical study of a clamped punch-loaded blister configuration: The quantitative relation of load and deflection. Int. *J. Mech. Sci.* **2010**, *52*, 928–936. [CrossRef]
22. Lian, Y.S.; Sun, J.Y.; Ge, X.M.; Yang, Z.X.; He, X.T.; Zheng, Z.L. A theoretical study of an improved capacitive pressure sensor: Closed-form solution of uniformly loaded annular membranes. *Measurement* **2017**, *111*, 84–92. [CrossRef]
23. Sun, J.Y.; Zhang, Q.; Li, X.; He, X. T. Axisymmetric large deflection elastic analysis of hollow annular membranes under transverse uniform loading. *Symmetry* **2021**, *13*, 1770. [CrossRef]
24. Fichter, W.B. *Some Solutions for the Large Deflections of Uniformly Loaded Circular Membranes*; NASA: Washington, DC, USA, 1997; TP-3658.
25. He, X.T.; Li, X.; Shi, B.B.; Sun, J.Y. A closed-form solution without small-rotation-angle assumption for circular membranes under gas pressure loading. *Mathematics* **2021**, *9*, 2269. [CrossRef]
26. Hencky, H. On the stress state in circular plates with vanishing bending stiffness. *Z. Angew. Math. Phys.* **1915**, *63*, 311–317.
27. Chien, W.Z. Asymptotic behavior of a thin clamped circular plate under uniform normal pressure at very large deflection. *Sci. Rep. Natl. Tsinghua Univ.* **1948**, *5*, 193–208.
28. Alekseev, S.A. Elastic circular membranes under the uniformly distributed loads. *Eng. Corpus.* **1953**, *14*, 196–198.
29. Lim, T.C. Large deflection of circular auxetic membranes under uniform load. *J. Mater. Technol.* **2016**, *138*, 041011. [CrossRef]
30. Yang, X.Y.; Yu, L.X.; Long, R. Contact mechanics of inflated circular membrane under large deformation: Analytical solutions. *Int. J. Solids Struct.* **2021**, *233*, 111222. [CrossRef]

31. Plaut, R.H. Effect of pressure on pull-off of flat cylindrical punch adhered to circular membrane. *J. Adhesion* **2022**, *98*, 1438–1460. [CrossRef]

32. Sun, J.Y.; Lian, Y.S.; Li, Y.M.; He, X.T.; Zheng, Z.L. Closed-form solution of elastic circular membrane with initial stress under uniformly-distributed loads: Extended Hencky solution. *Z. Angew. Math. Mech.* **2015**, *95*, 1335–1341. [CrossRef]

33. Xu, D.W.; Liechti, K.M. Analytical and experimental study of a circular membrane in Hertzian contact with a rigid substrate. *Int. J. Solids Struct.* **2010**, *47*, 969–977. [CrossRef]

34. Wang, T.F.; He, X.T.; Li, Y.H. Closed-form solution of a peripherally fixed circular membrane under uniformly-distributed transverse loads and deflection restrictions. *Math. Probl. Eng.* **2018**, *2018*, 5989010. [CrossRef]

35. Lian, Y.S.; Sun, J.Y.; Dong, J.; Zheng, Z.L.; Yang, Z.X. Closed-form solution of axisymmetric deformation of prestressed Föppl-Hencky membrane under constrained deflecting. *Stuct. Eng. Mech.* **2019**, *69*, 693–698.

36. Varma, M.A.; Jindal, S.K. Novel design for performance enhancement of a touch-mode capacitive pressure sensor: Theoretical modeling and numerical simulation. *J. Comput. Electron.* **2018**, *17*, 1324–1333. [CrossRef]

37. Li, K. Investigation of ring touch mode capacitive pressure sensor with an electrothermomechanical coupling contact model. *IEEE Sens. J.* **2019**, *19*, 9641–9652. [CrossRef]

38. Jindal, S.K.; Varma, M.A.; Thukral, D. Study of MEMS touch-mode capacitive pressure sensor utilizing flexible SiC circular diaphragm: Robust design, theoretical modeling, numerical simulation and performance comparison. *J. Circuits Syst. Comput.* **2019**, *28*, 1950206. [CrossRef]

39. Mishra, R.B.; Babatain, W.; El-Atab, N.; Hussain, M.M. Polymer/paper-based double touch mode capacitive pressure sensing element for wireless control of robotic arm. In Proceedings of the 2020 IEEE 15th International Conference on Nano/Micro Engineered and Molecular System (NEMS), San Diego, CA, USA, 27–30 September 2020; pp. 95–99.